

Molecularly Stratified and Combinatorial Approaches to Precision Cancer Therapy

Doctoral thesis at the Medical University of Vienna
for obtaining the academic degree

Doctor of Philosophy

Submitted by

Marco P. Licciardello, M.Sc.

Supervisor:

Stefan Kubicek, PhD

CeMM - Research Center for Molecular Medicine

of the Austrian Academy of Sciences

Lazarettgasse 14, AKH BT 25.3

1090 Vienna, Austria



Vienna, 04/2015

To all of you styling you hair in the morning
(or otherwise unstoppable).

ACKNOWLEDGMENTS

There have been many colleagues and friends that, certainly unknowingly at times, have contributed to the following pages and that here I would like to mention.

CeMM is a place of great science and scientists but it would never make it to the end of the day if it was not for the incredible support it receives from all administration departments. They all do an incredibly professional job and silently help us with our research day after day. Thank you so much.

I was honored to be advised by the members of my thesis committee: Denise Barlow, Christian Seiser, Walter Berger and Thijn Brummelkamp. They have followed the progress of my PhD and always provided invaluable help for my research. I would like to thank them here for the time and experience they have shared with me.

I would also like to thank the members of the Superti-Furga lab and especially my colleagues and friends in the Nijman lab. Thank you for your precious help and for all the fun we had together. In particular, I would like to express my gratitude to Sebastian Nijman. He has been a mentor and an inspiration for me over the past years. If my skin became thicker and my inquiring more critical I owe it to you.

Anneke, you just passed by but the time we spent working together in the lab or rolling down hills of snow very much stirred my motivation. You are simply incredible and I feel especially lucky I met you.

The work I present here would have never been possible without the support of the amazing Kubicek group. Derya, Tamara and Anna, I can only wish we would have had more time to get to know each other. Thank you for always providing company during the weekends Jin, please promise me you will take some time off to see more of Vienna eventually! Erika, you have been a great example of professionalism for us all, thank you for always being so nice and helpful. I was there when the robot was born Charles and I can tell you it was born again the day you joined the lab. Bernd, how can it be always so much fun around you? You made most of our lunch breaks unforgettable and some of

my dreams come true (you know what I mean). P.S.: thank you for always dressing up as good as an Italian. You did that too Freya and no need to say I will never forget all of the interesting “scientific” papers, YouTube and other funny web links you used to send me, and your proficiency with the Italian language of course. We laughed so much together and I deeply missed you this last year at CeMM. Sara, I know I will never find the right words to say it so I will just write it as it comes: thank you for always being so kind and such a good listener, for your enthusiasm and energy, thank you for cursing in Italian in the lab and for our long philosophical/psychological discussions. You have no idea how much I enjoyed them and how much I always wanted to have someone to do that with. You are a great friend and I hope that will stay like this forever.

A PhD is a tough journey on rough seas and you need to make sure a good captain steers the ship. I was incredibly lucky to have Stefan Kubicek as shipmaster and supervisor of my PhD. Stefan, it was an honor to be your first PhD student and I hope you enjoyed the journey as much as I did. Thank you for always being supportive, for the freedom you gave me and for always pushing me to the best of what I could do. Priceless are the things I have learnt and the knowledge I had access to by doing research in your lab. You made me the scientist I am today. It was a great and rewarding challenge, a lifetime experience and, above all, a lot of fun. I will never forget all of this.

Last but not least I want to thank you René. I know I am a tough one and believe me, I sometimes still wonder how all of this has happened and why you decided to stay. You have given me what I could not find anywhere else, you have showed me Vienna the way I had not seen it before, you were always there at the end of each day ready to catch me if I was about to fall. I would have never made it without you.

DECLARATION

This thesis describes already published results as well as unpublished data submitted for publication. The work presented here has been entirely performed at CeMM - Research Center for Molecular Medicine of the Austrian Academy of Sciences (Vienna, Austria).

Part of this thesis has been reported in the following publication:

Licciardello, M. P., Müllner, M. K., Dürnberger, G., Kerzendorfer, C., Boidol, B., Trefzer, C., Sdelci, S., Berg, T., Penz, T., Schuster, M., Bock, C., Kralovics, R., Superti-Furga, G., Colinge, J., Nijman, S. M. & Kubicek, S. *“NOTCH1 activation in breast cancer confers sensitivity to inhibition of SUMOylation”*, *Oncogene*, 2014, 1-11

M. P. L. designed and performed the loss-of-function screen, analyzed screening data, performed the vast majority of validation experiments and wrote the manuscript; M. K. M. and S. M. N. generated the collection of isogenic cell lines; G. D. and J. C. contributed to screening data analysis; C. K. assisted with the loss-of-function screen; B. B. performed shRNA knockdown experiments; C. T. and G. S.-F. performed multiple reaction monitoring experiments; S. S. contributed with immunofluorescence measurements; T. B. and R. K. performed sequencing of loss-of-function screen DNA libraries; T. P., M. S. and C. B. performed RNA sequencing and alignment of sequencing reads; S. K. designed the loss-of-function screen and wrote the manuscript.

Another important part of this work has been described in the following manuscript submitted for publication:

Licciardello, M. P., Markt, P., Klepsch, F., Lardeau C. -H., Dürnberger, G., Ivanov, V., Colinge, J. & Kubicek, S. *“A combinatorial screen of the CLOUD uncovers a synergy of approved drugs targeting the androgen receptor”*, (submitted)

M. P. L. designed and performed the combinatorial screen, analyzed screening data, performed all validation experiments and wrote the manuscript; **P. M.** designed and assembled the CLOUD library, **F. K.** assembled the library and contributed to the combinatorial screen; **C.-H. L.** assisted with the combinatorial screen; **G. D.** and **J. C.** performed DIPS score analysis; **V. I.** synthesized, provided and quality controlled the vast majority of CLOUD drugs; **S. K.** designed the CLOUD and wrote the manuscript.

TABLE OF CONTENTS

ACKNOWLEDGMENTS.....	v
DECLARATION.....	vii
TABLE OF CONTENTS.....	ix
ABSTRACT	x
ZUSAMMENFASSUNG	xii
ABBREVIATIONS	xiv
INTRODUCTION	1
Cancer: an evolving molecular circuitry	1
Cancer treatment	3
Surgery, radiation and chemotherapy	3
Oncogene addiction and targeted therapies	3
Non-oncogene addiction and synthetic lethality	5
Hurdles in cancer therapy	8
Intra- and intertumor heterogeneity	9
Mechanisms of resistance	13
Approaches to precision cancer medicine	16
RNAi-based loss-of-function screens	17
Multicomponent therapeutics	22
AIMS.....	26
RESULTS	27
NOTCH1 activation in breast cancer confers sensitivity to inhibition of SUMOylation.....	27
A combinatorial screen of the CLOUD uncovers a synergy of approved drugs targeting the androgen receptor	39
DISCUSSION.....	107
Targeting NOTCH1 breast cancer through inhibition of SUMOylation.....	108
A combination of approved drugs addressing resistance to flutamide in T877A AR prostate cancer	112
Conclusion & future prospects	116
REFERENCES.....	117
CURRICULUM VITAE.....	133

ABSTRACT

Recent developments in sequencing technologies and the establishment of systems biology approaches have unraveled the intricate genetic heterogeneity and complexity of cancer. Aberrations in both coding and non-coding regions of the genome, as well as altered epigenetic mechanisms, contribute to the rise of malignant neoplasms evolving according to Darwinian selection. Between the end of the 20th and the beginning of the 21st century, researches have described a broad range of key genes driving the tumorigenic process and involved in the maintenance of cancer. These important discoveries have fostered the development of the first targeted drugs, more specific pharmacological treatments compared to classical chemotherapeutics. Even though remarkable improvements have been witnessed with the advent of these molecules, therapeutic regimens fail, tumors relapse, drug development hobbles behind inefficient discovery pipelines and a large number of patients succumb to cancer or anticancer treatments. As we see it nowadays, cancer is an extremely heterogeneous disease not only among different patients but also within the same tumor. This large genetic diversity and intrinsic complexity has encouraged more stratified approaches and the development of precision cancer medicine. Here, we made use of technologies for the discovery of new cancer targets and the development of rationalized treatments in line with the concept of personalized cancer therapy. We have performed an RNA interference (RNAi)-based loss-of-function screen in a model depicting the heterogeneity of breast tumors and discovered a specific vulnerability of NOTCH1-activated breast cancer to inhibition of SUMOylation. We show that activation of NOTCH1 signaling in both isogenic and patient-derived breast cancer cells depletes unconjugated SUMO conferring sensitivity to SUMOylation inhibitors. Our observations indicate the SUMOylation cascade as a candidate cancer target and disclose a therapeutic potential for inhibitors of the SUMOylation cascade in the context of NOTCH1-activated breast tumors. The cellular circuitry of cancer cells is a redundant network evolving in response to cues from the environment. This intrinsic plasticity provides tumors with the ability of easily escaping therapies based on single drugs. Multicomponent therapeutics is regarded as another promising approach to the complexity of malignant neoplasms. In particular, combinations of approved drugs represent convenient alternatives as these chemically optimized entities have already been profiled in respect

to their pharmacokinetic and pharmacodynamic parameters. We have designed a non-redundant library of FDA-approved small molecules, the CeMM Library of Unique Drugs (CLOUD), and performed a pairwise combinatorial screen at physiologically relevant concentrations. This phenotypic screen has revealed a synergistic interaction between flutamide and phenprocoumon (PPC) impairing the growth of prostate cancer cells. We show that the combination interferes with the stability of the androgen receptor (AR) eventually leading to apoptosis. Interestingly, the combination reverts resistance of mutated AR to flutamide. Collectively, our data show that PPC could be repurposed in combination with flutamide for the treatment of prostate cancers harboring AR mutations such as T877A. Together, our approaches have expanded the spectrum of cancer targets and therapeutic possibilities as we need for truly personalized cancer medicine.

ZUSAMMENFASSUNG

Durchbrüche in den Sequenzierungstechnologien und die Etablierung der Systembiologie haben die komplexe genetische Heterogenität von Krebserkrankungen aufgezeigt. Aberrationen sowohl in codierenden und nicht-codierenden Regionen des Genoms sowie epigenetische Veränderungen tragen zur Entstehung der malignen Neoplasien und ihrer Ausbreitung nach Darwinistischer Selektion bei. Am Ende des 20. und Beginn des 21. Jahrhunderts haben Forscher eine breite Palette von Schlüsselgenen, die die Tumorigenese antreiben, beschrieben. Diese wichtigen Erkenntnisse haben die Entwicklung der ersten zielgerichteten Medikamenten gefördert, welche eine spezifischere pharmakologische Behandlung im Vergleich zu klassischen Chemotherapeutika ermöglichen. Obwohl diese Moleküle zu bemerkenswerten Verbesserungen geführt haben, sind das Versagen von Therapieschemata, die hohen Rezidivraten und die langsame ineffiziente Entwicklung neuer Wirkstoffe der Grund für die noch immer sehr hohe Mortalität von Krebserkrankungen. Heute wird Krebs als eine äußerst heterogene Erkrankung angesehen, nicht nur zwischen den verschiedenen Patienten sondern auch innerhalb des gleichen Tumors. Diese große genetische Vielfalt und inhärente Komplexität der Tumoren hat zur Forcierung von Patientenstratifikation und der Entwicklung des Konzepts der personalisierten Medizin geführt. In dieser Dissertation beschreibe ich unsere technologischen Ansätze neue therapeutische Targets für onkologische Erkrankungen zu finden und rational molekular begründete Therapien im Sinne einer personalisierten Medizin vorzuschlagen. In einem RNA-Interferenz (RNAi)-basierten Screening Modell, welches die Heterogenität von Brustkrebs nachahmt, haben wir die spezifische Sensitivität von NOTCH1-aktivierten Brustkrebszellen auf eine Hemmung der SUMOylierung entdeckt. Wir zeigen, dass die Aktivierung der NOTCH1 Signaltransduktion sowohl in isogenen als auch in patientenspezifischen Brustkrebszellen den Pool an unkonjugiertem SUMO reduziert und diese Zellen für Inhibitoren der SUMOylierung empfindlich macht. Unsere Beobachtungen identifizieren die SUMOylierungskaskade als potentielleres Krebstarget und offenbaren ein therapeutisches Potenzial für SUMO Inhibitoren im Kontext von NOTCH1-aktiviertem Brustkrebs. Die zellulären Prozesse von Krebszellen bilden ein redundantes Netzwerk, das in Reaktion auf Signale aus der Umwelt eine evolutionäre Entwicklung durchmacht. Diese intrinsische Plastizität verleiht Tumoren die Fähigkeit,

Resistenzen gegen Monotherapien zu entwickeln. Mehrkomponenten-Therapeutika werden daher als ein vielversprechender Ansatz angesehen, der Komplexität von malignen Neoplasmen zu begegnen. Insbesondere Kombinationen von zugelassenen Medikamenten stellen interessante Optionen dar, da diese chemisch optimierten Substanzen bereits in Bezug auf ihre pharmakokinetischen und pharmakodynamischen Parameter optimiert wurden. Wir haben eine nicht-redundante Bibliothek von der FDA-zugelassenen niedermolekularen Wirkstoffen, die CeMM Library of Unique Drugs (CLOUD), entwickelt und systematisch die Effekte paarweiser Kombination bei physiologisch relevanten Konzentrationen auf die Viabilität von Krebszellen getestet. Dieser phänotypische Screen hat eine synergistische Wechselwirkung zwischen Flutamid und Phenprocoumon (PPC) ergeben, die das Wachstum von Prostatakrebszellen beeinträchtigt. Wir zeigen, dass die Kombination die Stabilität des Androgen Rezeptors (AR) reduziert und schließlich zur Apoptose führt. Interessanterweise stellt diese Kombination die Sensibilität von Zellen mit mutiertem AR auf Flutamid wieder her. Insgesamt zeigen unsere Daten, dass PPC in Kombination mit Flutamid zur Behandlung von Prostatakrebs mit AR Mutationen wie T877A neuplatziert werden könnte. Zusammenfassend haben unsere Ansätze das Spektrum der Krebstargets und therapeutischen Möglichkeiten erweitert, was ein wichtiges Ziel für eine wirklich personalisierte Krebsmedizin ist.

ABBREVIATIONS

5-HT1A	5-hydroxytryptamine (serotonin) receptor 1A, G protein-coupled
5-HT1B	5-hydroxytryptamine (serotonin) receptor 1B, G protein-coupled
5-HT1D	5-hydroxytryptamine (serotonin) receptor 1D, G protein-coupled
5-HT1F	5-hydroxytryptamine (serotonin) receptor 1F, G protein-coupled
5-HT4	5-hydroxytryptamine (serotonin) receptor 4, G protein-coupled
ABC	ATP-binding cassette
ABL	Abelson proto-oncogene
AGO2	Argonaute RISC catalytic component 2
AKT1	v-akt murine thymoma viral oncogene homolog 1
AKT2	v-akt murine thymoma viral oncogene homolog 2
ALK	Anaplastic lymphoma receptor tyrosine kinase
ALL	Acute lymphoblastic leukemia
ALT	Alternative lengthening of telomeres
AML	Acute myeloid leukemia
AR	Androgen receptor
AR45	Androgen receptor 45 (isoform 2)
ARE	Androgen responsive elements
ARID1A	AT rich interactive domain 1A
ARID1B	AT rich interactive domain 1B
ARID2	AT rich interactive domain 2
ASXL1	Additional sex combs like transcriptional regulator 1
ATP	Adenosine triphosphate
AURKB	Aurora kinase B
BCR	Breakpoint cluster region
BRAF	B-Raf proto-oncogene, serine/threonine kinase
BRCA1	Breast cancer 1, early onset
BRCA2	Breast cancer 2, early onset
CARD11	Caspase recruitment domain family, member 11
CCND1	Cyclin D1
CDK1	Cyclin-dependent kinase 1
CDK2	Cyclin-dependent kinase 2
cDNA	Complementary DNA
CETSA	Cellular thermal shift
CGAN	Cancer Genome Atlas Network
CLOUD	CeMM Library of Unique Drugs
CMap	Connectivity Map
CML	Chronic myeloid leukemia
CRC	Colorectal cancer
CRPC	Castration-resistant prostate cancer
CYP17	Cytochrome P450, family 17
DAPI	4',6-diamidino-2-phenylindole
DAPT	N-[N-(3,5-Difluorophenacetyl)-L-alanyl]-S-phenylglycine t-butyl ester
DCIS	Ductal carcinoma in situ
DGCR8	DiGeorge syndrome critical region gene 8
DHT	Dihydrotestosterone

DIPS	Drug-induced gene expression profile similarity
DLBCL	Diffuse large B-cell lymphoma
DMSO	Dimethyl sulfoxide
DNA	Deoxyribonucleic acid
down	Downstream
dsRNA	Double-stranded RNA
ECFP	Extended Connectivity Fingerprints
EGFR	Epidermal growth factor receptor
EML4	Echinoderm microtubule associated protein like 4
EMT	Epithelial-mesenchymal transition
ER	Estrogen receptor
ERBB2	Erb-b2 receptor tyrosine kinase 2
FDA	Food and Drug Administration
flank	Flanking
FOXA1	Forkhead box A1
FPKM	Fragments per kilobase of exon per million fragments mapped
FW	Forward
GA	Ginkgolic acid
GAPDH	Glyceraldehyde-3-phosphate dehydrogenase
GATA3	GATA binding protein 3
GGCX	Gamma-glutamyl carboxylase
GIST	Gastrointestinal stromal tumor
GO	Gene Ontology
GPCR	G protein-coupled receptor
GRB7	Growth factor receptor-bound protein 7
GSI	Gamma-secretase inhibitor
HA	Hemagglutinin
HER2	Human epidermal growth factor receptor 2
HES1	Hairy and enhancer of split 1
HEY1	Hairy and enhancer of split related with YRPW motif 1
HIV	Human immunodeficiency virus
hPGK	Human phosphoglycerate kinase
HRAS	Harvey rat sarcoma viral oncogene homolog
HSP90	Heat shock protein 90
HTS	High-throughput screening
ICN1	Intracellular domain of NOTCH1
IDC NOS	Invasive ductal carcinoma, not otherwise specified
IKBKE	Inhibitor of kappa light polypeptide gene enhancer in B-cells, kinase epsilon
ILC	Invasive lobular carcinoma
KIT	v-kit Hardy-Zuckerman 4 feline sarcoma viral oncogene homolog
KLK2	Kallikrein-related peptidase 2
KLK3	Kallikrein-related peptidase 3
KO	Knockout
KRAS	Kirsten rat sarcoma viral oncogene homolog
lncRNA	Long non-coding RNA
LYN	LYN proto-oncogene, Src family tyrosine kinase
MAD	Median absolute deviation
MAML1	Mastermind-like 1
MAP3K1	Mitogen-activated protein kinase kinase kinase 1

MAP3K13	Mitogen-activated protein kinase kinase kinase 13
MDR	Multidrug resistance
MDR1	Multidrug resistance protein 1
MEK	Mitogen extracellular signal-regulated kinase
MIR10B	microRNA 10b
miRNA	microRNA
miRs	microRNA
MIT	Massachusetts Institute of Technology
MLL2	Mixed-lineage leukemia 2
MLL3	Mixed-lineage leukemia 3
MRM	Multiple reaction monitoring
mRNA	Messenger RNA
MTOR	Mechanistic target of rapamycin
MYC	v-myc avian myelocytomatosis viral oncogene homolog
NCGC	NIH Chemical Genomics Consortium
NCOR1	Nuclear receptor corepressor 1
NEU	Neuro/glioblastoma derived oncogene homolog
NF- κ B	Nuclear factor of kappa light polypeptide gene enhancer in B-cells
NME	New molecular entity
NOA	Non-oncogene addiction
NPC	Nuclear pore complex
NSCLC	Non-small cell lung cancer
PARP1	Poly (ADP-ribose) polymerase 1
PBP	Penicillin binding protein
PBS	Phosphate buffered saline
PCR	Polymerase chain reaction
PDGFR	Platelet-derived growth factor receptor
PIK3CA	Phosphatidylinositol-4,5-bisphosphate 3-kinase, catalytic subunit alpha
PKR	Protein kinase RNA-activated
PLK1	Polo-like kinase 1
PPC	Phenprocoumon
PR	Progesterone receptor
pre-miRNA	Precursor microRNA
pri-miRNA	Primary microRNA
PSA	Prostate specific antigen
PTEN	Phosphatase and tensin homolog
RB1	Retinoblastoma 1
RBPJ	Recombination signal binding protein for immunoglobulin kappa J region
RHOC	Ras homolog family member C
RIPA	Radioimmunoprecipitation assay
RISC	RNA-induced silencing complex
RNA	Ribonucleic acid
RNAi	RNA interference
RNA-seq	RNA sequencing
RT-qPCR	Reverse transcription quantitative PCR
RV	Reverse
SAE1	SUMO1 activating enzyme subunit 1
SETD2	SET domain containing 2
shRNA	Short hairpin RNA

siRNA	Small interfering RNA
SLC	Solute carrier
SLC39A6	Solute carrier family 39 member 6
SMAD4	SMAD family member 4
SMARCD1	SWI/SNF related, matrix associated, actin dependent regulator of chromatin, subfamily d, member 1
SMS	SUMOylation-dependent MYC switchers
STEAM	Systemic small molecule
Strep	Streptavidin
SUMO	Small ubiquitin-like modifier
SWI/SNF	Switch/Sucrose Non Fermentable
T-ALL	T-cell acute lymphoblastic leukemia
TARBP2	TAR (HIV-1) RNA binding protein 2
TBL1XR1	Transducin (beta)-like 1 X-linked receptor 1
TERT	Telomerase reverse transcriptase
TFF3	Trefoil factor 3
TKI	Tyrosine kinase inhibitor
TMPRSS2	Transmembrane protease, serine 2
TNBC	Triple negative breast cancer
TNRC6A	Trinucleotide repeat containing 6A
TP53	Tumor protein p53
TRC	The RNAi Consortium
TUB	Tubulin
UBA2	Ubiquitin-like modifier activating enzyme 2
UBC9	Ubiquitin conjugating enzyme 9
UBE2I	Ubiquitin-conjugating enzyme E2I
UPLC/MS	Ultra-performance liquid chromatography/Mass spectrometry
VEGF	Vascular endothelial growth factor
VKORC1	Vitamin K epoxide reductase complex, subunit 1
WB	Western blotting
XBP1	X-box binding protein 1
XPO1	Exportin 1
XPO5	Exportin 5
ZNF217	Zinc finger protein 217

INTRODUCTION

Cancer: an evolving molecular circuitry

The accumulation of genetic and epigenetic alterations may lead to uncontrolled cellular proliferation, a pathological condition commonly known as cancer. With around 40,000 new cases diagnosed every year, cancer is the second most common cause of death in Austria (WHOROE, 2012). In humans, cancers of the prostate (among men), breast (among women), lung and colorectum are the most frequent (WHOECO, 2012). Brain cancers and leukemias are the leading cause of cancer deaths among younger patients while lung cancer ranks first among adult men. Lung and breast cancer lead among women (WHOECO, 2012).

According to a number of studies, less than ten genetic events including point mutations, deletions, insertions, duplications or chromosomal translocations are required for the transformation of a cell and the development of a malignant tumor or neoplasm (Armitage & Doll, 1954; Hornsby et al, 2007; Renan, 1993). Aberrations of the genome predisposing to malignant transformations may be inherited but these events have been found to contribute to only 5-10% of all cancers (Fearon, 1997; Lichtenstein et al, 2000; Tomasetti & Vogelstein, 2015). The vast majority of cancer-causing genetic lesions are somatically acquired through exposure of the genome to mutagens such as chemicals, ionizing radiations, non-ionizing ultraviolet radiations and oncogenic viruses (Stratton et al, 2009). Some of these mutations are considered to play crucial roles in the tumorigenic event and are thus called “driver mutations” while others tend to accumulate at later stages and contribute only marginally to the development of a tumor (Stratton, 2011). The transformation of a cell into a cancer cell implies a series of new attributes related to cellular growth, mobility and the interaction with the tumor microenvironment (Figure 1). These traits have been referred to as hallmarks of cancer (Hanahan & Weinberg, 2000; Hanahan & Weinberg, 2011) and are commonly observed in virtually all neoplastic lesions. Malignant cells sustain their proliferation through gain-of-function mutations or the overexpression of oncogenes and evade growth inhibitors through loss-of-function mutations or the downregulation of tumor suppressors (Davies & Samuels, 2010; Yuan & Cantley, 2008). Similar mechanisms lay the fundamental molecular circuits for another hallmark of cancer: the ability to avoid

programmed cell death through apoptosis (Adams & Cory, 2007). The expression of the telomerase reverse transcriptase TERT or the activation of the Alternative Lengthening of Telomeres (ALT) provides cancer cells with unlimited replicative potential and the possibility to generate a substantial tumor mass (Flynn et al, 2015). Expanding solid tumors require oxygen and nutrients and thus release angiogenic signals inducing the sprouting of new blood vessels (Hanahan & Folkman, 1996). Cancer cells exploit newly formed capillaries not only to sustain their growth but also to disseminate to other tissues and give rise to secondary tumors or metastases (Fidler, 2011).

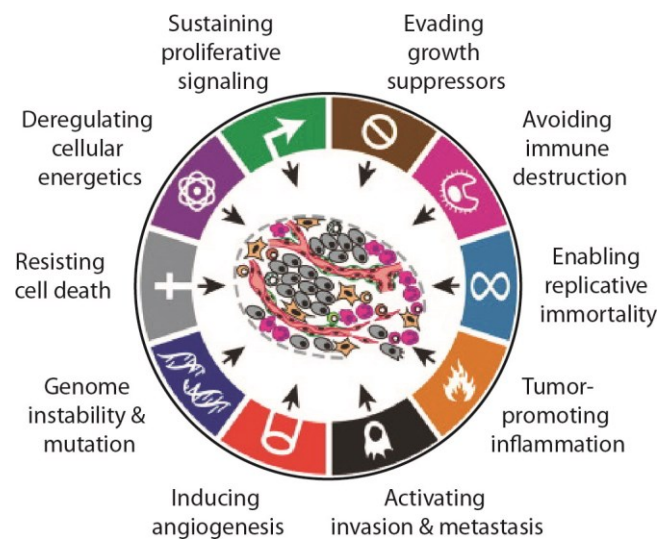


Figure 1. Hallmarks of cancer (adapted from Hanahan & Weinberg, 2011).

More recently, genome instability, deregulated cellular energetics and the ability to induce inflammation and avoid destruction by the immune system have been annotated as emerging hallmarks (Luo et al, 2009). Cancer cells experience genomic events giving rise to such hallmarks over time, in a multistep process that shares many analogies with Darwinian evolution (Greaves & Maley, 2012; Nowell, 1976). Once a cell has rewired its functional networks to achieve at least some of these traits it starts expanding in an uncontrolled manner generating a primary lesion. Secondary tumors usually arise at later stages of the disease. Primary tumors and metastases affect the correct functionality of organs, deprive the organism of essential capabilities and eventually lead to death.

Cancer treatment

Surgery, radiation and chemotherapy

Even though cancer death rates have decreased over the last twenty years (Siegel et al, 2013), treatment rarely results in complete disease remission. Surgical removal of the tumor mass is the most successful alternative for some confined solid cancers. However, surgery is invasive, efficient only at early stages of tumor development and particularly arduous for specific tissues. Two other mainstay cancer therapeutic approaches, radiation and chemotherapy, target the increased sensitivity of fast proliferating cells to DNA damage (Chabner & Roberts, 2005; Delaney et al, 2005). These strategies permit treatment of a broader variety of tumors but suffer from a significant number of side effects as some healthy tissues are also affected, particularly in the case of the systemically acting chemotherapy (Siegel et al, 2012). Although these alternatives have been used to successfully treat some forms of leukemias (Freedman, 2014; Nastoupil et al, 2012), their application to other cancers such as brain tumors has been rather disappointing (Rampling et al, 2004). Moreover, patients often develop resistance to multiple anticancer drugs (Brockman, 1963).

Oncogene addiction and targeted therapies

More recent approaches have tried to exploit alternative routes to treat cancer, targeting more specific traits of malignant cells. Studies of cancer genomes have revealed a number of genes contributing to the tumorigenic process and often essential for the maintenance of the malignant state (Futreal et al, 2004). Tumors tend to develop “oncogene addictions” becoming physiologically dependent on the activating mutation or overexpression of distinct proteins (Weinstein, 2002). For example, it has been shown that the overexpression of MYC in transgenic mice induces T-cell lymphomas and acute myeloid leukemia (AML) which regresses upon MYC withdrawal (Felsher & Bishop, 1999). Similar addictions to genes such as *HRAS* and the *BCR-ABL* fusion gene have been reported in mouse models developing, respectively, melanoma or leukemia upon oncogene overexpression (Chin et al, 1999; Huettner et al, 2000). Accordingly, tumor regression was observed upon downregulation of these genes. The idea that proteins sustaining these addictive mechanisms could be addressed using small molecule inhibitors led to the development of the first so-called targeted therapies

(Martini et al, 2011). Imatinib (Gleevec®), an ATP-competitive tyrosine kinase inhibitor (TKI) targeting ABL, was the first small molecule to be approved for the targeted treatment of chronic myeloid leukemia (CML) in patients harboring the Philadelphia chromosome derived from a t(9;22) translocation (Druker et al, 1996). Detailed target profiling of imatinib revealed also KIT and PDGFR among the inhibited tyrosine kinases and led to the approval of the same molecule for the treatment of advanced gastrointestinal stromal tumors (GIST) carrying KIT and PDGFR activating mutations (Croom & Perry, 2003). More recently, crizotinib (Xalkori®), a TKI targeting the kinase activity of ALK (Kwak et al, 2010), has been approved for the treatment of non-small cell lung cancer (NSCLC) harbouring the *EML4-ALK* fusion gene while the serine/threonine kinase inhibitor vemurafenib (Zelboraf®) has been developed to selectively target the V600E mutated BRAF protein and is currently used in the clinic for the treatment of melanoma (Flaherty et al, 2010). Targeted therapies rely not only on small molecule inhibitors hindering the enzymatic activity of oncogenes. The amplification and/or overexpression of HER2 (also known as NEU or ERBB2) in breast cancer can be targeted by the humanized murine monoclonal antibodies trastuzumab (Herceptin®) and pertuzumab (Perjeta®), directed against the extracellular domain of the transmembrane receptor (Nahta et al, 2004). Trastuzumab treatment has showed promising results also in combination with lapatinib (Tykerb®), a TKI targeting both HER2 and EGFR, for the treatment of HER2⁺ breast cancer (de Azambuja et al, 2014; Scaltriti et al, 2015). Cetuximab (Erbix®) and panitumumab (Vectibix®) are monoclonal antibodies targeting the EGFR. The improvement in response rate as well as the overall survival benefit observed in clinical settings has led to their approval for the treatment of colorectal cancer (CRC) (Di Nicolantonio et al, 2008).

One of the major limitations of targeted therapies is that cancer targets do not always present pockets that can easily accommodate chemical compounds (i.e. they are not always “druggable”). Moreover, cancers arise not only from the overexpression or activation of oncogenes but also from the deletion or inactivation of tumor suppressors. In the latter case, tumors become hypersensitive to the growth-inhibitory activity of such genes which are pharmacologically more challenging to restore. An alternative way that could address these more complicated instances would be to target other proteins which are not directly responsible for the malignant transformation of cancer cells but become necessary because of this transformation (Hartwell et al, 1997; Kaelin, 2009).

This new acquired essentiality may arise from intrinsic genetic or epigenetic changes of the cancer cells as well as from extrinsic alterations of the tumor microenvironment (Luo et al, 2009). Such an approach would have the important advantage of expanding the range of possible cancer targets while sparing at the same time cells with a normal genome and epigenome. In accordance with the previously described “oncogene addiction”, this alternative approach has been commonly referred to as “non-oncogene addiction” (NOA) or synthetic lethality.

Non-oncogene addiction and synthetic lethality

The concept of synthetic lethality has been originally described in 1922 by Charles Bridge (Bridges, 1922). His genetic experiments in *Drosophila melanogaster* showed that mutations occurring simultaneously in two distinct genes could result in cellular death even though disruption of one or the other gene alone would have been compatible with viability. It was, however, Theodore Dobzhansky that used the expression “synthetic lethality” for the first time referring to a similar phenomenon observed in *Drosophila pseudoobscura* (Dobzhansky, 1946). Lethality arising from the combination of two different entities (e.g. two mutated genes) is said to be synthetic in agreement with the original meaning of the ancient Greek word *σύνθεσις* – put together. If such a combination results in impairment of cellular fitness rather than death, the term “synthetic sickness” would be more appropriate (Nijman, 2011). Importantly, synthetic lethality applies to loss-of-function but also to gain-of-function mutations (i.e. a gene might be required to sustain the overexpression of a second gene) (Kaelin, 2005). Moreover, the concept might also be extended from gene-gene interactions to gene-drug or drug-drug interactions. Indeed, synthetic lethality may in principle arise from the combination of any specific cellular event with another and represents an alternative way to target tumor-intrinsic (i.e. within the cancer cell) and tumor-extrinsic (i.e. dependent on stromal or vascular cells) NOAs (Luo et al, 2009). In the ideal case, the pharmacological inactivation of a given gene would affect only the viability of cancer cells harboring already a mutation in another gene while being completely harmless to normal cells (Figure 2). However, scenarios where the cancer mutation simply shifts the response to the pharmacological intervention producing a therapeutic window are also likely (Kaelin, 2005).

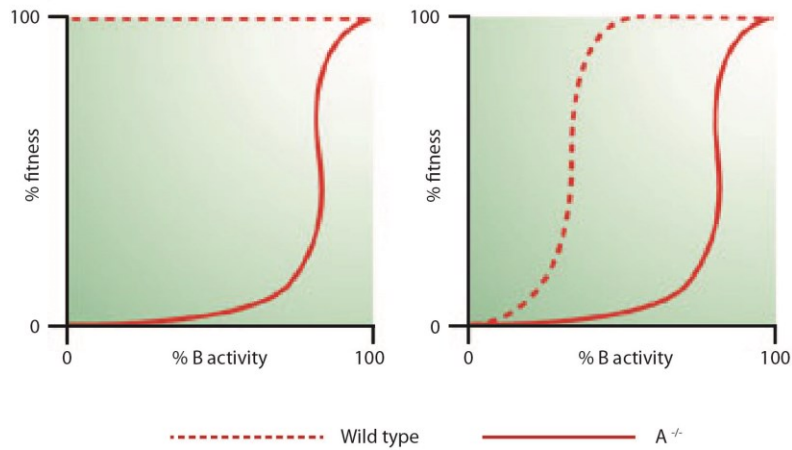


Figure 2. Synthetic lethality scenarios. In the ideal case the pharmacological inhibition of gene B impairs the fitness only in a gene A knockout, leaving the wild type unaffected (left panel). Otherwise inhibition of B can also create a therapeutic window shaping the curve of both wild type and knockout (right panel) (adapted from Kaelin, 2005).

Synthetic lethal interactions occur because of the complex and often redundant homeostatic machine regulating cellular processes (Hartman et al, 2001; Masel & Siegal, 2009). Accordingly, interactions involving loss-of-function mutations can sometimes be predicted based on protein activity. They might occur among functionally redundant genes (e.g. protein paralogs), subunits of the same protein complex, and important nodes of the same or convergent signaling pathways (Costanzo et al, 2010). For example, knockdown of genes related to mitotic spindle formation has been found to reduce the viability of NSCLC cells to otherwise sublethal concentrations of the mitotic inhibitor paclitaxel (Taxol®) (Whitehurst et al, 2007). Cellular co-localization, temporary physical interactions and co-expression might also hint at NOAs (Kaelin, 2005) while “capacitors” such as chromatin-related proteins or chaperons, which are able to buffer different genetic alterations, represent widespread hubs enriched in synthetic lethal partners (Costanzo et al, 2010; Lehner et al, 2006; Nijman & Friend, 2013; Rutherford & Lindquist, 1998). Chromatin modifying enzymes, in particular, have not been thoroughly addressed so far in the context of synthetic lethality and represent a pool of potential new drug targets yet to be investigated (Johnson & Dent, 2013; Mair et al, 2014).

Even though a comprehensive human genetic interaction network has not been assembled yet, synthetic lethal interactions involving cancer-causing genetic lesions have been described in humans. For example, the transcription factor MYC lacking an

ideal small molecule binding pocket has always been considered, at least so far, one of the most “undruggable” oncogenes. Nevertheless, different reports have described its synthetic lethal interaction with CDK1 and CDK2 inhibitors (Goga et al, 2007; Molenaar et al, 2009). In a similar way, exacerbation of or sensitization to various forms of stress experienced by cancer cells might also be regarded as a form of NOA that can be exploited through a synthetic lethal key (Luo et al, 2009). Tumor cells continuously face stress intrinsically related to DNA damage and replication, cell division, protein homeostasis and metabolism. Drug treatments that would intensify these forms of stress or make cancer cells more vulnerable to stress overload represent, ideally, valid therapeutic approaches. In this regard, inhibitors of the AURKB and PLK1 mitotic kinases have been tested in clinical trials (Carpinelli & Moll, 2008; Strebhardt & Ullrich, 2006) while increased proteotoxic stress might explain the efficacy of geldanamycin, an HSP90 inhibitor, and the proteasome inhibitor bortezomib (Velcade®) in the treatment of different forms of cancer (Richardson et al, 2006; Whitesell & Lindquist, 2005). Certainly, the sensitivity of breast and ovarian cancers harboring mutations in the *BRCA1* and *BRCA2* genes to PARP1 inhibitors such as the FDA-approved olaparib (Lynparza®) represents to date the most emblematic application of the synthetic lethality concept for the treatment of cancer (Bryant et al, 2005; Farmer et al, 2005a; Fong et al, 2009). In this example, impairment of double-strand breaks repair by homologous recombination mediated by *BRCA1* and *BRCA2* genes translates into dependence on another DNA damage response, the base-excision repair mechanism mediated by PARP1. Clearly, NOAs can also be extrinsic especially in the case of solid tumors establishing important interactions with the surrounding microenvironment. The anti-angiogenic antibody bevacizumab (Avastin®) targeting the vascular endothelial growth factor (VEGF) is the best example of cancer therapeutics targeting an extrinsic NOA (Ferrara et al, 2004).

Some NOA-based therapies have been successfully translated to the clinic but this repertoire is still very limited. The lack of a comprehensive genetic interaction map in human cells and cancer cells accounts for such a restricted range of therapeutically relevant synthetic lethalities. Initially, it was hypothesized that the genetic interaction network of mammalian cells could be extrapolated, at least in part, from genetic knockout experiments performed in model organisms (Tischler et al, 2008). The budding yeast *Saccharomyces cerevisiae*, for example, has been used for extensive

synthetic lethality studies. Boone and colleagues have reported around 80% of *Saccharomyces cerevisiae* genes not to be essential and that synthetic lethal interactions in this organism may account to up to 10 per gene (Tong et al, 2001; Tong et al, 2004). These numbers illustrate the genetic robustness of living organisms and their redundant homeostatic abilities. However, genetic interactions are poorly conserved hindering the application of prediction algorithms based on yeast genetic networks to higher organisms. Large-scale studies have shown, for instance, that the extent of yeast genetic interactions conserved in *Caenorhabditis elegans* amounts to less than 1% (Byrne et al, 2007; Tischler et al, 2008). These values are in stark contrast with the number of yeast essential genes that have been found to have an essential orthologue in *Caenorhabditis elegans* (61%) and protein-protein interactions conserved between these two organisms (31%) (Matthews et al, 2001; Tischler et al, 2006). Importantly, these differences do not correlate either with an overall decrease of synthetic interactions or with an increase in redundancy (Tischler et al, 2008). A potential explanation might be given by the “induced essentiality” model according to which synthetic lethalties originate from rewiring of the cellular circuitry following a first genetic event. Even though genes and protein functions might be conserved, cellular network rearrangements are not and, consequently, similar genetic events might induce different essentialities in different organisms (Tischler et al, 2008). In addition, many oncogenes and tumor suppressors involved in the development of human cancer do not have an orthologue in yeast. Therefore, synthetic lethal interactions in higher organisms have to be investigated and validated through experimental approaches using appropriate models.

Hurdles in cancer therapy

The establishment of targeted therapies over the last 15 years has changed and improved the therapeutic arsenal against cancer. However, in spite of recent insights into the biology of malignant transformation and more efficient therapeutic treatments, cancer remains a deadly disease especially at more advanced metastatic stages. Response to therapy varies greatly among patients carrying neoplasms affecting the same tissue and even after initial remission tumors often relapse. Research has just started elucidating the reasons behind failure of cancer therapy. Two strictly correlated

intrinsic features of cancer have emerged as main hurdles in the treatment of this complex disease.

Intra- and intertumor heterogeneity

According to the clonal evolution theory, neoplasms arise from a number of genetic and epigenetic alterations accumulating in a single cell, which then acquires hallmarks of sustained growth and inhibited apoptosis (Greaves & Maley, 2012; Hanahan & Weinberg, 2011; Nowell, 1976). The proliferation of this first tumor core generates the trunk of the cancer phylogenetic tree (Campbell et al, 2008). Genomic instability and selective pressures induce additional aberrations creating subclones branching out of the trunk, accumulating more mutations, branching out further and eventually competing with one another for space and nutrients in the tumor niche (Navin et al, 2011). Usually, one of the subclones dominates and constitutes the bulk of the tumor mass. The concomitant presence of genetically distinct clones accounts for the broad intratumor heterogeneity observed in recent genome-wide multiregion tumor sequencing studies (Gerlinger et al, 2012; Mullighan et al, 2008; Wang et al, 2014). Intratumor as well as intertumor (i.e. genetic differences among clinically undistinguishable neoplasms of the same tissue in different patients) heterogeneity has been observed in different cancers. Recent comprehensive genome-wide sequencing, mRNA profiling and copy number variation studies performed on extensive panels of patient-derived breast cancer samples provide an illustrative example (CGAN, 2012; Curtis et al, 2012; Nik-Zainal et al, 2012; Stephens et al, 2012).

Among women, breast cancer is the most common malignant neoplasm observed worldwide with more than 1,300,000 cases and 450,000 deaths per year (CGAN, 2012). Breast cancer commonly arises either in the lobules or in the ducts of the mammary gland (Figure 3). Both lobules and ducts are coated by a layer of luminal epithelial cells (immunohistochemically stained by keratin 8/18) and separated from the surrounding tissue by an external basement membrane (positive for keratin 5/6). A bed of myoepithelial cells belongs between these two structural layers. Cancer cells confined within a milk duct generate a ductal carcinoma in situ (DCIS) often defined as “stage zero” breast cancer. Historically treated with surgery, DCIS is no longer considered an immediate threat to the health of the patient but periodically monitored through mammography (Marshall, 2014). Tumors breaching the basement membrane constitute

the more dangerous invasive carcinomas. The most frequently encountered type of breast cancer is invasive ductal carcinoma, not otherwise specified (IDC NOS, accounting for about 75% of the cases) followed by invasive lobular carcinoma (ILC, 10%) (Li et al, 2005). Other types include: medullary, tubular, neuroendocrine, mucinous (A and B), comedo, apocrine, inflammatory, metaplastic, adenoid cystic and micropapillary breast neoplasms (Li et al, 2005; Weigelt et al, 2010).

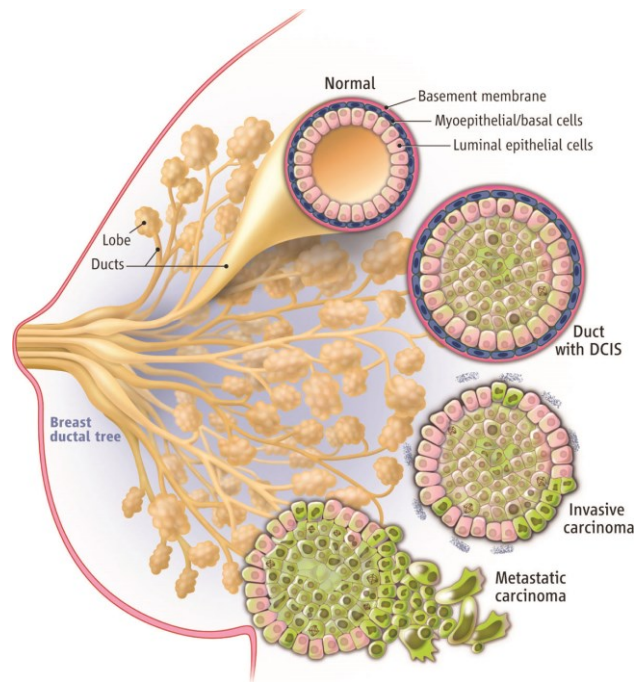


Figure 3. Breast anatomy and schematic illustration of DCIS, invasive and metastatic carcinoma (taken from Marshall, 2014).

A more common classification of breast cancer types, predominantly used in the first decade of targeted therapy, relies on the expression of specific biomarkers. The vast majority of breast tumors expresses the estrogen receptor (ER) and shows dependence on ER signaling. Often, concomitant expression of the progesterone receptor (PR) is observed (Maxmen, 2012). These breast cancers are usually treated with antiestrogens (i.e. endocrine therapy) such as tamoxifen (Nolvadex®) and are generally associated with better prognosis (Jordan & Brodie, 2007). The amplification of the HER2 receptor has been observed in around 25% of the cases and defines a more aggressive type of breast cancer for which therapeutic alternatives include the monoclonal antibodies trastuzumab and pertuzumab or the TKI lapatinib (Martini et al, 2011; Maxmen, 2012;

Ocana & Pandiella, 2008). These targeted treatments are often used in combination with one another or with other chemotherapeutics. Expression of these three markers in the same tumor has also been observed while breast cancers where no expression of ER, PR and HER2 can be detected represent another important class defined as triple negative breast cancer (TNBC)(Bertos & Park, 2011). Chemotherapy is the only available treatment for these tumors associated with the worst prognosis. Stratification of breast cancer patients according to this classification has supported the development of first targeted therapies directed against tumors of the mammary gland. However, more recent analyses have shown that breast cancer is a far more genetically heterogeneous disease providing an explanation for the nevertheless frequent cases of therapy failure (CGAN, 2012; Stephens et al, 2012).

An alternative classification of breast neoplasms proposed by Perou and colleagues defines three breast cancer portraits according to gene expression profiles (Perou et al, 2000). The basal-like subtype shows expression of genes typical of basal epithelial cells such as keratin 5, integrin- β 4 and laminin and broadly corresponds to TNBC; the HER2⁺ subtype where high levels of the tyrosine kinase receptor (and other genes included in the same amplicon such as *GRB7*) and low levels of the ER are observed; and the ER⁺/luminal subtype which has been subsequently further divided in three distinct molecular portraits namely ER⁺/luminal subtype A, with the highest expression of ER, GATA3, XBP1, TFF3 and SLC39A6, and ER⁺/luminal subtypes B and C with lower expression of ER and other luminal-specific genes (Sorlie et al, 2001). While expression of specific markers may lead to the conclusion that these subtypes originate from distinct differentiated cells of the milk duct, comparison of gene expression profiles suggests they arise rather from various stages of mammary epithelial differentiation (Prat & Perou, 2009). Basal-like and HER2⁺ tumors resemble early and late luminal progenitors, respectively, while luminal breast cancers seem to be closely related to differentiated luminal cells. Two other molecular subtypes have also been reported among the ER⁻ breast cancers using similar approaches: the claudin-low subtype shows stem cell features and an epithelial to mesenchymal transition (EMT) signature; the apocrine class displays instead HER2 and AR expression (Farmer et al, 2005b; Hennessy et al, 2009). These distinct groups correlate with clinical outcome and claudin-low, basal-like, HER2⁺ and ER⁺/luminal subtype C are indicative of a poorer prognosis. However, combinations of subtypes are also observed in breast cancer and such

classifications cannot precisely define the much broader genetic heterogeneity observed across patients (Bertos & Park, 2011).

The establishment of next-generation sequencing approaches has significantly improved cancer genetic analyses, has showed that malignant neoplasms frequently carry hundreds to thousands of passenger mutations and has highlighted the causative role of a vast collection of drivers in the context of cancers such as the one of the breast. Recent studies have extended our knowledge about cancer etiology and clarified that breast (but also other types of) neoplasms are a collection of molecularly distinct diseases rather than a pathological condition that can always be treated with the same drug (Figure 4).

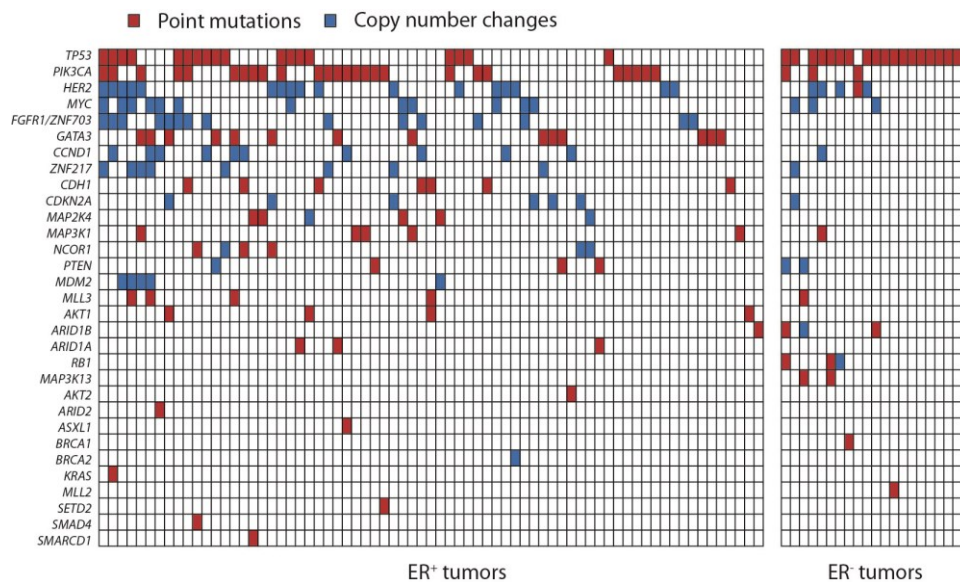


Figure 4. Mutational landscape of 92 breast tumors. Point mutations and copy number changes in breast cancer drivers are indicated in red and blue respectively (data taken from Stephens et al, 2012).

Mutations involved in breast cancer development have been identified in genes related to PI3K/AKT signaling (such as *PIK3CA*, *AKT1*, *PTEN*) and others such as *GATA3*, *CCND1*, *RB1* and *TP53* (CGAN, 2012; Stephens et al, 2012). Activation of the PI3K/AKT signaling pathway is frequently observed in breast cancer and small molecule inhibitors of MTOR such as everolimus (Afinitor®) have been evaluated for the treatment of advanced breast tumors in combination with exemestane (Aromasin®) (Beck et al, 2014). Whole exome-sequencing and copy number variation analyses performed on patient-derived samples

have expanded the collection of important driver mutations observed in breast tumors to genes observed already in other cancers (e.g. *ARID1A*, *ARID2*, *ASXL1*, *KRAS*, *MLL2*, *MLL3*, *SETD2*, *SMAD4*) or new cancer genes (e.g. *ARID1B*, *AKT2*, *MAP3K1*, *MAP3K13*, *NCOR1*, *SMARCD1*) (Stephens et al, 2012). Of note, different chromatin-related genes have been reported to be mutated in these samples (i.e. *MLL2*, *MLL3* as well as components of the SWI/SNF chromatin remodeling complex such as *SMARCD1* and *ARID1B*) highlighting the important contribution of epigenetics to the tumorigenic process. Interestingly, some of these mutations seem to co-segregate with breast cancer subtypes defined by gene expression profiling (CGAN, 2012). ER⁺/luminal subtype A tumors often show mutations in the *PIK3CA*, *MAP3K1* and *GATA3* genes. Instead, TP53 mutations are more frequent in basal-like and HER2⁺ subtypes. Copy number variations are also observed with focal amplifications of genes such as *HER2*, *PIK3CA*, and *FOXA1* and deletions of *RB1*, *PTEN* and *MLL3*.

These mutational landscapes depicting complex intra- and intertumor heterogeneity explain why response to current drugs varies among patients and fails to eradicate the disease. Importantly, heterogeneity affects also specific targets as different mutations may occur on the same gene conferring resistance to treatment and preventing broad efficacy of cancer therapies among patients. Clearly, there is a need for new and more sophisticated treatments based on accurate patient stratification.

Mechanisms of resistance

Unsuccessful therapeutic regimens are often due to cancer heterogeneity but can also arise because of other complications outside of the tumor (Brockman, 1963). Resistance to treatment represents one of the major hurdles in current cancer therapy and an active field of cancer research (Girotti et al, 2015; Steiner et al, 2006). Primary (or *de novo*) resistance mechanisms arise from intrinsic characteristics of the patient and can be detected prior to treatment. The selective pressure exerted by the pharmacological therapy may also promote secondary resistance mechanisms in patients initially responding to therapy. Both are, however, associated with genetic and/or epigenetic alterations of key targets (Garraway & Janne, 2012; Gottesman, 2002).

Another convenient classification defines targeted-dependent and target-independent mechanisms as intrinsic and extrinsic resistance, respectively (Lamontanara et al, 2013). Kinase inhibitors, the most successful class of cancer targeted therapies over the last

decade, provide different examples of intrinsic resistance mechanisms. Few years after the approval of imatinib, resistance to inhibition of BCR-ABL activity emerged as a shortcoming of the pharmacological treatment of CML. Point mutations in the catalytic domain of ABL were described as the predominant resistance mechanism. In particular, mutations such as T315I affecting the “gatekeeper” residue of the binding pocket (i.e. an amino acid providing crucial interactions and selectivity to binding molecules) abrogated the effect of imatinib (Gorre et al, 2001). A similar “gatekeeper” mutation has been observed also in NSCLC patients resistant to gefitinib (Iressa®) and erlotinib (Tarceva®) treatment. While the T315I mutation disrupts imatinib binding to ABL, the “gatekeeper” T790M EGFR mutant observed in NSCLC patients increases the affinity of the receptor to the endogenous ligand ATP (Yun et al, 2008). Alterations in the binding site have been described also in non-kinase receptors. The T877A mutation, for instance, has been reported to increase the promiscuity of the AR and to confer resistance to antiandrogens therapy in prostate cancer (Veldscholte et al, 1992). More difficult to elucidate is the resistance mediated by amino acids that are distant from the binding site or located outside of the kinase domain. For example, mutations located outside of the binding pocket of ALK have been reported in patients resistant to crizotinib (Choi et al, 2010; Sasaki et al, 2010). Of note, these mutations can already be present in naïve (i.e. untreated) patients and become selected upon pharmacological treatment (Al-Lazikani et al, 2012). Importantly, the initial mutation on a targeted oncogene modulates response to treatment. In the case of GIST, patients with mutations in the exon 9 of the *KIT* gene are less responsive to imatinib compared to the most frequent genetic lesions occurring on exon 11 (Debiec-Rychter et al, 2006; Heinrich et al, 2003). Similarly, NSCLC patients respond better to TKI therapy when they carry a deletion on the exon 19 of the *EGFR* gene while exon 21 mutations have been associated to shorter overall survival (Gazdar, 2009). Amplification and/or overexpression of the drug target are other frequently observed intrinsic mechanisms of resistance. Increased levels of BCR-ABL as well as other proteins have been described in the context of pharmacological resistance (Feldman & Feldman, 2001; Gorre et al, 2001). In addition, alternative splicing of oncogenes has also been annotated as a potential resistance mechanism. A BRAF^{V600E} variant lacking the RAS binding domain (p61BRAFF^{V600E}) has been detected in tumor samples of patients showing resistance to vemurafenib (Poulikakos et al, 2011).

Cancer cells can also take advantage of a broad range of extrinsic resistance mechanisms upon treatment with both chemotherapeutics and targeted agents. Patient-specific pharmacokinetic and pharmacodynamic parameters may hamper the efficacy of an otherwise successful drug. Poor adsorption, distribution or metabolism may be observed sporadically in some patients even for optimized molecules (Brockman, 1963). Some cancer drugs exert their pharmacological action on plasma membrane proteins while others have intracellular targets and need to reach the cytoplasm through diffusion, active transport or endocytosis (Gottesman, 2002). Even though changes in the lipid composition of the plasma membrane might affect diffusion and endocytosis, a much more common extrinsic resistance mechanism observed in cancer treatment relates to active transport of drugs in and out of the cell. Often, drug transporters at the plasma membrane are not specific and alterations in these carriers may lead to so-called multidrug resistance (MDR). One of the first examples was provided by the observation that many cancers overexpress the *MDR1* gene (also known as P-glycoprotein or P-gp) (Kartner et al, 1983). The product of this gene belongs to the wide family of ATP-binding cassette (ABC) transporters and works as an energy-dependent drug efflux pump (Dean & Annilo, 2005; Szakacs et al, 2006). The solute carrier (SLC) family represents another important family of membrane transporters that has been shown to play a pivotal role in the mechanism of action of cancer drugs (Hediger et al, 2004; Winter et al, 2014).

Extrinsic resistance may also occur upon alterations of signaling upstream or downstream of the main drug target. Upstream amplification of BRAF, for example, has been shown to confer resistance to the MEK inhibitor AZD6244 (Little et al, 2011). Alternatively, activation of different signaling pathways and mutations on genes other than the primary pharmacological target may substantially influence the effect of a specific treatment. For instance, the presence of KRAS or BRAF mutations in CRC abrogates the benefits observed upon cetuximab administration and stands as a paradigmatic predictor of anti-EGFR antibody therapy efficiency (Benvenuti et al, 2007). The outcome of anti-EGFR therapy in CRC might decline also in the presence of specific mutations in the *PIK3CA* gene and activation of this kinase or downregulation of its negative regulator PTEN have been shown to affect response to trastuzumab in breast cancer (Berns et al, 2007; De Roock et al, 2011). Extrinsic resistance might also be mediated by the overexpression of genes not directly targeted by therapy as illustrated

by the increased expression of LYN in different models of TKI-resistant CML (Mahon et al, 2008).

Increasing drug concentrations can overcome the effect of some mutations but toxicity and additional side effects might be experienced (Kantarjian et al, 2009). Targeting allosteric sites and engaging a target outside of its main binding pocket is another alternative (Hantschel, 2012; Hantschel et al, 2011). Intrinsic resistance can also be addressed with more sophisticated molecules optimized to bind wild type as well as mutated oncogenes. TKIs provide again an illustrative example with second generation inhibitors such as nilotinib (Tasigna®), dasatinib (Sprycel®) and bosutinib (Bosulif®) inhibiting also some mutated variants of BCR-ABL but not the T315I gatekeeper mutation while the third generation inhibitors ponatinib (Iclusig®) and rebastinib target also the gatekeeper (Lamontanara et al, 2013). However, effective alternatives are not always available for every drug target. Furthermore, extrinsic resistance mechanisms are more difficult to tackle and often require additional molecules targeting different proteins. Indeed, combinations of drugs are currently seen as the most promising alternative for cancer treatment and successful applications have already been described (Al-Lazikani et al, 2012).

Approaches to precision cancer medicine

Essentially, the first cancer pharmacological treatments have been devised to target features of malignant cells such as fast division. Sequencing of cancer genomes has molecularly refined these specific traits and produced the first targeted therapies. However, these early attempts have missed the intrinsic heterogeneity of cancer and underestimated the plasticity of redundant cellular networks. Moreover, they often deliver “undruggable” answers. Furthermore, they can only provide direct information on the tumor generating machinery overlooking alternative targets provided by synthetic lethal interactions. Genetic and chemical phenotypic screens are currently the most promising alternatives for the comprehensive characterizations of synthetic lethal drug targets and the discovery of new cancer therapies (Kaelin, 2009; Luo et al, 2009). Similar to classical genetic approaches, forward synthetic lethality screens explore loss-of-functions impairing a given phenotype (e.g. cancer embodied in a collection of different cell lines). However, complex genotypes such as those of cell lines often hinder

the molecular dissection of genetic interactions. On the other hand, reverse approaches focus on specific genetic changes and isogenic models. Even though artificially created, isogenic cell lines provide an elegant way to accurately describe synthetic lethalties (Nijman, 2011). Comprehensive loss-of-function screens have been long restricted to model organisms such as *Saccharomyces cerevisiae* and *Caenorhabditis elegans* but the discovery of the RNAi process has completely revolutionized the field empowering researchers with the possibility to knockdown every gene in a human cell lines.

Finding novel cancer targets is of extreme importance for the development of personalized medicine. However, targeting one single protein or cellular pathway in the redundant circuitry of the cell might not be sufficient to hinder tumor proliferation. The successful application of multicomponent therapeutics to other complex diseases such as HIV infection has inspired similar strategies for the treatment of malignant neoplasms (Bock & Lengauer, 2012). Indeed, we believe that combinatorial chemical screenings and RNAi-based loss-of-function studies represent technically distinct but complementary technologies for the development of more personalized and efficient cancer treatments. They are, therefore, the approaches that we chose to implement to contribute to the field of precision cancer medicine (Collins & Varmus, 2015; Gonzalez de Castro et al, 2013).

RNAi-based loss-of-function screens

The RNAi mechanism was originally described in *Caenorhabditis elegans* where post-transcriptional gene silencing was reported to be mediated by double-stranded RNA (dsRNA) (Fire et al, 1998). The very first observation of RNAi occurred, however, in plants during genetic experiments conducted by Jorgensen and colleagues who described as “co-suppression” a very similar phenomenon (Napoli et al, 1990). Biochemical studies in *Drosophila* embryo extracts have shown that dsRNA molecules are processed to smaller sequences called small interfering RNAs (siRNAs) which are the effective mediators of post-transcriptional gene silencing (Zamore et al, 2000). In mammals, RNAi is mediated by microribonucleic acids (microRNAs, miRNAs or miRs), which are short (around 22 nucleotides), single-stranded RNA molecules (Roberts, 2014). The genome encodes for longer miRNA precursors called primary-miRNAs (pri-miRNAs) with a stem-loop hairpin structure (Figure 5). The ribonuclease III DROSHA converts pri-miRNAs to precursor-miRNAs (pre-miRNAs) which are then exported to

the cytoplasm through the nuclear pore complex (NPC) by the karyopherin XPO5. In the cytoplasm, pre-miRNAs are further processed by DICER1, an endoribonuclease that removes the loop of the hairpin and generates small RNA duplexes resembling the siRNA molecules observed in *Drosophila*. The RNA duplex is subsequently loaded on the Argonaute protein (e.g. AGO2) of the RNA-induced silencing complex (RISC). At this stage, one RNA strand is discarded according to the thermodynamic asymmetry rule leaving a mature single-stranded miRNA which guides the RISC complex to the complementary messenger RNA (Hutvagner, 2005).

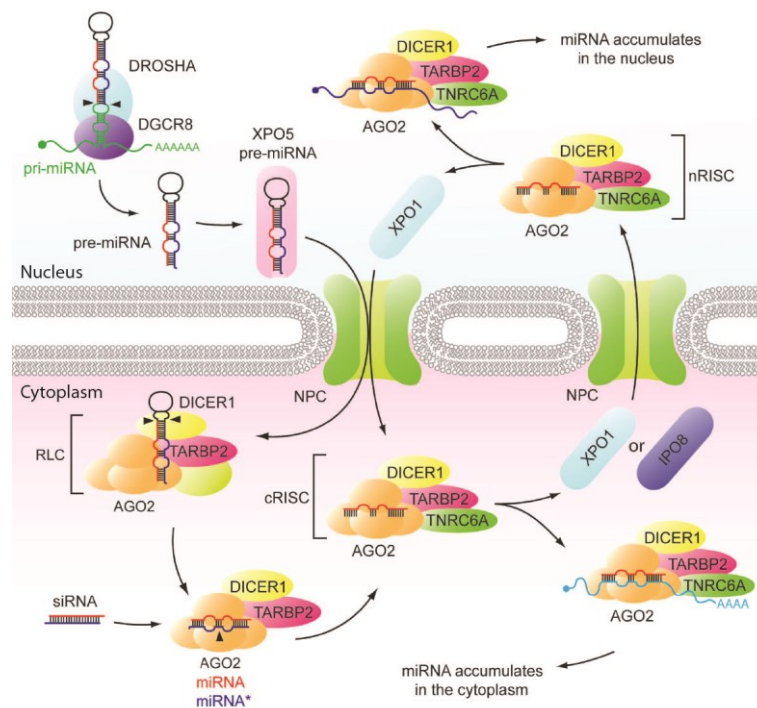


Figure 5. RNAi in mammals. Transcribed pri-miRNAs are processed by the DROSHA/DGCR8 complex to pre-miRNA and translocated to the cytoplasm by XPO5 through the Nuclear Pore Complex (NPC). Here, the pre-miRNA is further modified by the RISC loading complex (RLC) consisting of the Argonaute protein AGO2, DICER1, TARBP2 and other members. One strand of the mature miRNA is discarded and the AGO2 protein loaded with the remaining one. The cytoplasmic RISC (cRISC) binds the silencing factor TNRC6A and can then either target cytoplasmic messenger RNAs or be exported to the nucleus by XPO1. Here, the nuclear RISC (nRISC) may bind to other proteins and target nuclear transcripts (taken from Roberts, 2014).

Recognition of a specific mRNA requires perfect matching between the transcript and the “seed region” (i.e. nucleotides 2-7) of the miRNA while some mismatches are allowed

in the rest of the sequence. Of note, perfect matching throughout the entire sequence usually determines mRNA degradation via the catalytic activity of the Argonaute protein while lower complementarity results in post-transcriptional gene silencing through alternative mechanisms such as inhibition of protein translation (Roberts, 2014). Importantly, miRNAs have been described not only in the cytoplasm of mammalian cells but also in the nucleus (Jeffries et al, 2011; Park et al, 2010). The nuclear function of miRNAs remains unclear but evidence suggests they might be involved in regulation of long noncoding RNAs (lncRNAs) or other miRNAs transcription, epigenetic gene silencing and alternative splicing (Allo et al, 2009; Kim et al, 2008; Leucci et al, 2013).

Since the first observations, RNAi was regarded as a revolution in the field of functional genomics. Knockdown of gene expression through dsRNA provided an innovative tool to perform studies on gene function that were previously restricted to lower organisms. Initially, researchers thought that the activation of interferon response, the dsRNA-dependent protein kinase (PKR) pathway and general protein translation arrest would have hampered the application of dsRNA-induced RNAi to somatic mammalian cells. However, these responses are triggered mainly by long dsRNA molecules (i.e. >30 bp) apart from particular circumstances in specific cell types. The first RNAi experiments in mammalian cells involved chemically synthesized short (21-22 base pair) siRNAs modelled on the small RNA duplexes observed in *Drosophila* and delivered by means of transfection (Elbashir et al, 2001). However, in contrast to the systemic and heritable nature of dsRNA-mediated post-transcriptional gene silencing in *Caenorhabditis elegans* and plants, RNAi mediated by siRNA in *Drosophila* and mammals is transient, cell-autonomous and non-heritable (Hannon, 2002). Moreover, many mammalian cells cannot be readily transfected. Short hairpin RNAs (shRNAs) resemble endogenous mammalian miRNAs and provide an alternative to these limitations. Extensive studies have been conducted to elucidate the structural features essential for an efficient shRNA molecule both in terms of length of the stem-loop and sequence complementarity to the intended target (Gu et al, 2012; Paddison et al, 2002). As for siRNAs, shRNAs can be chemically synthesized and transfected in cells where they would anyway elicit a transient effect (Brummelkamp et al, 2002b; Paddison et al, 2002). However, these hairpin-like RNAi triggers can also be encoded by self-inactivating retroviral or lentiviral constructs integrating in the genome of the target cell upon infection (Abbas-Terki et al, 2002; Brummelkamp et al, 2002a). This feature allows delivery to a broader range of

mammalian cells. After genomic integration, a stem-loop hairpin resembling natural miRNAs is produced and processed by the endogenous RNAi machinery. Stable integration allows sustained expression of shRNA molecules also in daughter cells and prolonged gene knockdown effects that can be observed for weeks. Furthermore, shRNA-encoding vectors can be propagated and stored indefinitely. Different shRNA constructs have been reported in the literature. For example, The RNAi Consortium (TRC) at the Broad Institute of MIT and Harvard (Cambridge, MA, USA) developed the pLKO.1 vector adapting a previously reported lentiviral construct (Moffat et al, 2006) (Figure 6). In pLKO.1, the human U6 RNA polymerase III promoter drives the transcription of a 21-base pair stem and a 6-nucleotide loop shRNA while expression of a puromycin-resistance gene under the control of the human phosphoglycerate kinase (hPGK) promoter allows for selection of infected cells.

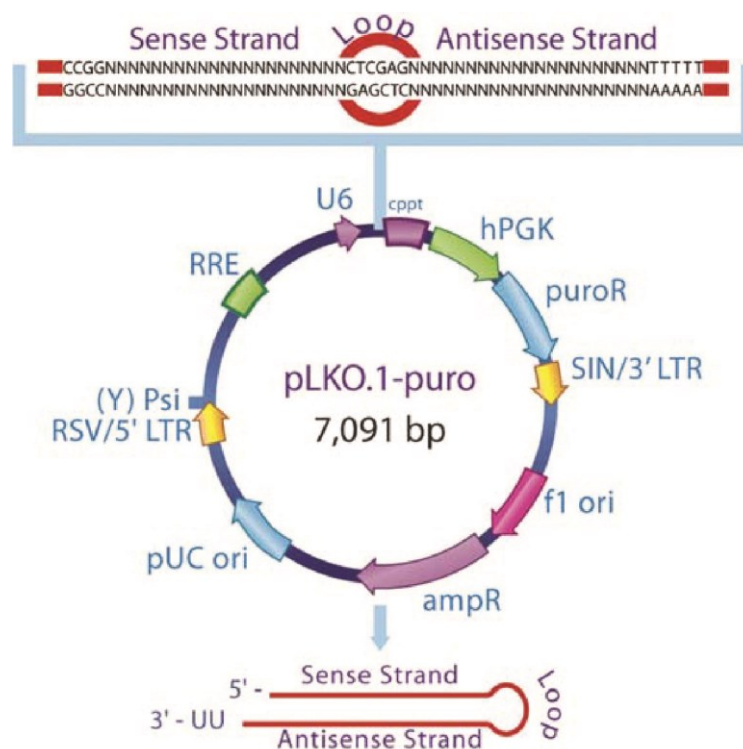


Figure 6. Schematic illustration of the pLKO.1 vector used by The RNAi Consortium (taken from Moffat et al, 2006).

The sustained expression of a shRNA targeting an essential gene can be toxic and induce cellular death preventing analyses of gene function. In this regard, engineered vectors

allowing inducible expression of RNA hairpins have been described (Ngo et al, 2006; Zuber et al, 2011a).

Certainly, the most exciting potential of RNAi resides in the possibility to build extensive shRNA libraries targeting focused gene sets or an entire genome. Such libraries represent an unprecedented technology that can be employed to investigate gene functions, gene-gene interactions and new therapeutic targets in humans. Arrayed or pooled loss-of-function genetic screens can be performed using libraries of shRNAs (Bernards et al, 2006; Brummelkamp et al, 2006; Luo et al, 2008; Silva et al, 2005). In arrayed screens shRNA constructs targeting different genes are separately administered to cells in, for example, a 96-well plate format. This type of genetic screens is usually more sensitive, provides direct information on genes responsible for a particular phenotype and allows implementation of more sophisticated read-outs such as fluorescence imaging-based high-content screenings. The array format can be used for both positive selection screens, where gene knockdown confers some sort of advantage or increase of a specific property, and negative selections, where gene downregulation leads to cellular growth impairment or death. Paddison and colleagues, for example, looked for impaired proteasome function in an arrayed shRNA screen based on a fluorescent reporter (Paddison et al, 2004). However, arrayed screens of genome-wide libraries require extensive automation and only allow for short-term phenotypes to be monitored as prolonged culture of cells in multi-well plates is rather impractical. On the other hand, cells can be infected with pooled libraries. The specific sequence of a shRNA molecule can be seen as a molecular barcode that can be PCR-amplified from the genomic DNA of infected cells and deconvoluted out of a pool by microarray analysis or, more recently, through next-generation sequencing (Sims et al, 2011). Moreover, additional barcodes inserted during PCR amplifications permit higher multiplexing. Pooled shRNA screens do not require extensive pipetting and are usually performed in standard cell culture dishes allowing for long-term proliferation assays. Negative selection screens are, however, more difficult in the pooled format as the detrimental phenotype has to be sufficiently pronounced to be robustly detected in the pool. In a successful example, Ngo et al. uncovered a role for CARD11 in the regulation of NF- κ B signaling and its therapeutic potential in diffuse large B-cell lymphoma (DLBCL) through the pooled screen of an inducible shRNA library (Ngo et al, 2006). Undoubtedly, shRNA screens represent a powerful investigation tool for the discovery of new molecular

targets in cancer. Notably, loss-of-function screens using shRNA libraries have been also successfully conducted *in vivo* (Dow et al, 2012; Zuber et al, 2011b).

A caveat to the use of RNAi molecules such as siRNA or shRNA is represented by off-target effects. Both siRNA and shRNA molecules have been reported to induce knockdown of genes different from the intended target (Echeverri et al, 2006). Even though RNAi molecules are designed in order to minimize such off-target effects, results from loss-of-function screens carried with these triggers have to be validated with secondary experiments. A way around this complication is the inclusion of different constructs targeting the same gene in shRNA libraries as molecules with different targeting sequences are less likely to show overlapping off-targets.

Multicomponent therapeutics

Pharmacological treatments based on complex mixture of active natural products have largely been used in traditional medicinal approaches. Multi-drug regimens have been in vogue till the beginning of the twentieth century when some investigators developed a concrete interest in the defined action of single molecules. Pioneering research conducted by Paul Ehrlich generated considerable excitement about so-called “magic bullets” effective against specific diseases (Ehrlich, 1913). This trend dominated till the second half of last century when it became clear that the multifactorial basis and molecular complexity of diseases such as cancer could not always be addressed by single molecules. Recently, it has been proposed that cancer heterogeneity and resistance mechanisms would be better undertaken by multicomponent therapeutics emulating successful anti-HIV strategies (Bock & Lengauer, 2012).

Cancer is often treated with a combination of surgery, radiation and/or pharmacological approaches. The chemotherapy regimen for childhood acute lymphoblastic leukemia (ALL) based on a mixture of methotrexate, vincristine, 6-mercaptopurine and prednisone was among the first drug-only combinatorial treatments (Chabner & Roberts, 2005). More recent targeted drugs are regularly used in combination with classical chemotherapeutic agents. For example, the monoclonal antibody trastuzumab is often prescribed in combination with paclitaxel for the treatment of breast cancer while cetuximab can be administered together with irinotecan (Camptosar®) in CRC (Cunningham et al, 2004; Slamon et al, 2001). Combinatorial approaches based exclusively on targeted drugs have also been explored and are usually referred to as

“vertical” if the distinct molecules target the same oncogenic pathway (or even the same target) or “horizontal” if parallel pathways are addressed. Combinatorial treatments based on the CYP17 inhibitor abiraterone (Zytiga®) and the antiandrogen enzalutamide (Xtandi®), both targeting the AR signaling, are being evaluated for the treatment of castration-resistant prostate cancer (CRPC) (Al-Lazikani et al, 2012). In a more “horizontal” example, the efficacy of the MEK inhibitor AZD6244 has been shown to improve by concomitant administration of an allosteric AKT inhibitor in the context of NSCLC (Tolcher et al, 2015). Importantly, all combinatorial approaches must carefully evaluate the appropriate concentrations of the agents to be combined as well as a potential administration time lag. Studies on breast cancer have shown that hormonal therapy can be combined with chemotherapeutics and that better results are obtained if the two drugs are administered sequentially rather than concomitantly (Albain et al, 2009; Lee et al, 2012).

Hypothesis-driven combination strategies based on knowledge about the underlying cancer mechanisms have improved treatment but cannot probe the entire combinatorial space and could miss important non-obvious interactions. In the future, network/systems biology will likely be able to provide more sophisticated *in silico* tools for rational drug combinations design based on integrated information from (functional) genomics and proteomics. Currently, high-throughput screening (HTS) technologies provide the most resourceful strategy for combinatorial drug discovery. Even though genome-wide genetic loss- or gain-of-function screens can uncover key interactions sustaining sensitivity or resistance mechanisms, phenotypic screens of large compound collections have the advantage of providing a direct connection between phenotypes, “druggable” targets and a compound. Moreover, HTS of diverse compound libraries can identify unexpected interactions and lead to the formulation of syncretic drug combinations (in contrast to more obvious congruous ones) where at least one of the active ingredients is not used individually for the treatment of the targeted disease (Keith et al, 2005). Combinations of drugs are usually explored using factorial designs (also referred to as dose-response matrices) where all possible permutations of different doses of two or more compounds are systematically analyzed. As illustrated by Lehar et al., these representations might also reveal different types of interaction between drug targets (Lehar, 2007). Ultimately, multicomponent therapeutics in the clinic has to be justified by a significant improvement over the administration of

individual drugs. Addition of a second molecule, can improve the efficacy of another by either boosting the maximal effect at the highest concentrations or by shifting potency to lower doses (Lehar et al, 2008). Synergy (from the Greek *συνεργία*, meaning cooperation) has historically been used in pharmacology to indicate a combinatorial effect that is greater than the simple addition of the effects of the single compounds (Berenbaum, 1989). In contrast, drugs producing a combination effect which is poorer compared to the predicted additivity are said to antagonize. Two distinct models are usually employed for synergy assessment in multicomponent therapeutics (Figure 7).

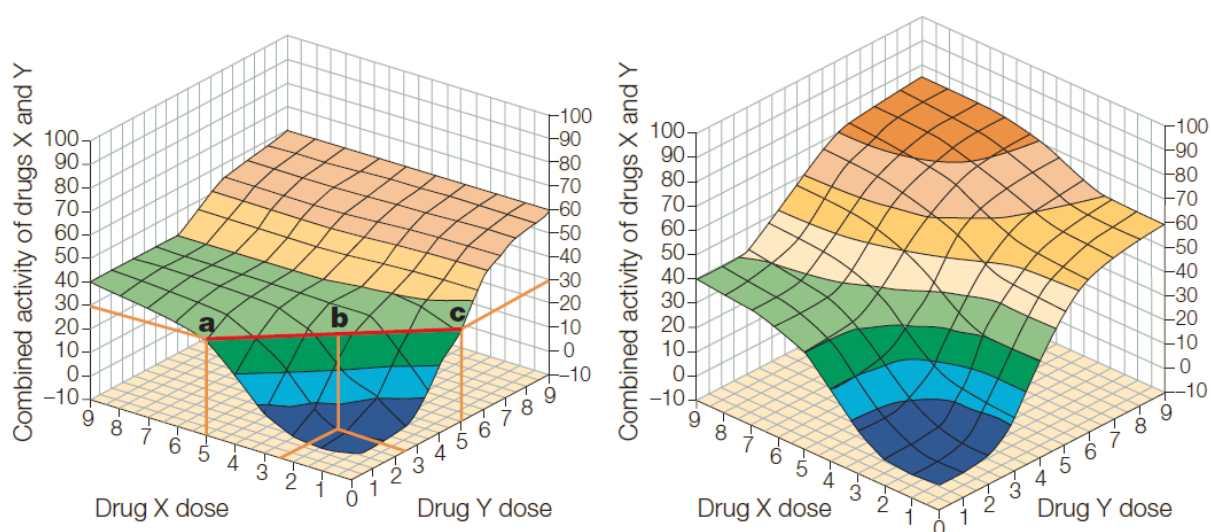


Figure 7. Synergy evaluation models. Dose-response surfaces describing the combinatorial activity of drugs X and Y according to the Loewe additivity model (left) or the Bliss independence model (right) (taken from Keith et al, 2005).

The assumption of the Loewe additivity model is that when combined with itself, a compound must be, by definition, additive (Loewe, 1928; Loewe, 1953). Consequentially, in order to achieve the specific effect generated by either drug X alone at C_X concentration or by drug Y alone at C_Y concentration, X and Y have to be combined at doses C_{X1} and C_{Y1} respectively, satisfying the equation $C_{X1}/C_X + C_{Y1}/C_Y = 1$. Chou and Talalay extended the Loewe additivity model defining a Combination Index (CI) given by the equation $C_{X1}/C_X + C_{Y1}/C_Y = CI$ (Chou & Talalay, 1984). CI values describe multicomponent synergy when $CI < 1$, antagonism when $CI > 1$ or Loewe additivity when $CI = 1$. A disadvantage of the Loewe additivity model is that dose-response curves of the drugs alone are necessary to evaluate the effect of a combination. The Bliss

independence model refers to combinations of drugs acting independently and, in contrast to Loewe additivity, does not require dose-response information about the single compounds to assess potential combinatorial synergy or antagonism (Bliss, 1939). According to this model the effect of two drugs X and Y can be predicted to be equal to $A_X + A_Y - A_X * A_Y$ where A_X and A_Y are the activities of the two individual drugs. Deviations between experimental and predicted values define synergy (deviation > 0), additivity (deviation = 0) or antagonism (deviation < 0).

For a compound library of n molecules there are $n*(n-1)/2$ possible pairwise combinations. Therefore, even a relatively small library of 1,000 compounds, would generate almost 500,000 pairwise combinations to be investigated. Such numbers easily exceed the standard throughput of many screening facilities. A way around this scale issue might be provided by sophisticated screening strategies (Borisy et al, 2003) or more focused libraries such as collections of kinase inhibitors or epigenetic molecules. Libraries of approved drugs, especially, represent a convenient resource not only because they contain highly optimized small molecules that can be used as chemical biology tools but also because they could easily allow repurposing (i.e. repositioning) of individual drugs or combinations thereof (Ashburn & Thor, 2004). Followed by a proper assessment of pharmacokinetic and pharmacodynamic parameters of concomitantly administered molecules, combinatorial HTS of approved drugs have the potential to deliver clinically relevant ready-to-use multicomponent therapeutics bypassing most of the hurdles of a standard drug discovery pipeline.

AIMS

The aim of the work described here was to define novel therapeutic targets and to develop stratified treatments contributing to more personalized cancer medicine. In particular, we aimed at the establishment of a robust pooled shRNA screening pipeline to allow for the systematic investigation of the role of chromatin-related proteins in a model for breast cancer heterogeneity. Using a collection of isogenic cell lines we wanted to evaluate the therapeutic potential of chromatin modifying enzymes in specific breast cancer genetic backgrounds and disclose new “druggable” targets for the development of more personalized therapies.

We also aimed at a comprehensive evaluation of combinations of approved drugs to uncover clinically relevant synergistic interactions. By means of combinatorial HTS we wanted to assess congruous relations as well as non-obvious connections between seemingly unrelated drugs and repurpose clinical compounds for more patient-specific pharmacological treatments.

RESULTS

NOTCH1 activation in breast cancer confers sensitivity to inhibition of SUMOylation

In order to evaluate the therapeutic potential of chromatin-related proteins for the development of breast cancer treatments specific for distinct genetic backgrounds described in patients, we have performed a pooled shRNA screen on a panel of isogenic cell lines and uncovered the sensitivity of NOTCH1-activated breast cancer cells to inhibition of SUMOylation, a post-translational modification that occurs on histones as well as on other proteins. The findings of the screen together with the molecular characterization of the genetic interaction and the evaluation of its clinical relevance in patient-derived breast cancer cell lines have been reported in the following publication.



ORIGINAL ARTICLE

NOTCH1 activation in breast cancer confers sensitivity to inhibition of SUMOylation

MP Licciardello¹, MK Müllner¹, G Dürnberger^{1,3}, C Kerzendorfer¹, B Boidol^{1,2}, C Trefzer¹, S Sdelci¹, T Berg¹, T Penz¹, M Schuster¹, C Bock¹, R Kralovics¹, G Superti-Furga¹, J Colinge¹, SM Nijman¹ and S Kubicek^{1,2}

Breast cancer is genetically heterogeneous, and recent studies have underlined a prominent contribution of epigenetics to the development of this disease. To uncover new synthetic lethalties with known breast cancer oncogenes, we screened an epigenome-focused short hairpin RNA library on a panel of engineered breast epithelial cell lines. Here we report a selective interaction between the NOTCH1 signaling pathway and the SUMOylation cascade. Knockdown of the E2-conjugating enzyme UBC9 (*UBE2I*) as well as inhibition of the E1-activating complex SAE1/UBA2 using ginkgolic acid impairs the growth of NOTCH1-activated breast epithelial cells. We show that upon inhibition of SUMOylation NOTCH1-activated cells proceed slower through the cell cycle and ultimately enter apoptosis. Mechanistically, activation of NOTCH1 signaling depletes the pool of unconjugated small ubiquitin-like modifier 1 (SUMO1) and SUMO2/3 leading to increased sensitivity to perturbation of the SUMOylation cascade. Depletion of unconjugated SUMO correlates with sensitivity to inhibition of SUMOylation also in patient-derived breast cancer cell lines with constitutive NOTCH pathway activation. Our investigation suggests that SUMOylation cascade inhibitors should be further explored as targeted treatment for NOTCH-driven breast cancer.

Oncogene advance online publication, 29 September 2014; doi:10.1038/onc.2014.319

INTRODUCTION

Breast cancer is the most common type of cancer in women and is usually classified according to the expression status of the estrogen, progesterone and HER2/neu receptors.¹ Recent whole-genome sequencing efforts have revealed that all breast cancer subtypes show a broad heterogeneity of genetic alterations.^{2–4} This genetic complexity might explain why some patients do not respond to current therapies and calls for more stratified approaches in the treatment of breast cancer.

Tumor cells tend to become addicted to the activity of cancer-causing mutated proteins (oncogene addiction).⁵ This observation has led to the development of several types of targeted therapies geared toward directly inhibiting the function of these oncoproteins.^{6–8} However, oncogenes are not always directly 'druggable'. More recently, it has been hypothesized that the molecular changes occurring during tumor development may also lead to addiction to genes that are not directly involved in the tumorigenic process and are normally not essential.^{9–11} This non-oncogene addiction or synthetic lethality principle has been corroborated through different examples^{12,13} and provides a further way to treat cancer.

Chromatin pathways control all aspects of transcription and are hubs enriched in synthetic lethal interactions with diverse signaling pathways.^{14,15} In order to comprehensively investigate the function of chromatin-modifying proteins in cancer and prioritize targets that could emerge as new synthetic lethalties, we screened an epigenome-focused short hairpin RNA (shRNA) library on a panel of engineered breast epithelial cell lines. In this study, we tested >3000 gene–gene interactions in a multiplexed

fashion revealing a specific interaction between the NOTCH1 signaling pathway and the SUMOylation cascade.

Activation of NOTCH signaling in breast cancer through mutations or overexpression of the NOTCH1 receptor or loss of the negative regulator NUMB has been described recently.^{16,17} The NOTCH pathway regulates cellular proliferation and differentiation^{18,19} and is frequently activated in different tumors.^{20–22} Its role in tumorigenesis is not well understood and appears to be strictly context-dependent.^{21,23} Activation of the pathway results in the cleavage of the transmembrane receptor NOTCH1 by γ -secretase, releasing the intracellular domain of NOTCH1 (ICN1) in the cytoplasm. ICN1 translocates into the nucleus where it forms a complex with other proteins, such as MAML1 and RBPJ, and promotes the transcription of NOTCH1 target genes.^{18,24} Specific targeting of NOTCH1-driven cancers currently focuses on the use of antibodies against both receptor and ligands,^{25,26} stapled peptides interfering with ICN1/MAML interaction²⁷ and γ -secretase inhibitors (GSIs).²⁵ GSIs are currently in clinical trial but have shown significant side effects.^{28,29} Furthermore, γ -secretase-independent activation of NOTCH signaling has also been described.³⁰

Small ubiquitin-like modifier (SUMO) is a posttranslational modification similar to ubiquitin. Mammals encode four isoforms of SUMO: SUMO1, SUMO2 and SUMO3 sharing 97% sequence identity and SUMO4 whose expression seems to be restricted only to certain tissues.^{31,32} This posttranslational modification is established by a cascade similar to the one of ubiquitin with an E1-activating complex SAE1/UBA2, an E2-conjugating enzyme UBC9 (*UBE2I*) and several E3 ligases.³¹ SUMOylation occurs mainly

¹CeMM Research Center for Molecular Medicine of the Austrian Academy of Sciences, Vienna, Austria and ²Christian Doppler Laboratory for Chemical Epigenetics and Antiinfectives, CeMM Research Center for Molecular Medicine of the Austrian Academy of Sciences, Vienna, Austria. Correspondence: Dr S Kubicek, CeMM Research Center for Molecular Medicine of the Austrian Academy of Sciences, Lazarettgasse 14 AKH BT 25.3, Vienna 1090, Austria.

E-mail: skubicek@cemm.oew.ac.at

³Current address: Research Institute of Molecular Pathology (IMP), Vienna, Austria.

Received 17 March 2014; revised 29 July 2014; accepted 13 August 2014



2

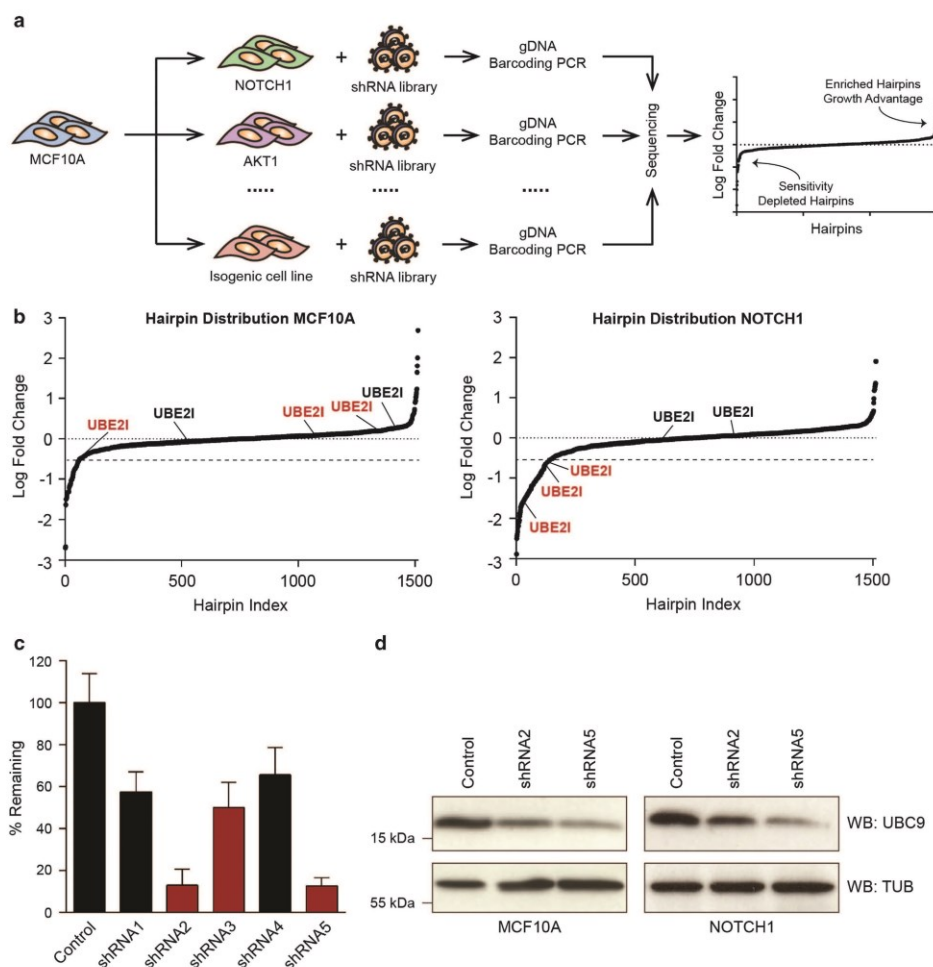


Figure 1. An shRNA screen uncovers the genetic interaction between NOTCH1 signaling and the SUMOylation cascade. **(a)** Schematic representation of the pooled shRNA screen on a panel of isogenic breast cancer cells. **(b)** Hairpin distributions for MCF10A and NOTCH1 cells. Hairpins are ranked according to the Log of the fold change in abundance over the median. *UBE2I* hairpins are indicated in red or black according to knockdown efficiency. **(c)** Quantitative reverse transcriptase-PCR measurement of *UBE2I* knockdown efficiency. RNA was harvested 4 days after infection. Data are normalized to actin expression, and control infection is set to 100%. Error bars are s.d. of three biological replicates. **(d)** Western blotting showing reduced UBC9 levels upon knockdown of *UBE2I* with two different hairpins. Samples were collected 6 days after infection. Tubulin was used as a loading control.

on nuclear proteins,^{33,34} including histones,³⁵ and has been shown to regulate the activity of SUMOylation enzymes themselves.³⁶ In contrast to ubiquitination, SUMOylation is usually not associated with protein degradation but rather modifies activity, binding partners and localization of its targets.³¹ Notably, recent reports have linked SUMOylation and the components of the SUMOylation cascade to cancer.^{37,38}

Here we show that overexpression of ICN1 in MCF10A breast epithelial cells confers sensitivity to knockdown of *UBE2I*. We also observe growth impairment upon treatment with a small-molecule inhibitor of the SAE1/UBA2 complex. Importantly, these effects are conserved in different patient-derived

NOTCH-activated breast tumor models. Collectively, our data suggest targeting of the SUMOylation cascade for the treatment of NOTCH-driven breast cancer.

RESULTS

Cancer cell lines have been used extensively in genetic and drug screens aiming at the discovery of new therapies and insights in the biology of the disease.^{39–41} However, they do not always allow for an easy mechanistic interpretation of findings, due to their genetic complexity. In addition, available breast cancer cell lines do not comprehensively represent the genetic heterogeneity of

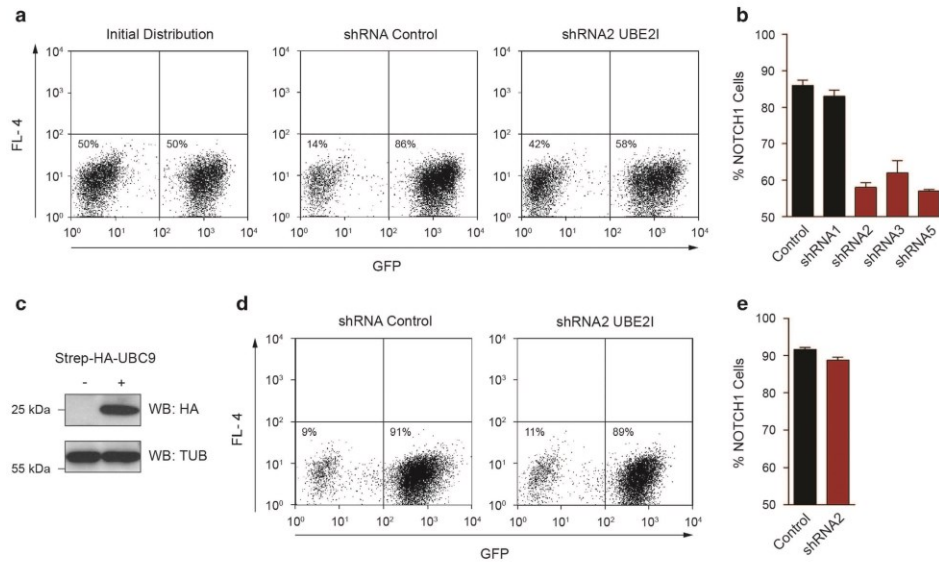


Figure 2. Knockdown of *UBE2I* impairs the growth of NOTCH1 cells. **(a)** Flow cytometry analysis of a co-culture of MCF10A and NOTCH1 cells. Distribution of the two cell lines at the beginning of the experiment (left panel), 12 days after infection with a control hairpin (middle panel) and 12 days after infection with *UBE2I* shRNA2 (right panel). **(b)** Quantification of the percentage of NOTCH1 cells 12 days after infection with control or different *UBE2I* hairpins. Colors refer to knockdown efficiency as indicated in Figure 1. Error bars are s.d. of two biological replicates. **(c)** Western blotting confirming overexpression in NOTCH1 cells infected with a retrovirus encoding Strep-HA-UBC9. Tubulin was used as a loading control. **(d and e)** Same as in panels **(a and b)**, only here both MCF10A and NOTCH1 cells overexpress a knockdown-resistant Strep-HA-UBC9. *UBE2I* shRNA2 targets the 3'-UTR of the transcript, which is not present in the Strep-HA-UBC9 overexpression construct. Error bars are s.d. of two biological replicates.

the disease in patients. Moreover, the different culture requirements demand context-dependent data analysis. In order to overcome these difficulties and focus on specific breast cancer oncogenes, we used a collection of genetically engineered isogenic breast cancer cell lines that has been already validated and successfully employed to identify resistance of NOTCH1-activated breast cancers to phosphatidylinositol 3'-kinase inhibitors.⁴² Briefly, the cDNA of 10 breast cancer oncogenes was overexpressed in the immortalized non-tumorigenic breast cell line MCF10A (Supplementary Table S1). On this panel of isogenic cell lines, we screened an epigenome-focused shRNA library in a pooled fashion (Figure 1a). The library targets 305 chromatin-related genes with three to five different hairpins for each target giving a total of 1519 hairpins (Supplementary Figure S1 and Supplementary Table S2). This setup allowed for the investigation of > 3000 gene-gene interactions.

We initially assessed the variability of the assay through correlation scatter plots of the hairpin sequencing reads from different biological replicates and found good reproducibility ($R^2 > 0.7$, Supplementary Figure S2). We then analyzed the hairpin distributions for all cell lines of the panel and compared them with the MCF10A cell line not expressing any oncogene. This analysis revealed the specific depletion of three hairpins targeting *UBE2I*, the gene coding for the UBC9 E2-conjugating enzyme of the SUMOylation cascade, in cells overexpressing ICN1 (NOTCH1 cells) (Figure 1b, Supplementary Figure S3 and Supplementary Table S3). Notably, the distribution of the five *UBE2I* hairpins correlated to the knockdown efficiency assessed for the individual shRNAs by quantitative reverse transcriptase-PCR and western blotting (Figures 1c and d). Overexpression of ICN1 results in the activation of the NOTCH1 pathway. We confirmed this activation

in a NOTCH luciferase reporter assay³⁰ (Supplementary Figure S4a) and by measuring the relative expression of NOTCH1 canonical targets *HES1*, *HEY1*, *MYC* and *CCND1*. NOTCH1 cells showed increased mRNA levels for these genes compared with MCF10A cells (Supplementary Figure S4b).

In order to validate the finding from our screen, we monitored the relative growth of NOTCH1 cells in a co-culture with MCF10A control cells. NOTCH1 cells express green fluorescent protein thus allowing the design of a flow cytometry-based assay. Moreover, they overgrow MCF10A cells in co-cultures, as expected from cells expressing a potent oncogene. Upon infection with a control vector, these growth properties remained unchanged (Figure 2a); knockdown of *UBE2I* with different hairpins instead abolished the growth advantage of NOTCH1 cells recapitulating the finding of the screen (Figures 2a and b). Furthermore, overexpression of an shRNA-resistant *UBE2I* construct (Figure 2c) rescued the growth advantage of NOTCH1 cells upon knockdown of *UBE2I* (Figures 2d and e).

Ginkgolic acid (GA) has been reported to inhibit the SUMOylation cascade through direct binding to SAE1/UBA2, the E1-activating complex of the cascade, in both biochemical and cellular assays.⁴³ Treatment of the co-culture with GA resulted in a faster and stronger depletion of NOTCH1 cells compared with that observed with shRNAs (Figure 3a). This is probably due to greater inhibition of the SUMOylation cascade upon treatment with the small molecule compared with incomplete knockdown of *UBE2I*. We also examined the effect of GA on the two cell lines in independent growth curves. Again we observed a selective impairment of the growth of NOTCH1 cells upon inhibition of the SUMOylation cascade (Figure 3b). In order to exclude effects due to growth speed differences between the two cell lines,



4

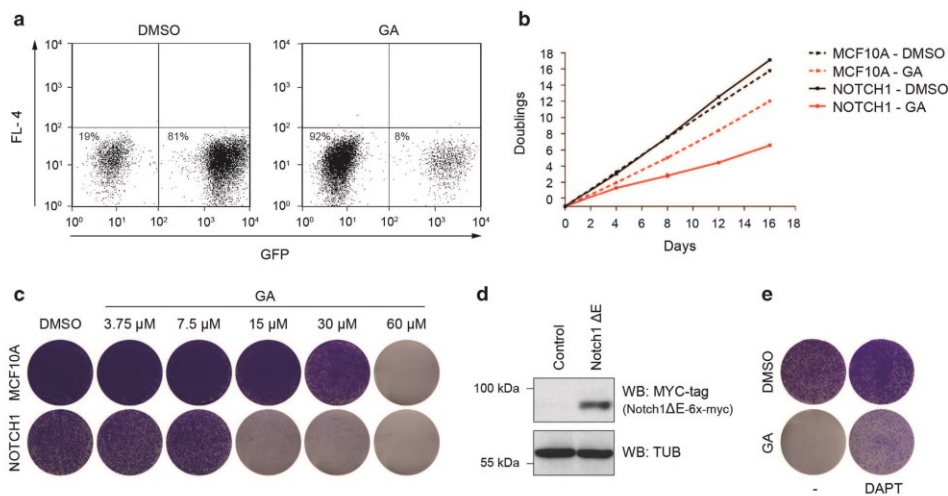


Figure 3. Sensitivity of NOTCH1 cells to GA. **(a)** Flow cytometry analysis of a co-culture of MCF10A and NOTCH1 cells treated with either DMSO or 30 μM GA. Distribution was assessed after 15 days. **(b)** Growth curves of MCF10A and NOTCH1 cells treated with either DMSO or 30 μM GA. Error bars are s.d. of three biological replicates. **(c)** Colony-formation assay of MCF10A and NOTCH1 cells treated with either DMSO or indicated concentrations of GA for 6 days. **(d)** Western blotting showing overexpression of Notch1 ΔE -6x-Myc in MCF10A cells. Tubulin was used as a loading control. **(e)** Colony-formation assay showing sensitivity of Notch1 ΔE cells to 30 μM GA partly rescued by co-treatment with 10 μM DAPT for 6 days.

we performed a colony-formation assay. A dose-response treatment over 6 days revealed a fourfold greater sensitivity of NOTCH1 cells to GA (Figure 3c). Notably, none of the other cell lines of our isogenic panel showed the same sensitivity to inhibition of SUMOylation (Supplementary Figure S5). To further corroborate the specific interaction between the NOTCH1 pathway and the SUMOylation cascade, we overexpressed a different GSI-sensitive NOTCH1 construct in MCF10A cells (Notch1 ΔE)⁴⁴ (Figure 3d). Notch1 ΔE cells also showed greater sensitivity to inhibition of SUMOylation (Figure 3e) while co-treatment with the GSI N-[N-(3,5-Difluorophenacetyl)-L-alanyl]-S-phenylglycine t-butyl ester (DAPT) partly rescued the effect of GA (Figure 3e). All together, these results indicate that NOTCH1-activated cells are more susceptible to inhibition of SUMOylation.

In order to unravel the mechanism behind this selective interaction, we assessed whether inhibition of the SUMOylation cascade could impair NOTCH1 signaling and affect the transcription of its canonical targets. Treatment with GA upregulated HES1 and HEY1 but downregulated MYC in both cell lines after 3 days (Supplementary Figure S6). Previous knockdown experiments performed on the same cell lines have shown that MYC downregulation does not impair the growth of NOTCH1 cells.⁴² Furthermore, the remaining MYC levels in NOTCH1 cells treated with GA are higher than in untreated MCF10A cells, suggesting MYC-independence of the observed phenotype. We addressed the effect of inhibition of the SUMOylation cascade at a broader level by gene expression profiling. We compared GA-treated cells with their corresponding dimethyl sulfoxide (DMSO) control, selected only significantly upregulated or downregulated genes ($\log_2(\text{fold change}) > 1.5$, $P < 0.001$) and performed Gene Ontology (GO) term enrichment analysis. This revealed a strong enrichment of terms associated with cell cycle among the genes upregulated by GA in both cell lines (Figure 4a and Supplementary Table S4). However, the enrichment was more significant in NOTCH1 cells. Gene Set Enrichment Analysis⁴⁵ led to the same conclusion (Figure 4b). Notably, cell cycle-related proteins having an

important role during S phase and mitosis have been reported to be SUMOylated.^{46,47} We then monitored the cell cycle of synchronized MCF10A and NOTCH1 cells. Upon treatment with GA, we observed slower progression of NOTCH1 cells through the S phase after 6 h (Figure 4c and Supplementary Figure S7). Similarly, NOTCH1 cells showed a delay in the G2/M phase between 10 and 12 h of treatment (Figure 4d and Supplementary Figure S7). Moreover, propidium iodide/Annexin V staining revealed increased early and late apoptotic cells in NOTCH1 cells treated with GA for 6 days (Figure 4e). Taken together, these experiments indicate that inhibition of SUMOylation impairs the growth of NOTCH1 cells by affecting the S and the G2/M phase of the cell cycle eventually leading to apoptosis.

To better assess the effects of inhibition of SUMOylation in both cell lines, we analyzed global SUMOylation levels using antibodies specific for the different SUMO isoforms. Strikingly, NOTCH1 cells showed a dramatic reduction in both global SUMO1 and SUMO2/3 levels upon treatment with 15 or 30 μM GA, whereas no change was observed for MCF10A cells (Figure 5a). Particularly, the SUMO2/3 antibody marked a specific pattern of differentially SUMOylated proteins in NOTCH1 cells (Figure 5a). Similar differences were also observed upon knockdown of *UBE2I* (Supplementary Figure S8) and in immunofluorescence experiments performed with the SUMO1 antibody (Figure 5b). In order to exclude effects related to general toxicity and global protein degradation or inhibition of translation, we analyzed the same samples for global protein content: a Coomassie staining revealed only minor differences between the different conditions (Supplementary Figure S9a). We also inquired whether the sensitivity of NOTCH1 cells could simply be explained by a greater amount of intracellular GA. However, a Multiple Reaction Monitoring (MRM) experiment revealed comparable GA uptake by the two cell lines (Supplementary Figure S9b).

We then questioned whether the levels of unconjugated SUMO1 and SUMO2/3 in our models could already be different prior to treatment. Indeed, depleted SUMO1 and SUMO2/3 levels

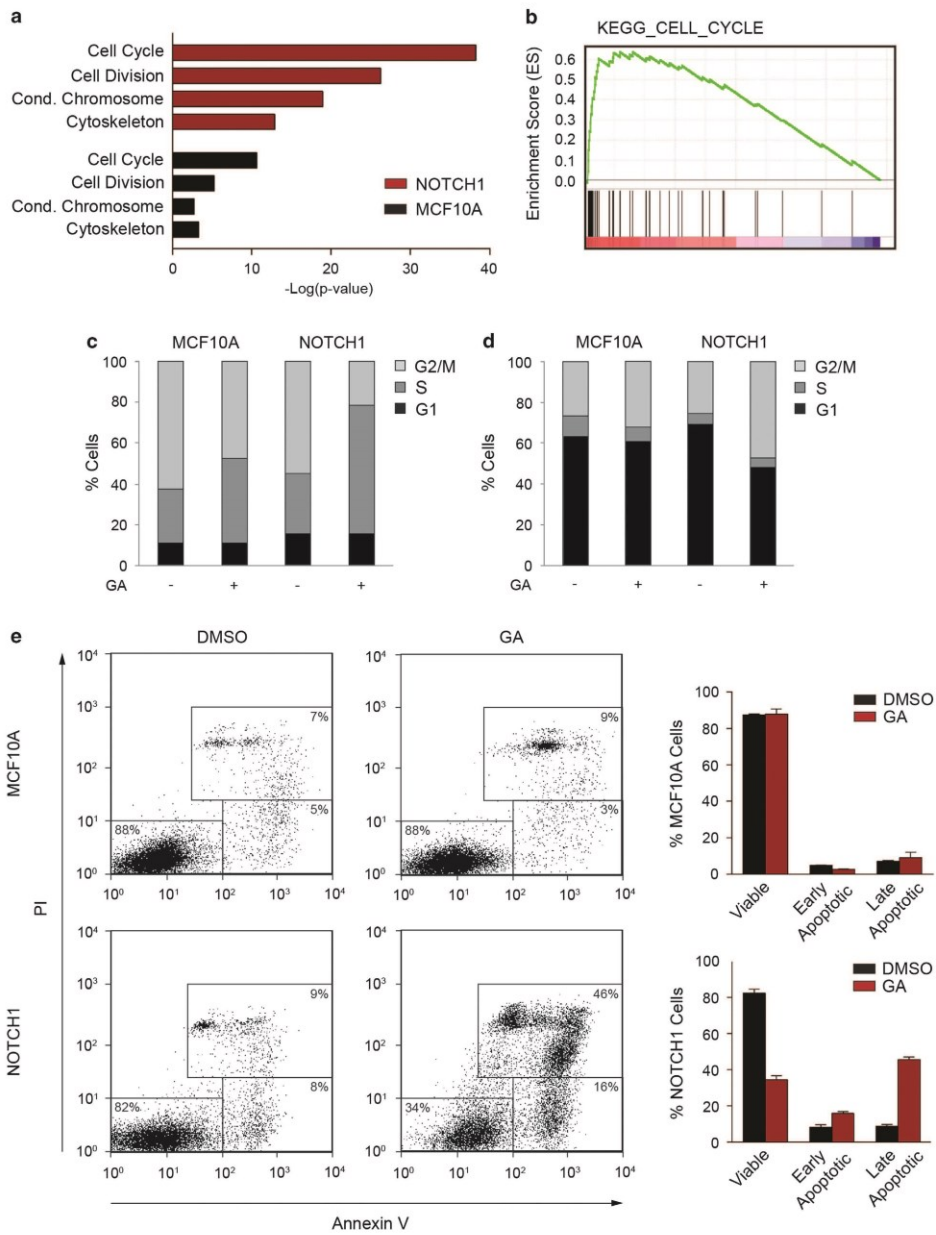


Figure 4. NOTCH1 cells proceed slower through the cell cycle and enter apoptosis upon inhibition of SUMOylation. **(a)** GO term enrichment analysis of genes with significant expression changes in MCF10A and NOTCH1 cells (GA treatment vs DMSO control). **(b)** Preranked Gene Set Enrichment Analysis showed enrichment of cell cycle-related terms among the genes upregulated by GA in NOTCH1 cells. **(c and d)** Analysis of cell cycle progression of synchronized MCF10A and NOTCH1 cells after 6 **(c)** or 12 h **(d)** treatment with either DMSO or 30 μ M GA. **(e)** Annexin V/propidium iodide staining of MCF10A and NOTCH1 cells treated with DMSO or 30 μ M GA for 6 days. Quantifications on the right indicate mean and s.d. of two biological replicates.

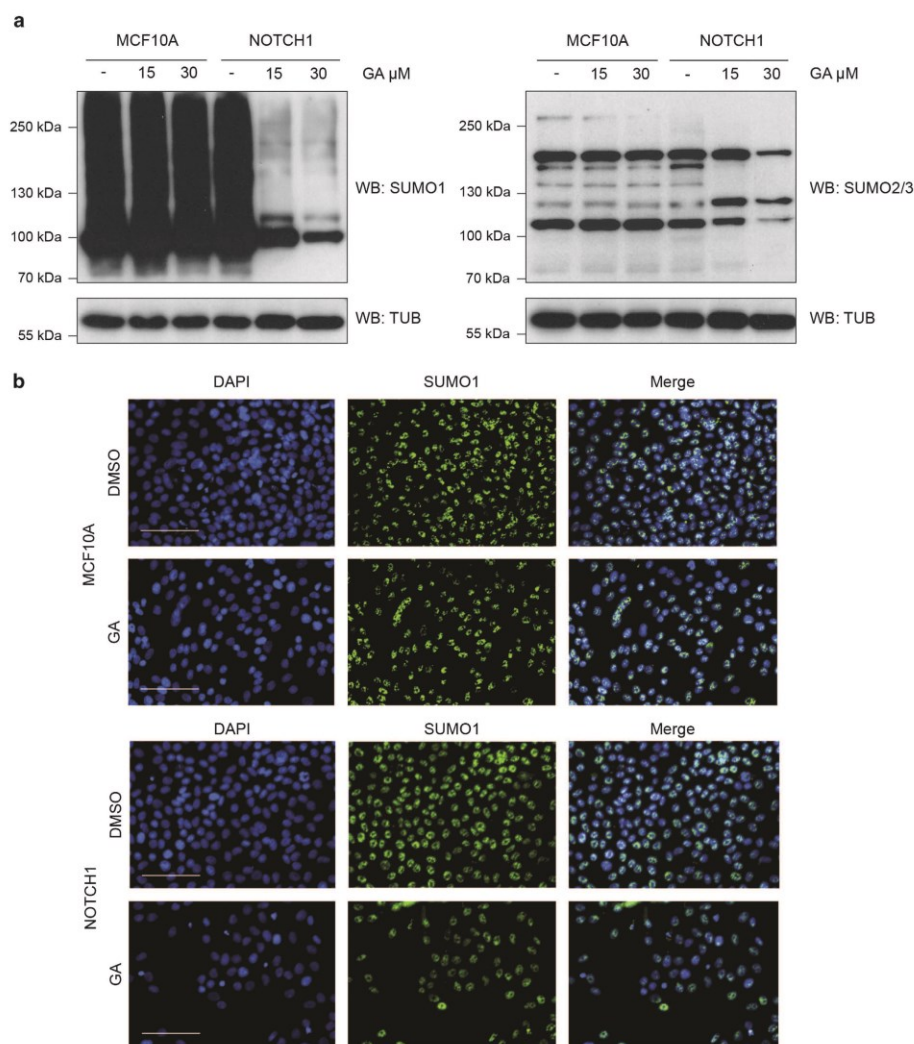


Figure 5. NOTCH1 cells show greater SUMOylation impairment upon treatment with GA. **(a)** Western blotting analysis of global SUMO1 (left) and SUMO2/3 (right) in MCF10A and NOTCH1 cells treated with DMSO, 15 μ M or 30 μ M GA for 3 days. Tubulin was used as a loading control. **(b)** Immunofluorescence analysis of global SUMO1 in MCF10A (top) and NOTCH1 (bottom) cells treated with either DMSO or 30 μ M GA for 3 days. Scale bar = 100 μ m.

were observed in NOTCH1 cells compared with control MCF10A cells (Figure 6a). Interestingly, Notch1 Δ E cells also showed depleted levels of unconjugated SUMO1 (Figure 6b), which increased upon treatment with the GSI DAPT (Figure 6c). Furthermore, NOTCH1 cells had the lowest levels of unconjugated SUMO1 and SUMO2/3 among the isogenic cell lines of our panel (Figure 6d). Depletion in the levels of unconjugated SUMO1 and SUMO2/3 could explain the greater sensitivity to inhibition of SUMOylation in NOTCH1-activated cells: in the presence of a reduced pool of one of its key players, the SUMOylation cascade would be more sensitive to any external perturbation such as

knockdown or inhibition of one of its enzymes. To test this hypothesis, we used different shRNA constructs targeting SUMO1, SUMO2 and SUMO3 to reduce the levels of unconjugated SUMO in our models (Supplementary Figures S10a and b). Upon knockdown of different SUMO isoforms, MCF10A control cells showed greater sensitivity to GA in colony-formation assays (Figure 6e). Moreover, due to the increased sensitivity of MCF10A cells to inhibition of SUMOylation upon knockdown of SUMO, NOTCH1 cells could no longer be depleted in a flow cytometry-based competition assay (Figure 6f and Supplementary Figure S10c). Collectively, these results show that depletion of

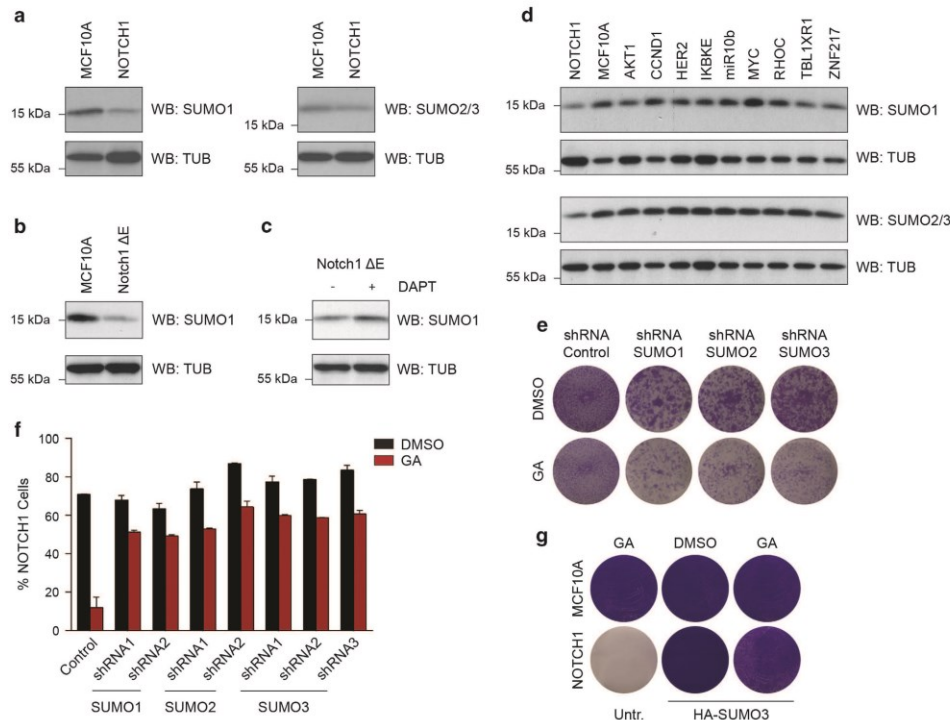


Figure 6. NOTCH1 activation depletes unconjugated SUMO1 and SUMO2/3. (a) Western blotting analysis of unconjugated SUMO1 (left) and SUMO2/3 (right) levels in MCF10A and NOTCH1 cells. Tubulin was used as a loading control. (b) Western blotting showing depletion of unconjugated SUMO1 in Notch1 ΔE cells. Tubulin was used as a loading control. (c) Western blotting showing increased unconjugated SUMO1 levels in Notch1 ΔE cells treated with 10 μM DAPT for 3 days. Tubulin was used as a loading control. (d) Western blotting showing NOTCH1 cells having the strongest depletion of unconjugated SUMO1 (top) and SUMO2/3 (bottom) among the cell lines of the isogenic panel. Tubulin was used as a loading control. (e) Colony-formation assay of MCF10A cells infected with either control or SUMO hairpins and treated with either DMSO or 30 μM GA for 6 days. (f) NOTCH1 cells infected with control vector were seeded with MCF10A cells infected with either control vector or different SUMO shRNAs as indicated and treated with either DMSO or 30 μM GA. Percentage of NOTCH1 cells was assessed after 15 days. Error bars are s.d. of two biological replicates. (g) Colony-formation assay of MCF10A and NOTCH1 cells untransfected or overexpressing HA-SUMO3. Cells were treated with DMSO or 30 μM GA. After 6 days, survival cells were allowed to grow in the fresh medium for 3 days.

unconjugated SUMO1 and SUMO2/3 increases susceptibility to perturbations of the SUMOylation cascade. Finally, to rescue the sensitivity phenotype we overexpressed HA-tagged SUMO3 in MCF10A and NOTCH1 cells (Supplementary Figure S11) and treated them with GA. NOTCH1 cells overexpressing HA-SUMO3 lost their specific sensitivity to inhibition of SUMOylation (Figure 6g).

NOTCH1 signaling has been found to be activated in breast cancer through increased expression or stability of the receptor or loss of negative regulators, such as NUMB.¹⁶ More recently, transcriptome analyses performed on a panel of 89 breast cancer cell lines and tumors revealed NOTCH fusion transcripts leading to constitutive activation of the NOTCH pathway.³⁰ We examined the levels of unconjugated SUMO and sensitivity to GA in the breast cancer cell lines HCC-38, HCC-1187, HCC-1599, HCC-2218 and BT-20, which have been reported to express NOTCH fusion transcripts (Supplementary Table S5). Almost all cell lines showed increased expression of NOTCH1 target genes *HES1*, *HEY1* and *CCND1* in quantitative PCR experiments, albeit with differences most likely due to context dependence (Supplementary Figure S12). Increased expression of MYC was observed only in

HCC-1599 cells (Supplementary Figure S12). Notably, the cell lines HCC-2218 and HCC-1187 showed strong depletion of unconjugated SUMO1 (Figure 7a) while HCC-1599 cells showed the most prominent SUMO2/3 depletion (Figure 7a). Of note, these three cell lines are the ones showing greater activation of the NOTCH pathway both phenotypically (that is, growth in suspension or as weakly adherent clusters and decreased cell–matrix adhesion) and at the mRNA level (Supplementary Figure S12). Finally, we assessed sensitivity to inhibition of SUMOylation for all five cell lines (Figures 7b–d). In agreement with our previous observations, sensitivity to GA correlated with the levels of unconjugated SUMO.

DISCUSSION

In this study, we performed a pooled shRNA screen on a breast cancer model and uncovered specific interactions between seven common breast cancer oncogenes and chromatin factors (Supplementary Table S3). The combination of a multiplexed next-generation sequencing-based technology with a panel of isogenic cell lines enabled the cost and time-effective interrogation of >3000 gene–gene interactions. Moreover, the



8

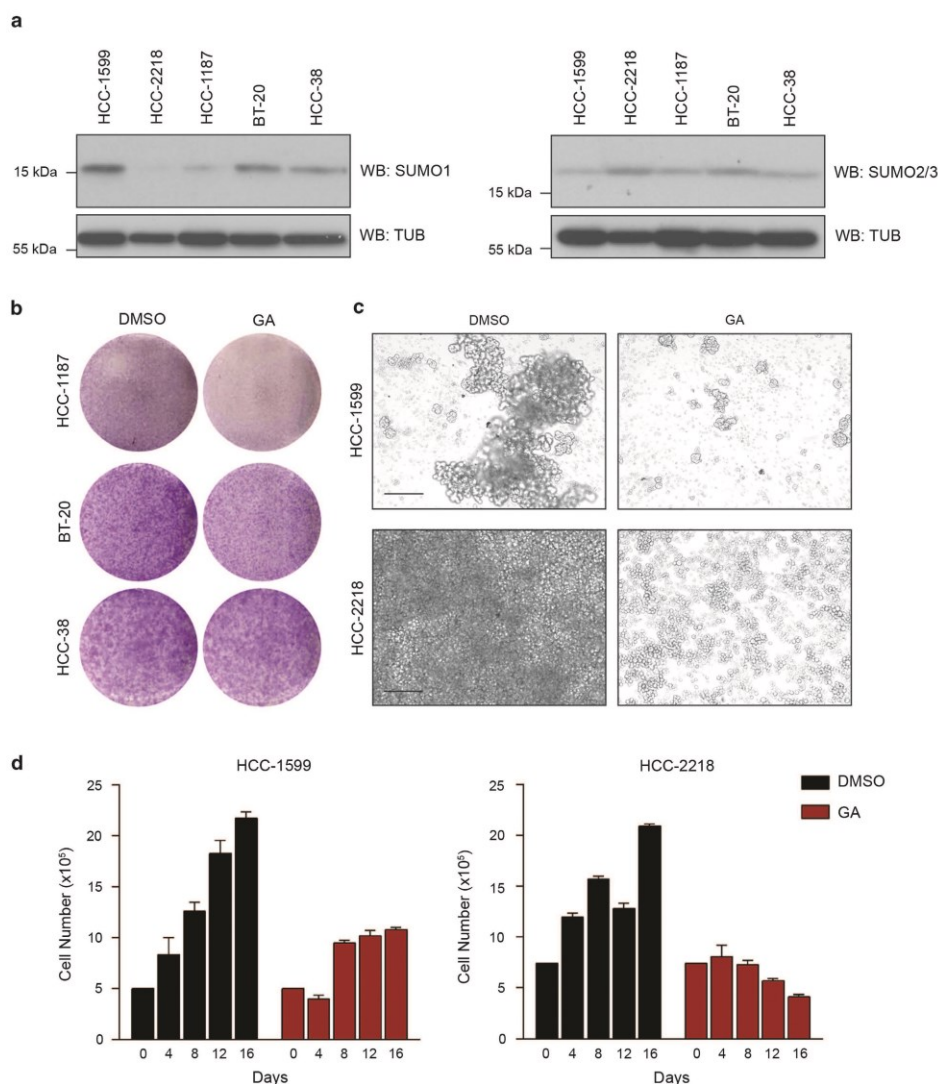


Figure 7. Sensitivity to GA correlates to SUMO levels in NOTCH breast cancer cell lines. **(a)** Western blotting analysis of unconjugated SUMO1 (left) and SUMO2/3 (right) levels in breast cancer cell lines bearing NOTCH translocations. Tubulin was used as a loading control. **(b)** Colony-formation assay of adherent NOTCH breast cancer cell lines treated with either DMSO or 30 μ M GA for 6 days. **(c)** Brightfield pictures of suspension NOTCH breast cancer cell lines treated with either DMSO or 30 μ M GA for 4 days. Scale bar = 100 μ m. **(d)** Cell counts of HCC-1599 and HCC-2218 cells treated with either DMSO or 30 μ M GA for the indicated time.

simplicity of our model allowed for an easier characterization of the mechanism behind the reported interaction. Among the top hits, we decided to focus on the interaction between NOTCH1 and *UBE2I*, given the potential to pharmacologically modulate the pathway using the recently published SUMOylation inhibitors.

We show that inhibition of SUMOylation through either knockdown of *UBE2I* or inhibition of SAE1/UBA2 with GA selectively impairs the growth of NOTCH1-activated cells. Notably,

a recent study reported on the sensitivity of MYC-overexpressing breast epithelial cells to inhibition of SUMOylation.⁴⁵ In this analysis, downregulation of a specific group of MYC-induced transcripts called SUMOylation-dependent MYC switchers (SMS genes) was observed upon inhibition of SUMOylation. The downregulation of these genes caused abnormal spindle formation and G2/M arrest in MYC-overexpressing cells. However, the MYC cell line from our panel showed only a weak depletion of the

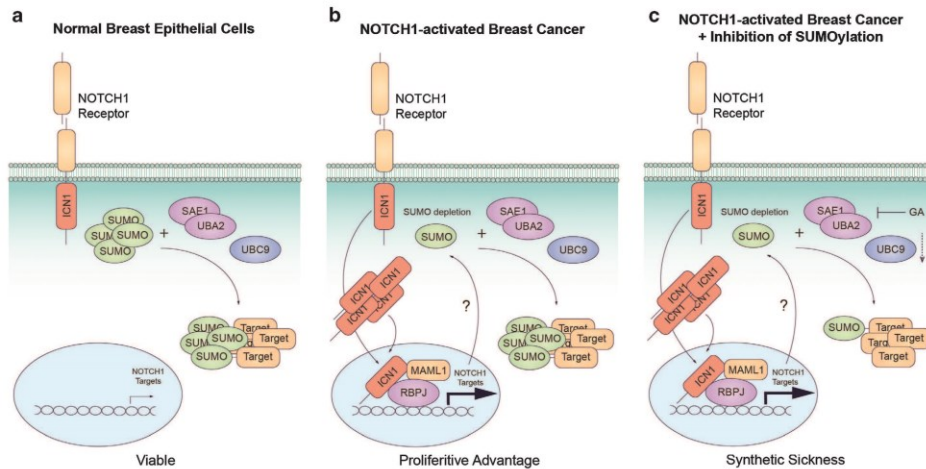


Figure 8. NOTCH1 activation depletes unconjugated SUMO and increases sensitivity to inhibition of SUMOylation cascade. **(a)** Breast epithelial cells show normal levels of unconjugated SUMO and are less susceptible to inhibition of SUMOylation. **(b)** NOTCH1 signaling activation leads to depletion of unconjugated SUMO leaving global protein SUMOylation unaffected. **(c)** Depleted SUMO in NOTCH1 cells increases sensitivity to knockdown of *UBE2I* (*UBC9*) or inhibition of *SAE1/UBA2* with GA.

hairpins targeting *UBE2I* (Supplementary Figure S3) with only one hairpin markedly over the selected fold change threshold. As reported, sensitivity to inhibition of SUMOylation correlates with MYC dependence and shows up only in the case of MYC addiction. MYC is also a downstream target of NOTCH1 signaling. However, we observed neither downregulation of SMS genes (Supplementary Figure S13) nor complete G2/M arrest upon inhibition of SUMOylation in NOTCH1 cells (data not shown); rather, they grow slower upon treatment with GA with evident delays in the S and G2/M phases before entering apoptosis. Therefore, we concluded that the interaction between NOTCH1 signaling and the SUMOylation cascade occurs through a different mechanism.

We showed greater inhibition of the SUMOylation cascade in NOTCH1 cells with both western blotting and immunofluorescence experiments. GA is a relatively lipophilic molecule ($\log P = 5.56$). It is not known how this small molecule enters the cell, but we speculated that it would simply diffuse through the plasma membrane. Indeed, our MRM experiments showed that there is no significant difference in the uptake of the molecule by MCF10A and NOTCH1 cells. Furthermore, our initial discovery was made using shRNAs against the SUMOylation cascade, again arguing against a compound uptake effect. Interestingly, NOTCH1 cells showed depleted levels of unconjugated SUMO1 and SUMO2/3 compared with MCF10A cells. Although we cannot rule out additional mechanisms, these differences could explain the observed selectivity (Figure 8): NOTCH1 activation depletes unconjugated SUMO1 and SUMO2/3 down to levels that are not detrimental to the cells but prompt for greater sensitivity to external perturbation of the SUMOylation cascade. In such a context, depletion of *UBC9* or inhibition of *SAE1/UBA2* would result in synthetic sickness. We support this hypothesis with SUMO knockdown experiments increasing the sensitivity of control MCF10A cells to inhibition of SUMOylation and overexpression experiments rescuing NOTCH1 cells from GA treatment. Finally, we recapitulated our finding in a clinically relevant breast cancer model: we observed similar correlations in patient-derived breast cancer cell lines recently reported to bear NOTCH1 and NOTCH2 translocations leading to constitutive activation of the pathway. Although NOTCH

receptors behave non-redundantly, a partial overlap of downstream targets could account for a common mechanism.

It is still not clear how NOTCH1 activation would deplete unconjugated SUMO levels. Regulation seems to occur at the protein level as we do not observe significant differences in SUMO mRNA levels (Supplementary Figure S14). NOTCH1-induced expression of proteins that are normally SUMOylated could deplete the cellular pool of SUMO down to levels that would not impair cellular fitness. Altered SUMO turnover by changes in the translation and degradation rates could provide another explanation.

Using a genetically engineered breast cancer model, we were able to uncover and characterize the specific interaction between two cellular pathways. Moving to a more clinically relevant context, we described the same interaction in patient-derived breast cancer cell lines. Our data support a model in which activation of NOTCH1 signaling pathway results in SUMO depletion and greater sensitivity to inhibition of SUMOylation and suggest SUMOylation cascade should be further investigated as a potential Achilles' heel of NOTCH1-driven breast cancer.

MATERIALS AND METHODS

Cell culture, plasmids and reagents

MCF10A (ATCC, Manassas, VA, USA, CRL10317) and all isogenic cell lines were cultured in Dulbecco's modified Eagle's medium/F12 supplemented with 5% horse serum (Thermo Fisher Scientific, Waltham, MA, USA), 1% penicillin-streptomycin (Sigma-Aldrich, St Louis, MO, USA), insulin (10 $\mu\text{g}/\text{ml}$, Thermo Fisher Scientific), cholera toxin (100 ng/ml, Sigma-Aldrich), epidermal growth factor (20 ng/ml, Sigma-Aldrich) and hydrocortisone (500 ng/ml, Sigma-Aldrich). HCC-38 (ATCC CRL-2314), HCC-1599 (ATCC CRL-2331), HCC-1187 (ATCC CRL-2322) and HCC-2218 (ATCC CRL-2343) were cultured in RPMI-1640 supplemented with 10% fetal bovine serum (Thermo Fisher Scientific) and 1% penicillin-streptomycin (Sigma-Aldrich). BT-20 (ATCC HTB-19) cells were cultured in Minimum Essential Medium α supplemented with 10% fetal bovine serum (Thermo Fisher Scientific) and 1% penicillin-streptomycin (Sigma-Aldrich). pcDNA3-HA-SUMO3⁴⁹ (plasmid 17361) was purchased from Addgene (Cambridge, MA, USA). *UBE2I* was cloned in the retroviral vector pMSCV-StrepHA-GW-hPGK-Bla using Gateway Cloning (Thermo Fisher Scientific). Ginkgolic acid C15:1 was purchased from Sigma-Aldrich. DAPT was purchased from Selleck Chemicals (Houston, TX, USA).



Epigenome-focused shRNA library and pooled shRNA screen

The lentiviral library has been produced at The RNAi Consortium (TRC) of the Broad Institute and is based on the pLKO.1 vector carrying a puromycin-resistance cassette. Pooled lentiviral screens have been extensively described elsewhere.^{50,51} Briefly, hairpins of comparable titers were pooled, and the library was titrated together with puromycin on MCF10A cells to define optimal multiplicity of infection and concentration, respectively. In the screen, cells were infected at a multiplicity of infection of 3 and selected with 2 µg/ml puromycin. One million cells per sample were infected and maintained in culture until the end of the experiment. The screen was performed in duplicates. At the end, cell pellets were collected and genomic DNA was extracted using the DNA Wizard kit (Promega, Fitchburg, WI, USA). A first outer PCR was performed with ExTaq polymerase (Millipore, Billerica, MA, USA) on a total amount of 3 µg of genomic DNA for each sample. PCR products were then barcoded during an inner PCR. After purification, PCR products were quantified with Nanodrop (Wilmington, DE, USA) and pooled accordingly. Pooled samples were sequenced with a HiSeq2000 (Illumina, San Diego, CA, USA) using a 50-bp single-read protocol. Primers are listed in Supplementary Table S6.

Data analysis

Raw data from the pooled shRNA screen were initially processed and deconvoluted using a Pipeline Pilot protocol (Accelrys, San Diego, CA, USA) requiring perfect matches of the sequencing reads to the 4-base barcode and the 21-base hairpin sequences. Cell lines showing poor hairpin reads correlation between biological replicates ($R^2 < 0.7$) were excluded from any further analysis (that is, FGFR1, CCND1, IKBKE). Normalization of the data was performed using an adapted version of a previously described procedure.⁵² The Log of the fold change over the median across all samples was calculated for all hairpins. A 3.2-fold change threshold (Log(fold change) < -0.5) was arbitrarily selected as a first hit criterion. Gene hits scoring with ≥ 2 hairpins were then prioritized. We also used available data on knockdown efficiency to further discriminate among candidate hits.

Quantitative reverse transcriptase-PCR

RNA was extracted using the RNeasy kit (Qiagen, Venlo, Netherlands). cDNA was synthesized using a kit from Thermo Fisher Scientific. Quantitative reverse transcriptase-PCR was performed using the SYBR Green Master mix from Thermo Fisher Scientific on a LightCycler 480 (Roche, Basel, Switzerland). Primers are listed in Supplementary Table S6.

Western blotting

Cells were lysed using RIPA buffer supplemented with a cocktail of protease inhibitors (Roche) and the SUMO protease inhibitor *N*-ethylmaleimide (50 mM) for the SUMOylation analysis. Lysates were resolved using sodium dodecyl sulfate-polyacrylamide gel electrophoresis. UBC9, SUMO1, SUMO2/3, HA-tag and α TUB antibodies were purchased from Abcam (Cambridge, UK). MYC-tag antibody was purchased from Cell Signaling Technology (Danvers, MA, USA).

Competition assay

An equal amount of MCF10A and NOTCH1 cells was seeded in six-well plates. Co-cultures of MCF10A and NOTCH1 cells were infected with either a control vector or *UBE2I* hairpins after 24 h. After puromycin selection, cells were analyzed using flow cytometry (FACSCalibur, BD Biosciences, San Jose, CA, USA), reseeded and then analyzed every 3 days. When the experiment was performed with the inhibitor, cells were treated the day after the seeding with DMSO or 30 µM GA and analyzed using flow cytometry after 3 days; cells were then reseeded and treated again to continue the experiment.

Growth curves

In all, 50 000 cells/well were seeded in six-well plates and treated after 24 h with either DMSO or 30 µM GA. After 3 days, cells were counted using a CASY counter (Roche), reseeded and treated again to continue the experiment.

Colony-formation assay

In all, 25 000 cells/well (MCF10A or other isogenic cells) were seeded in six-well plates and treated with DMSO or GA after 24 h. Treatment with the inhibitor was refreshed after 3 days. Cells were washed with phosphate-

buffered saline (PBS) after 6 days, fixed using 3.7% paraformaldehyde and stained with crystal violet. For the SUMO3 overexpression experiment, 100 000 cells/well were seeded in six-well plates. Cells were transfected 24 h later using Lipofectamine 2000 (Thermo Fisher Scientific) with a transfection efficiency of around 30%. After 48 h, cells were treated with DMSO or 30 µM GA as above. At day 6, surviving cells were allowed to grow in fresh medium for 3 more days. In all, 100 000 or 35 000 cells/well were seeded in six-well plates for HCC-1187 and HCC-38 or BT-20 cells, respectively.

Gene expression profiling

Cells were treated with either DMSO or 30 µM GA, and RNA was extracted after 3 days. Libraries were prepared using the ScriptSeq Complete Gold Kit (Epicentre, Illuminia). Pooled libraries were sequenced with a HiSeq2000 (Illumina) using a 50-bp single-read protocol. RNA-seq reads were aligned to the human genome using TopHat (Johns Hopkins University, Baltimore, MD, USA). Cufflinks was employed to normalize the data and perform relevant comparisons among the different samples. Experiment was performed in duplicates. FPKM (fragments per kilo bases of exons per million mapped reads) values and fold changes of significantly upregulated and downregulated genes are reported in Supplementary Table S4.

Cell cycle analysis

Cells were synchronized using the double thymidine treatment as described previously.⁵² At the end of the synchronization procedure, cells were released and treated with either DMSO or 30 µM GA for 12 h. Samples were taken every 2 h for cell cycle analysis. The cell cycle was analyzed using propidium iodide staining. Briefly, cells were harvested, resuspended in PBS and fixed with cold 70% ethanol for 15 min. After centrifugation, ethanol was removed, and the cells were rehydrated in PBS for 10 min. RNase A was added to a final concentration of 1 µg/ml, and the cells were incubated at 37 °C for 30 min. Propidium iodide was finally added at a final concentration of 1 µg/ml. Cells were then analyzed using flow cytometry.

Apoptosis assay

In all, 25 000 cells/well were seeded in six-well plates and treated with DMSO or 30 µM GA after 24 h. GA was refreshed after 3 days. At day 6, cells were harvested, washed with PBS, labeled in Annexin V-binding buffer with Alexa Fluor 647 Annexin V antibody (Biolegend, San Diego, CA, USA) and propidium iodide and analyzed using flow cytometry.

Immunofluorescence

Cells were washed with PBS and fixed with cold methanol for 1 h. Blocking was performed in PBS 3% bovine serum albumin and 0.1% Triton for 20 min. Cells were then incubated with primary antibody for 30 min at room temperature. After washing, they were incubated with secondary antibody (Alexa Fluor 488 Goat Anti-Rabbit, Thermo Fisher Scientific) and DAPI (4,6-diamidino-2-phenylindole) for 30 min at room temperature in the dark. After washing with PBS, cells were analyzed using an Operetta microscope (PerkinElmer, Waltham, MA, USA).

MRM

Cells were seeded in six-well plates and treated with DMSO or 30 µM GA for the indicated time. After washing with cold PBS, cells were lysed using 80% methanol. After centrifugation, the supernatant was immediately injected in a UPLC/MS system (Xevo, Waters, Milford, MA, USA) to analyze the abundance of GA. The amount of inhibitor was normalized to the protein content and using a GA standard curve. The MRM method on the mass spectrometer was established using the IntelliStart Technology (Waters).

CONFLICT OF INTEREST

The authors declare no conflict of interest.

ACKNOWLEDGEMENTS

We thank John Doench, Serena Silver and David E Root (Broad Institute of MIT and Harvard) for shRNA tools and screening protocols; Johannes Bigenzahn (CeMM) for providing the pMSCV-StrepHA-GW-hPGK-Bla vector; and Erika Schirghuber (CeMM) and Berend Snijder (CeMM) for critically reading the manuscript. SK acknowledges support by a Marie Curie Career Integration Grant, the Austrian Federal Ministry of

Science, Research and Economy and the National Foundation for Research, Technology and Development.

REFERENCES

- Maxmen A. The hard facts. *Nature* 2012; **485**: 550–551.
- Stephens PJ, Tarpey PS, Davies H, Van Loo P, Greenman C, Wedge DC *et al*. The landscape of cancer genes and mutational processes in breast cancer. *Nature* 2012; **486**: 400–404.
- Curtis C, Shah SP, Chin S-F, Turashvili G, Rueda OM, Dunning MJ *et al*. The genomic and transcriptomic architecture of 2000 breast tumours reveals novel subgroups. *Nature* 2012; **486**: 346–352.
- Cancer Genome Atlas Network. Comprehensive molecular portraits of human breast tumours. *Nature* 2012; **490**: 61–70.
- Weinstein IB. Addiction to oncogenes—the Achilles heel of cancer. *Science* 2002; **297**: 63–64.
- Druker BJ, Talpaz M, Resta DJ, Peng B, Buchdunger E, Ford JM *et al*. Efficacy and safety of a specific inhibitor of the BCR-ABL tyrosine kinase in chronic myeloid leukemia. *New Engl J Med* 2001; **344**: 1031–1037.
- Vogel CL, Cobleigh MA, Tripathy D, Guthell JC, Harris LN, Fehrenbacher L *et al*. Efficacy and safety of trastuzumab as a single agent in first-line treatment of HER2-overexpressing metastatic breast cancer. *J Clin Oncol* 2002; **20**: 719–726.
- Flaherty KT, Puzanov I, Kim KB, Ribas A, McArthur GA, Sosman JA *et al*. Inhibition of mutated, activated BRAF in metastatic melanoma. *New Engl J Med* 2010; **363**: 809–819.
- Luo J, Solimini NL, Elledge SJ. Principles of cancer therapy: oncogene and non-oncogene addiction. *Cell* 2009; **136**: 823–837.
- Kaelin WG. The concept of synthetic lethality in the context of anticancer therapy. *Nat Rev Cancer* 2005; **5**: 689–698.
- Nijman SMB. Synthetic lethality: general principles, utility and detection using genetic screens in human cells. *FEBS Lett* 2011; **585**: 1–6.
- Neshat MS, Mellinghoff IK, Tran C, Stiles B, Thomas G, Petersen R *et al*. Enhanced sensitivity of PTEN-deficient tumors to inhibition of FRAP/mTOR. *Proc Natl Acad Sci* 2001; **98**: 10314–10319.
- Fong PC, Boss DS, Yap TA, Tutt A, Wu P, Mergui-Roelvink M *et al*. Inhibition of poly (ADP-ribose) polymerase in tumors from BRCA mutation carriers. *New Engl J Med* 2009; **361**: 123–134.
- Mair B, Kubicek S, Nijman SM. Exploiting epigenetic vulnerabilities for cancer therapeutics. *Trends Pharmacol Sci* 2014; **35**: 136–145.
- Johnson David G, Dent Sharon YR. Chromatin: receiver and quarterback for cellular signals. *Cell* 2013; **152**: 685–689.
- Al-Hussaini H, Subramanyam D, Reedijk M, Sridhar SS. Notch signaling pathway as a therapeutic target in breast cancer. *Mol Cancer Ther* 2010; **10**: 9–15.
- Mazzone M, Selfors LM, Albeck J, Overholtzer M, Sale S, Carroll DL *et al*. Dose-dependent induction of distinct phenotypic responses to Notch pathway activation in mammary epithelial cells. *Proc Natl Acad Sci* 2010; **107**: 5012–5017.
- Kopan R, Ilagan MXG. The canonical notch signaling pathway: unfolding the activation mechanism. *Cell* 2009; **137**: 216–233.
- Radtke F, Fasnacht N, MacDonald HR. Notch signaling in the immune system. *Immunity* 2010; **32**: 14–27.
- Aifantis I, Raetz E, Buonamici S. Molecular pathogenesis of T-cell leukaemia and lymphoma. *Nat Rev Immunol* 2008; **8**: 380–390.
- Ranganathan P, Weaver KL, Capobianco AJ. Notch signalling in solid tumours: a little bit of everything but not all the time. *Nat Rev Cancer* 2011; **11**: 338–351.
- Grabher C, von Boehmer H, Look AT. Notch 1 activation in the molecular pathogenesis of T-cell acute lymphoblastic leukaemia. *Nat Rev Cancer* 2006; **6**: 347–359.
- Lobry C, Oh P, Aifantis I. Oncogenic and tumor suppressor functions of Notch in cancer: it's NOTCH what you think. *J Exp Med* 2011; **208**: 1931–1935.
- Bray SJ. Notch signalling: a simple pathway becomes complex. *Nat Rev Mol Cell Biol* 2006; **7**: 678–689.
- Andersson ER, Lendahl U. Therapeutic modulation of Notch signalling—are we there yet? *Nat Rev Drug Discov* 2014; **13**: 357–378.
- Falk R, Falk A, Dyson MR, Melidoni AN, Parthiban K, Young JL *et al*. Generation of anti-Notch antibodies and their application in blocking Notch signalling in neural stem cells. *Methods* 2012; **58**: 69–78.
- Moeller RE, Cornejo M, Davis TN, Bianco CD, Aster JC, Blacklow SC *et al*. Direct inhibition of the NOTCH transcription factor complex. *Nature* 2009; **462**: 182–188.
- Rao SS, O'Neil J, Liberator CD, Hardwick JS, Dai X, Zhang T *et al*. Inhibition of NOTCH signaling by gamma secretase inhibitor engages the RB pathway and elicits cell cycle exit in T-cell Acute lymphoblastic leukemia cells. *Cancer Res* 2009; **69**: 3060–3068.
- Purov B. Notch inhibition as a promising new approach to cancer therapy. *Adv Exp Med Biol* 2012; **727**: 305–319.
- Robinson DR, Kalyana-Sundaram S, Wu Y-M, Shankar S, Cao X, Ateeq B *et al*. Functionally recurrent rearrangements of the MAST kinase and Notch gene families in breast cancer. *Nat Med* 2011; **17**: 1646–1651.
- Geiss-Friedlander R, Melchior F. Concepts in sumoylation: a decade on. *Nat Rev Mol Cell Biol* 2007; **8**: 947–956.
- Gareau JR, Lima CD. The SUMO pathway: emerging mechanisms that shape specificity, conjugation and recognition. *Nat Rev Mol Cell Biol* 2010; **11**: 861–871.
- Gill G. SUMO and ubiquitin in the nucleus: different functions, similar mechanisms? *Genes Dev* 2004; **18**: 2046–2059.
- Seeler J-S, Dejean A. Nuclear and unclear functions of SUMO. *Nat Rev Mol Cell Biol* 2003; **4**: 690–699.
- Shiio Y, Eisenman RN. Histone sumoylation is associated with transcriptional repression. *Proc Natl Acad Sci* 2003; **100**: 13225–13230.
- Knipscheer P, Flotho A, Klug H, Olsen JV, van Dijk WJ, Fish A *et al*. Ubc9 sumoylation regulates SUMO target discrimination. *Mol Cell* 2008; **31**: 371–382.
- Mo Y-Y, Yu Y, Theodosiou E, Rachel EL, Beck WT. A role for Ubc9 in tumorigenesis. *Oncogene* 2005; **24**: 2677–2683.
- Moschos SJ, Smith AP, Mandic M, Athanassiou C, Watson-Hurst K, Jukic DM *et al*. SAGE and antibody array analysis of melanoma-infiltrated lymph nodes: identification of Ubc9 as an important molecule in advanced-stage melanomas. *Oncogene* 2007; **26**: 4216–4225.
- Garnett MJ, Edelman EJ, Heidorn SJ, Greenman CD, Dastur A, Lau KW *et al*. Systematic identification of genomic markers of drug sensitivity in cancer cells. *Nature* 2012; **483**: 570–575.
- Barretina J, Caponigro G, Stransky N, Venkatesan K, Margolin AA, Kim S *et al*. The Cancer Cell Line Encyclopedia enables predictive modelling of anticancer drug sensitivity. *Nature* 2012; **483**: 603–607.
- Marcotte R, Brown KR, Suarez F, Sayad A, Karamboulas K, Krzyzanowski PM *et al*. Essential gene profiles in breast, pancreatic, and ovarian cancer cells. *Cancer Discov* 2011; **2**: 172–189.
- Muellner MK, Uras IZ, Gapp BV, Kerzendorfer C, Smida M, Lechtermann H *et al*. A chemical-genetic screen reveals a mechanism of resistance to PI3K inhibitors in cancer. *Nat Chem Biol* 2011; **7**: 787–793.
- Fukuda I, Ito A, Hirai G, Nishimura S, Kawasaki H, Saitoh H *et al*. Ginkgolic acid inhibits protein SUMOylation by blocking formation of the E1-SUMO intermediate. *Chem Biol* 2009; **16**: 133–140.
- Jarriault S, Brou C, Loegeat F, Schroeter EH, Kopan R, Israel A. Signalling downstream of activated mammalian Notch. *Nature* 1995; **377**: 355–358.
- Subramanian A, Tamayo P, Mootha VK, Mukherjee S, Ebert BL, Gillette MA *et al*. Gene set enrichment analysis: a knowledge-based approach for interpreting genome-wide expression profiles. *Proc Natl Acad Sci* 2005; **102**: 15545–15550.
- Pfander B, Moldovan G-L, Sacher M, Hoegge C, Jentsch S. SUMO-modified PCNA recruits Srs2 to prevent recombination during S phase. *Nature* 2005; **436**: 428–433.
- Hay RT. Sumo: a history of modification. *Mol Cell* 2005; **18**: 1–12.
- Kessler JD, Kahle KT, Sun T, Meerbrey KL, Schlabach MR, Schmitt EM *et al*. A SUMOylation-dependent transcriptional subprogram is required for Myc-driven tumorigenesis. *Science* 2011; **335**: 348–353.
- Kamitani T, Nguyen HP, Kito K, Fukuda-Kamitani T, Yeh ET. Covalent modification of PML by the sentrin family of ubiquitin-like proteins. *J Biol Chem* 1998; **273**: 3117–3120.
- Moffat J, Grueneberg DA, Yang X, Kim SY, Kloepper AM, Hinkle G *et al*. A lentiviral RNAi library for human and mouse genes applied to an arrayed viral high-content screen. *Cell* 2006; **124**: 1283–1298.
- Sims D, Mendes-Pereira AM, Frankum J, Burgess D, Cerone M-A, Lombardelli C *et al*. High-throughput RNA interference screening using pooled shRNA libraries and next generation sequencing. *Genome Biol* 2011; **12**: R104.
- Whitfield ML, Zheng LX, Baldwin A, Ohta T, Hurt MM, Marzluff WF. Stem-loop binding protein, the protein that binds the 3' end of histone mRNA, is cell cycle regulated by both translational and posttranslational mechanisms. *Mol Cell Biol* 2000; **20**: 4188–4198.

Supplementary Information accompanies this paper on the Oncogene website (<http://www.nature.com/onc>)

A combinatorial screen of the CLOUD uncovers a synergy of approved drugs targeting the androgen receptor

Resistance mechanisms contribute to the complexity of cancer and are better addressed by multicomponent therapeutics. Drug repurposing has been shown to be a valid alternative for the formulation of new cancer treatments (Ashburn & Thor, 2004) but has not been thoroughly evaluated in the context of drug combinations mainly because combinatorial screens of even relatively small libraries easily overcome the standard throughput of screening platforms. To address this problem, we defined a non-redundant library of FDA-approved drugs containing structurally and biologically unique representatives of clinical compounds. We named this collection of small molecules the CeMM Library of Unique Drugs (CLOUD) and performed a pairwise combinatorial screen to uncover synergies of approved drugs that could be repurposed as more efficient and patient-specific cancer pharmacological treatments. A description of the combinatorial screen and the validation of a synergistic interaction have been collected in the following manuscript submitted for publication.

A combinatorial screen of the CLOUD uncovers a synergy of approved drugs targeting the androgen receptor

Authors: M. P. Licciardello¹, P. Markt^{1†}, F. Klepsch^{1‡}, C.-H. Lardeau¹, G. Dürnberger^{1§}, V. Ivanov³, J. Colinge^{1¶}, S. Kubicek^{1,2*}

Affiliations:

¹CeMM Research Center for Molecular Medicine of the Austrian Academy of Sciences, Vienna, Austria.

²Christian Doppler Laboratory for Chemical Epigenetics and Antiinfectives, CeMM Research Center for Molecular Medicine of the Austrian Academy of Sciences, Vienna, Austria.

³Enamine Ltd, Kiev, Ukraine.

†Current address: LKI Pharmacy, Innsbruck, Austria.

‡Current address: Chemical Computing Group Inc., Cologne, Germany.

§Current address: Gregor Mendel Institute, Vienna, Austria.

¶Current address: Faculté de Médecine, Université de Montpellier, France; Institut de Recherche en Cancérologie de Montpellier, Inserm U1194, France; Institut régional du Cancer Montpellier, France.

*Correspondence: Dr Stefan Kubicek, CeMM Research Center for Molecular Medicine of the Austrian Academy of Sciences, Lazarettgasse 14 AKH BT 25.3 1090 Vienna, Austria. Phone +43-1/40160-70 036 Fax +43-1/40160-970 000
E-mail: skubicek@cemm.oeaw.ac.at

One Sentence Summary: We performed a combinatorial screen of a library of FDA-approved drugs and uncovered a synergistic interaction between flutamide and phenprocoumon that could be clinically translated for the treatment of prostate cancer.

Abstract: Approved drugs are invaluable tools to study biochemical pathways playing important roles in human health and disease. Moreover, further functional and mechanistic characterization of clinical compounds may lead to repurposing of single drugs or combinations. Here, we describe the cheminformatic approach that led to a collection of small molecules representing all FDA-approved chemical entities: the CeMM Library of Unique Drugs (CLOUD). The CLOUD is designed to best represent the chemical and biological space of approved drugs, cover prodrugs and active forms, and allow for combinatorial screens at pharmacologically relevant concentrations. In one such screen we discovered the synergistic interaction between flutamide and phenprocoumon (PPC). We show that PPC modulates the stability of the androgen receptor (AR) and resensitizes AR mutant prostate cancer cells to flutamide. Collectively, our data suggest that PPC might be clinically repurposed to tackle resistance to antiandrogens in prostate cancer patients.

Introduction

Drug discovery is a challenging process easily spanning 10-15 years (1). In spite of the recent advances in screening and sequencing technologies, the number of new molecular entities (NMEs) (2) approved every year still hobbles below expectations (2, 3). Recently, both industry and academia have tried to bypass the hurdles in the drug discovery process by repositioning clinical compounds for additional indications (so-called drug repurposing) (4).

Patient diversity and drug resistance still represent significant obstacles in long-term pharmacological treatment of diseases such as cancer or infections (5, 6). Multicomponent therapeutics has been shown to be an effective alternative in these circumstances (7) providing a new strategy for more personalized medicine. Notably, combinations of already approved products would have the obvious advantage of dealing with safe, effective and bioavailable drugs. Moreover, approved drugs comprise some of the best studied organic small molecules and for many of them the biological target and mechanism of action are known.

These unique features have prompted two recent academic efforts to take on the challenge of cataloguing and collecting all drugs approved for human or veterinary use (8, 9). However, access to these comprehensive libraries is limited to scientists affiliated to the corresponding institutions or to external collaborators when screenings are performed on site. Moreover, a systematic pairwise combinatorial high-throughput screen (HTS) of all 14,814 molecules currently in the NCGC pharmaceutical collection (9) would generate more than 100 million data points, an effort beyond the current capacity of screening facilities. There are also several commercially available libraries of approved drugs containing between 780 and 1600 compounds. However, these collections do not cover all drug classes.

In this study, we report a strategy to computationally derive a set of representative FDA-approved drugs. Our aim was to generate a collection that optimally captures the chemical and biological diversity of all clinical compounds while fitting to a single 384-well screening plate. We annotated this collection with human maximum plasma concentrations reported in the literature to encourage HTS at pharmacologically relevant ranges. Moreover, for all substances administered as prodrugs we included the respective active form. We named this collection of clinical compounds the CeMM Library of Unique Drugs (CLOUD).

The non-redundant nature of our library allows for the systematic investigation of all combinations of CLOUD drugs. In one such combinatorial HTS we uncovered the synergistic interaction between flutamide (10), an AR antagonist, and PPC (11), a vitamin K epoxide reductase complex subunit 1 (VKORC1) (12) inhibitor. The AR normally resides in the cytoplasm bound to chaperones such as HSP90 (13). Upon binding of dihydrotestosterone (DHT) the AR changes its conformation and translocates into the nucleus where it binds androgen responsive elements (AREs) driving the transcription of canonical targets such as *KLK3* (also known as prostate specific antigen PSA), *TMPRSS2* and *KLK2* (14, 15). Flutamide is a non-steroidal antiandrogen approved for the treatment of prostate cancer (16). It competes with DHT working as an AR antagonist (10). However, AR mutations such as T877A have been reported to switch the activity of flutamide from antagonist to agonist (17, 18) and have been described as a resistance mechanism to antiandrogen therapy (19). Vitamin K is an important cofactor of the enzyme γ -glutamyl carboxylase (GGCX) which catalyzes the γ -carboxylation of glutamic acid residues in proteins involved in the coagulation cascade (20, 21). In this reaction, GGCX oxidizes vitamin K hydroquinone to vitamin K epoxide (22). The VKORC1 enzyme converts oxidized vitamin K back to its reduced form (23) sustaining the cellular pool of the cofactor. PPC, a coumarin anticoagulant used for the treatment of thrombosis, inhibits VKORC1 and therefore vitamin K-dependent γ -carboxylations and the coagulation cascade (11). Here, we show that PPC restrains the induction of AR canonical targets by flutamide in a prostate cancer cell line carrying a T877A mutated AR and where flutamide normally behaves as an agonist. The combination of these two approved drugs leads to AR degradation and apoptosis of an AR-dependent prostate cancer model. Our findings suggest that PPC could be repurposed in the clinic to address prostate cancer resistance to AR antagonists mediated by AR mutations such as T877A.

Results

A representative library of approved drugs

In order to generate a representative library of clinical compounds we retrieved all approved products from the Drugs@FDA Database (www.fda.gov). This resource contains prescription and over-the-counter small molecules and therapeutic biologicals approved for human use together with drugs discontinued for reasons other than safety (e.g. for economic reasons). First, we determined and extracted the 2,171 unique active ingredients responsible for the biological effects of the 26,800 products retrieved from the database (Fig. 1A). In order to obtain a small molecule collection suitable for HTS we discarded all macromolecules (e.g. enzymes, antibodies, polysaccharides) narrowing our set down to 1,929 small molecules. We proceeded removing all salt fragments and keeping only 1,416 unique molecular entities. Furthermore, all FDA-approved molecules exerting their biological effects through mechanisms other than DNA alteration/interaction, protein-ligand interaction or that are not used to treat diseases (e.g. diagnostic agents, dietary supplements, disinfectant, blood substitutes, perfusion solutions, metabolism products, surfactants, stomatological preparations, throat preparations) or that can only be found in topical products (e.g. dermatologicals, nail polish) were removed. This filtering scheme produced a collection of 955 systemically active small molecules that we called the STEAM (SystEMic smAll Molecules) (table S1). To condense the STEAM into the CLOUD we temporarily removed 35 drugs with unknown target. The remaining small molecules were annotated with their biological activity and grouped into classes accordingly (table S1). Each class contains all drugs for a specific target or protein family (e.g. DNA, androgen receptor, histone deacetylases) with the same mechanism of action (e.g. agonist, antagonist). Drugs belonging to the same class are often structurally very similar: this is due to many so-called “me too” drugs (24) developed by competing pharmaceutical companies. While minor structural differences might change important pharmacological parameters and side effects *in vivo*, we reasoned that structurally very similar molecules belonging to the same class would behave redundantly in most screening assays. Therefore, we decided to keep only representative compounds for each of these classes. We clustered all drugs within a specific class according to their chemical structure and selected molecules at cluster centers (Materials and Methods). For example, out of four structurally very similar dihydrofolate reductase inhibitors only methotrexate was selected by the clustering

algorithm (Fig. 1A). However, some drug classes are populated by structurally different molecules. For instance, histone deacetylases can be inhibited by the small hydroxamic acid vorinostat and the cyclic peptide romidepsin: in such cases all different structures were kept (Fig. 1B). Moreover, some drug classes cover a broader range of therapeutic activities. Depending on their receptor subtypes serotonin receptor agonists can be used to treat anxiety (5-HT_{1A}), migraine (5-HT_{1B/1D/1F}) and disorders of gastrointestinal motility (5-HT₄). For such drug classes the clustering parameters were relaxed to allow for the selection of structurally more related compounds covering a broader range of therapeutic indications (table S1). Structural clustering of 176 classes resulted in 239 representative drugs optimized for chemical diversity and coverage of biological activities. To enable detection of compound activity in both biochemical and cellular assays, we searched the literature for prodrugs among these 239 molecules. We identified 35 prodrugs for which the corresponding active form was included in our screening collection (table S2). Finally, the 35 drugs with unknown target from the STEAM were directly added to this final collection of 309 approved small molecules that we named the CLOUD – the CeMM Library of Approved Drugs. The CLOUD covers more drug classes compared to other commercially available libraries containing FDA-approved drugs (fig. S1A) and exclusively provides active forms of prodrugs (fig. S1B).

The CLOUD covers target and physicochemical space of FDA-approved drugs

We addressed the clustering procedure for potential biases in target organisms, target proteins or physicochemical properties. The 955 STEAM drugs with known mechanism of action target mostly human proteins (80%, fig. S2A) followed by bacterial (14%), viral (4%), protozoal, fungal and helminthic (2%) targets. CLOUD drugs showed a similar distribution with a minor reduction in drugs targeting bacterial proteins (fig. S2A): this difference is easily explained by the high number of structurally similar antibiotics acting on the dihydropteroate synthase, penicillin-binding proteins and the ribosome. A protein target classification of STEAM drugs showed that the majority of approved small molecules target G protein-coupled receptors (GPCRs, 27%, fig. S2B) as already reported (25). Other prominent targets are ion channels (14%), oxidoreductases (10%), transferases (8%), nuclear receptors (7%) and hydrolases (7%). Again, CLOUD drugs showed a similar pattern (fig. S2B). Furthermore, drugs usually obey to the so-called Lipinski's rule of five (26). As expected STEAM drugs tend not to violate this rule (Fig.

1C) and CLOUD drugs showed the same trend. Moreover, when the physicochemical properties contemplated by the Lipinski's rule of five (i.e. molecular weight, hydrogen bond acceptors/donors, logP) as well as the number of rotatable bonds were analyzed individually, no significantly different distribution was observed comparing the CLOUD to the STEAM (fig. S3A-E). This confirmed that the 239 CLOUD drugs with known target did not only reflect the target distribution but also covered the physicochemical space of the 955 initially selected FDA-approved small molecules.

Approved drugs have been extensively annotated with pharmacological data including peak plasma concentrations in humans. These concentrations vary over several orders of magnitude (Fig. 1D). In order to reproduce conditions close to clinical settings we prepared stocks of CLOUD drugs so to allow screens in the range of their plasma concentration. Furthermore, we arranged all CLOUD drugs in a single 384-well plate with the aim of creating an easily accessible reference library for repurposing and annotating clinical compounds.

Finally, to ensure that this library functionally preserved most of the biological activities addressed by STEAM drugs, we analyzed gene expression profiles reported for compounds belonging to the same class. The Connectivity Map (CMap) (27) represents an optimal database for such analyses. To eliminate batch-effects from CMap data, we used DIPS scores (28) as they provide efficient data normalization. Pairwise DIPS scores within CLOUD clusters are significantly increased compared to random drug pairs indicating a similar influence of co-clustered drugs on cellular responses (Fig. 1E).

A synergistic interaction between flutamide and PPC

Drug repurposing has already produced successful new applications of approved drugs (29, 30). More recently, it has been emphasized that combinations of different molecules can improve the outcome of pharmacological therapies (7). The CLOUD allows for effective combinatorial screenings of clinical compounds using different assays. In one such screen we investigated the effect of 40,470 pairwise combinations of CLOUD drugs on the viability of KBM7 cells, a near haploid human chronic myeloid leukemia (CML) cell line (31) that allows for rapid downstream functional characterizations of drug targets and mechanisms of action (32, 33). Combinations of CLOUD drugs were analyzed for potential synergy or antagonism according to the Bliss independence model (34) and 254 hits were selected for a counter-screen (Fig. 2A). We then selected the top 20

synergies and antagonisms among the hits that validated in the counter-screen (Fig. 2B and table S3) and investigated these further in dose-response matrices: the synergistic interaction between flutamide and PPC stood out as the most significant hit of the screen (fig. S4 and Fig. 2C).

KBM7 cells allow for the generation of human gene knockouts by insertional mutagenesis (35, 36). In order to validate the specificity of the target we addressed the effect of the drug combination on a KBM7 clone carrying a gene-trap in the *AR* gene (AR KO KBM7). We first validated the knockout of the *AR* gene using reverse transcription quantitative polymerase chain reaction (RT-qPCR) (Fig. 2D) and western blotting (Fig. 2E). Upon treatment with different concentrations of flutamide and PPC in combination, AR KO KBM7 cells showed increased resistance compared to wild type KBM7 cells (Fig. 2F). A closer inspection of the position of the gene-trap locus revealed an AR isoform (AR45) (37) downstream of the inserted cassette (fig. S5A). The presence of this alternative isoform and residual transcripts of the full length AR in AR KO KBM7 cells (fig. S5B) might explain the incomplete resistance to the combination.

Flutamide and PPC induce apoptosis in LNCaP cells

AR signaling has been shown to play a crucial role in the development of prostate cancer (38). Current pharmacological treatments aim at a reduction of androgen levels or inhibition of the pathway with AR antagonists (39). Even though patients usually respond well to antiandrogen therapy initially, cancer cells inevitably develop resistance mechanisms hampering the efficiency of the treatment (40). Drug combinations have proven to be a valid alternative to circumvent drug resistance and the use of already approved drugs entails different pharmacological and clinical benefits. In order to evaluate the translational potential of the CLOUD and of the synergistic interaction we have uncovered in our combinatorial screen, we addressed the effect of the combination of flutamide and PPC on prostate cancer cell lines. We performed dose-response measurements on LNCaP cells, an AR-dependent prostate cancer cell line carrying a T877A mutation in the *AR* gene (17). This mutation has been described in prostate cancer patients (18) and reported to confer resistance to AR antagonists. LNCaP cells showed a marked sensitivity to the combination of flutamide and PPC while PC-3 prostate cancer cells, which express very low levels of AR (41), were only mildly affected at very high concentrations (Fig. 3A and fig. S6). Notably, we obtained similar results

exchanging PPC with warfarin, another VKORC1 inhibitor, or flutamide with bicalutamide, another AR antagonist (fig. S7A). Two other antiandrogens, namely enzalutamide and nilutamide, also showed a synergistic interaction with PPC, albeit to a lower extent compared to flutamide (fig. S7B). To better elucidate the cellular death mechanism triggered by the two compounds, we performed Annexin V staining and flow cytometry analysis of LNCaP cells treated with either the drugs alone or in combination. Only the treatment with both flutamide and PPC induced apoptosis in this prostate cancer cell line (Fig. 3B).

Binding of flutamide in the presence of PPC leads to AR downregulation

To better understand the effect of the combination on LNCaP cells we repeated the dose-response treatment in the absence of steroids, confirming the sensitivity of these cells to the combination (fig. S8). RT-qPCR experiments showed that flutamide alone behaves indeed as an agonist in these cells increasing the expression of AR signaling canonical targets such as *KLK3*, *TMPRSS2* and *KLK2* after 24 hours while PPC alone did not affect the expression of these genes (Fig. 4A). Notably, treatment of LNCaP cells with both flutamide and PPC restrains the expression of *KLK3* and *KLK2* to levels similar to vehicle treatment (Fig. 4A). Interestingly, the combination decreased also *AR* expression (Fig. 4A). Of note, PPC did not interfere with induction of AR signaling promoted by the potent agonist R1881 (fig. S9). We assessed the stability of AR mRNA and found no difference between DMSO and treatment with flutamide and PPC (Fig. 4B) over 10 hours. By means of immunofluorescence (Fig. 4C) and western blotting (Fig. 4D) experiments we observed downregulation of AR upon treatment with the combination also at the protein level. Notably, AR decreased already after 8 hours (fig. S10). Treatment of LNCaP cells with a proteasome inhibitor reduced AR protein levels as already described (42) (Fig. 4E). Of note, bortezomib could partly restore the levels of AR upon treatment with the combination (Fig. 4E) suggesting proteasomal degradation of the receptor in the presence of flutamide and PPC. In addition, turnover measurements revealed decreased AR half-life in LNCaP cells treated with the combination (Fig. 4F) hinting at changes in protein stability upon administration of the two drugs.

PPC inhibits the γ -carboxylation of glutamic acid residues of proteins involved in the coagulation cascade. We hypothesized that this modification could occur also on

glutamic acid residues of the AR and induce global conformational changes affecting protein stability and binding of antiandrogens. To test this hypothesis, we performed a cellular thermal shift assay (CETSA), a recently described (43) technique for the measurement of direct and indirect cellular interactions between proteins and small molecules. CETSA measurements showed that PPC affects the thermal stability of the AR receptor (Fig. 4G). Importantly, this shift in stability was observed only upon administration of PPC to LNCaP cells for 2 days before the experiment. In the absence of such a pretreatment, the addition of PPC to the cell lysate did not stabilize the AR (Fig. 4G), arguing against a direct engagement of the receptor by PPC. Without providing unambiguous evidence of AR γ -carboxylation, this experiment indicates that PPC affects the conformation and the stability of the AR by means other than direct binding.

Discussion

Approved drugs are highly optimized molecules that can be used to address important biological questions. Moreover, a comprehensive library of clinical compounds allows for drug repurposing through one-molecule and combinatorial HTS. In our attempts to physically obtain a complete set of all approved drugs for screening purposes, we realized that no commercially available compound collection covers all drug classes and that combinatorial screenings of even relatively small libraries would overload the infrastructure of most screening platforms. Therefore, we performed an extensive literature search and cheminformatics analyses to generate a set of FDA-approved drugs representing the target and chemical space of all clinical compounds. Using a clustering algorithm on systemically active approved drugs with known targets, we selected only structurally unique molecules. To these compounds we added approved drugs with unknown targets and the active forms of prodrugs to allow for both biochemical and cellular screens. We call this compound set the CeMM Library of Unique Drugs (CLOUD). In contrast to previous collections, all CLOUD drugs fit to a single 384-well plate, are screened at their plasma concentration, and include active forms of compounds clinically administered as prodrugs.

The non-redundant nature of the CLOUD allows for combinatorial screenings of drugs which are already used in clinical settings entailing a strong translational potential. In an HTS of all pairwise combinations of CLOUD drugs we uncovered the synergistic interaction between flutamide and PPC. Flutamide is an AR antagonist approved for the treatment of prostate cancer while PPC, which has been approved as an anticoagulant for treatment of thrombosis, inhibits vitamin K-dependent protein γ -carboxylation. Here, we show that the combination of these two drugs impairs the growth of the AR-dependent LNCaP prostate cancer cell line leading to apoptosis. Importantly, LNCaP cells carry a T877A mutation in the AR that switches flutamide to an agonist. The same mutation has been validated as a resistance mechanism to AR antagonists in prostate cancer patients. Our results indicate that resistance of T877A mutant AR to flutamide can be addressed by the concomitant administration of PPC.

Mechanistically, we observe decreased AR protein stability and proteasomal degradation upon treatment of LNCaP cells with the combination. The downregulation of this important nuclear receptor operates very likely as the main death trigger in the AR-dependent LNCaP cells. We speculate that the concomitant administration of

flutamide and PPC induces conformational changes in the receptor leading to protein degradation and AR signaling downregulation. As the AR regulates its own expression (44), transcriptional changes are likely contributing to decreased protein abundance. Importantly, PPC did not alter the induction of AR signaling by the potent synthetic agonist R1881. Hence, it seems reasonable to assume that flutamide still binds to the receptor in the presence of PPC.

It is not known whether glutamic acid residues of the AR are γ -carboxylated but we speculate this post-translational modification might occur on the nuclear receptor. In this regard, we provide evidence that PPC affects the thermal stability of the AR. Our data support a model where PPC precludes γ -carboxylation of the AR and the uncarboxylated receptor would bind to flutamide incurring in a different conformational change that induces protein degradation.

In summary, we have assembled a representative library that offers structurally unique approved drugs for chemical biology studies and drug repurposing screenings. Through one such screen we found that the combination of PPC with flutamide induces proteasomal degradation of the T877A mutated AR and apoptosis in an AR-dependent prostate cancer cell line. T877A mutated AR has been reported in prostate cancer patients and associated with resistance to flutamide. Our results suggest that PPC could be clinically repurposed for the formulation of more specific prostate cancer treatments.

Materials and Methods

Cell Culture

KBM7 cells were grown in Iscove's modified Dulbecco's medium supplemented with 10% fetal bovine serum (Thermo Fisher Scientific, Waltham, MA, USA) and 1% penicillin/streptomycin (Sigma-Aldrich, St Louis, MO, USA). AR KO KBM7 cells were obtained from Haplogen (Vienna, Austria). LNCaP (ATCC, Manassas, VA, USA, CRL-1740) and PC-3 (ATCC, CRL-1435) cells were grown in RPMI-1640 supplemented with 10% fetal bovine serum (Thermo Fisher Scientific) and 1% penicillin/streptomycin (Sigma-Aldrich). For steroid-deprived experiments, LNCaP cells were cultured in RPMI-1640 supplemented with 10% charcoal stripped fetal bovine serum (Thermo Fisher Scientific) and 1% penicillin/streptomycin (Sigma-Aldrich).

Generation of the STEAM

The complete list of all approved FDA products was downloaded from the Drugs@FDA database (www.fda.gov, 2011) and the names of all active ingredients were extracted. Information on biological activity, CAS numbers, canonical smiles, and molecular weights was retrieved mainly from the DrugBank or the Therapeutic Target Database. Other sources included Clarke's Analysis of Drugs and Poisons, the KEGG drug database, the Handbook of Clinical DrugData, and Martindale. Active ingredients were filtered as described in the text to obtain 955 systemically active small molecules.

Generation of the CLOUD

Structural clustering of the 955 STEAM drugs with known targets was performed using a Pipeline Pilot protocol (Accelrys, San Diego, CA, USA). Structures were represented as Extended Connectivity Fingerprints (ECFP) and the Tanimoto coefficient was applied as a measurement of structural distance. For cluster formation, the Tanimoto dissimilarity was set to 0.85. If this threshold could not cover most of the therapeutic activities within a drug class, the threshold was lowered in a stepwise procedure. The script was used to identify the cluster centers within each of the 176 drug classes. Cluster centers were kept providing a final set of 239 structurally unique CLOUD drugs. To these, we added 35 STEAM drugs with unknown target and the active forms of 35 prodrugs. Compounds were mainly purchased from Enamine Ltd (Kiev, Ukraine), Toronto Research Chemical

(Toronto, Canada) and Sigma-Aldrich. Controlled substances and unstable/unavailable compounds are indicated in table S1 and table S2. The CLOUD will be distributed by Enamine Ltd.

Physicochemical property calculations

Molecular weight, logP, the number of rotatable bonds, hydrogen bond acceptors/donors, and violations of the Lipinski's rule of five were calculated using the chemistry components of the software Pipeline Pilot (Accelrys).

KBM7 cells viability screen

CLOUD drugs and combinations thereof were transferred on 384-well plates using an acoustic liquid handler (Echo, Labcyte, Sunnyvale, CA, USA) and 5,000 cells/well were dispensed on top of the drugs using a dispenser (Thermo Fisher Scientific) for a total of 50 μ l/well. Viability was measured after 72 hours using CellTiter-Glo (Promega, Fitchburg, WI, USA) in a multilabel plate reader (EnVision, PerkinElmer, Waltham, MA, USA). Signal was then normalized to negative (DMSO) and positive (10 μ M dasatinib) controls and set between 0 and 100. Noisy compounds, defined according to median absolute deviation (MAD), were excluded from the analysis together with their corresponding combinations. Drug combinations were analyzed according to the Bliss independence model (34). Briefly, the effect of the combination of drug A and drug B can be predicted to be $A+B-A*B$ where A and B are the effects of the single drugs expressed as fractional inhibition between 0 and 1. A deviation of the experimental value from the Bliss prediction was calculated. Positive deviations denote synergies while negative deviations denote antagonisms. Top hits were selected setting thresholds for deviation (>0.7 for synergies and <-0.5 for antagonisms) and Z score (>1). 254 hits have been selected and tested again in a counter-screen. The top 20 validated synergies and antagonisms were further validated in 4 concentrations dose-response matrices and analyzed in a similar way. Here, synergisms and antagonisms were measured calculating differential volumes representing the sum of all deviation values within a specific matrix. Differential volumes > 1 indicate robust synergies while differential volumes < -1 indicate robust antagonisms.

Reverse transcription quantitative polymerase chain reaction

Performed as already described (45). Primers are listed in table S4.

Western blotting

Cells were lysed in RIPA buffer supplemented with a cocktail of protease inhibitors (Roche). Lysates were resolved by sodium dodecyl sulfate–polyacrylamide gel electrophoresis. AR (#5153) and GAPDH (#5174) antibodies were purchased from Cell Signaling Technology (Danvers, MA, USA). α TUB antibody (ab7291) was purchased from Abcam (Cambridge, UK).

Immunofluorescence

Performed as already described (45). AR antibody (#5153) was purchased from Cell Signaling Technology.

Apoptosis assay

In all, 50,000 cells/well were seeded in 6-well plates and treated with DMSO, 15 μ M flutamide, 35 μ M PPC or flutamide and PPC in combination after 24 h. After 3 days, cells were labeled with Alexa Fluor 647 Annexin V antibody (Biolegend, San Diego, CA, USA) and propidium iodide and analyzed using flow cytometry (BD FACSCalibur, BD Biosciences, Franklyn Lake, NJ, USA).

Cellular thermal shift assay

LNCaP cells were treated with DMSO or 35 μ M PPC for 2 days and then harvested maintaining a constant concentration of PPC in all subsequent handling buffers. Otherwise, lysates were directly treated with the drug as already described (43).

List of Supplementary Materials

Fig. S1. The CLOUD compared to other commercial libraries.

Fig. S2. STEAM and CLOUD distribution of organisms and targets.

Fig. S3. Physicochemical properties of STEAM and CLOUD drugs.

Fig. S4. Screen dose-response matrix for flutamide and PPC.

Fig. S5. AR KO KBM7 clone.

Fig. S6. Differential volumes of LNCaP and PC-3.

Fig. S7. Dose-response matrices with alternative VKORC1 inhibitors and antiandrogens.

Fig. S8. Dose-response matrix of starved LNCaP cells.

Fig. S9. AR signaling activation by R1881.

Fig. S10. AR and AR canonical targets downregulation.

Table S1. STEAM and CLOUD drugs.

Table S2. Prodrugs and active forms.

Table S3. Top 20 synergies and antagonisms.

Table S4. RT-qPCR primers used.

References and Notes:

1. S. M. Paul, D. S. Mytelka, C. T. Dunwiddie, C. C. Persinger, B. H. Munos, S. R. Lindborg, A. L. Schacht, How to improve R&D productivity: the pharmaceutical industry's grand challenge. *Nat. Rev. Drug Discov.* **9**, 203-214 (2010).
2. A. Mullard, 2013 FDA drug approvals. *Nat. Rev. Drug Discov.* **13**, 85-89 (2014).
3. J. W. Scannell, A. Blanckley, H. Boldon, B. Warrington, Diagnosing the decline in pharmaceutical R&D efficiency. *Nat. Rev. Drug Discov.* **11**, 191-200 (2012).
4. T. T. Ashburn, K. B. Thor, Drug repositioning: identifying and developing new uses for existing drugs. *Nat. Rev. Drug Discov.* **3**, 673-683 (2004).
5. C. Holohan, S. Van Schaeybroeck, D. B. Longley, P. G. Johnston, Cancer drug resistance: an evolving paradigm. *Nat. Rev. Cancer* **13**, 714-726 (2013).
6. F. Clavel, A. J. Hance, HIV drug resistance. *N. Engl. J. Med.* **350**, 1023-1035 (2004).
7. C. Bock, T. Lengauer, Managing drug resistance in cancer: lessons from HIV therapy. *Nat. Rev. Cancer* **12**, 494-501 (2012).
8. C. R. Chong, X. Chen, L. Shi, J. O. Liu, D. J. Sullivan, Jr., A clinical drug library screen identifies astemizole as an antimalarial agent. *Nat. Chem. Biol.* **2**, 415-416 (2006).
9. R. Huang, N. Southall, Y. Wang, A. Yasgar, P. Shinn, A. Jadhav, D. T. Nguyen, C. P. Austin, The NCGC pharmaceutical collection: a comprehensive resource of clinically approved drugs enabling repurposing and chemical genomics. *Sci. Transl. Med.* **3**, 80ps16 (2011).
10. S. Liao, D. K. Howell, T. M. Chang, Action of a nonsteroidal antiandrogen, flutamide, on the receptor binding and nuclear retention of 5 alpha-dihydrotestosterone in rat ventral prostate. *Endocrinology* **94**, 1205-1209 (1974).
11. J. S. Paikin, J. W. Eikelboom, J. A. Cairns, J. Hirsh, New antithrombotic agents--insights from clinical trials. *Nat. Rev. Cardiol.* **7**, 498-509 (2010).
12. T. Li, C. Y. Chang, D. Y. Jin, P. J. Lin, A. Khvorova, D. W. Stafford, Identification of the gene for vitamin K epoxide reductase. *Nature* **427**, 541-544 (2004).
13. A. O. Brinkmann, L. J. Blok, P. E. de Rooter, P. Doesburg, K. Steketeer, C. A. Berrevoets, J. Trapman, Mechanisms of androgen receptor activation and function. *J. Steroid Biochem. Mol. Biol.* **69**, 307-313 (1999).

14. C. Tran, S. Ouk, N. J. Clegg, Y. Chen, P. A. Watson, V. Arora, J. Wongvipat, P. M. Smith-Jones, D. Yoo, A. Kwon, T. Wasielewska, D. Welsbie, C. D. Chen, C. S. Higano, T. M. Beer, D. T. Hung, H. I. Scher, M. E. Jung, C. L. Sawyers, Development of a Second-Generation Antiandrogen for Treatment of Advanced Prostate Cancer. *Science* **324**, 787-790 (2009).
15. P. Murtha, D. J. Tindall, C. Y. Young, Androgen induction of a human prostate-specific kallikrein, hKLK2: characterization of an androgen response element in the 5' promoter region of the gene. *Biochemistry (Mosc.)* **32**, 6459-6464 (1993).
16. Y. Chen, N. J. Clegg, H. I. Scher, Anti-androgens and androgen-depleting therapies in prostate cancer: new agents for an established target. *Lancet Oncol.* **10**, 981-991 (2009).
17. J. Veldscholte, C. A. Berrevoets, C. Ris-Stalpers, G. G. Kuiper, G. Jenster, J. Trapman, A. O. Brinkmann, E. Mulder, The androgen receptor in LNCaP cells contains a mutation in the ligand binding domain which affects steroid binding characteristics and response to antiandrogens. *J. Steroid Biochem. Mol. Biol.* **41**, 665-669 (1992).
18. J. P. Gaddipati, D. G. McLeod, H. B. Heidenberg, I. A. Sesterhenn, M. J. Finger, J. W. Moul, S. Srivastava, Frequent detection of codon 877 mutation in the androgen receptor gene in advanced prostate cancers. *Cancer Res.* **54**, 2861-2864 (1994).
19. B. J. Feldman, D. Feldman, The development of androgen-independent prostate cancer. *Nat. Rev. Cancer* **1**, 34-45 (2001).
20. J. Stenflo, P. Fernlund, W. Egan, P. Roepstorff, Vitamin K dependent modifications of glutamic acid residues in prothrombin. *Proc. Natl. Acad. Sci. U. S. A.* **71**, 2730-2733 (1974).
21. S. Rost, A. Fregin, V. Ivaskevicius, E. Conzelmann, K. Hortnagel, H. J. Pelz, K. Lappégard, E. Seifried, I. Scharrer, E. G. Tuddenham, C. R. Muller, T. M. Strom, J. Oldenburg, Mutations in VKORC1 cause warfarin resistance and multiple coagulation factor deficiency type 2. *Nature* **427**, 537-541 (2004).
22. J. W. Suttie, Vitamin K-dependent carboxylase. *Annu. Rev. Biochem.* **54**, 459-477 (1985).
23. M. J. Rieder, A. P. Reiner, B. F. Gage, D. A. Nickerson, C. S. Eby, H. L. McLeod, D. K. Blough, K. E. Thummel, D. L. Veenstra, A. E. Rettie, Effect of VKORC1 haplotypes

- on transcriptional regulation and warfarin dose. *N. Engl. J. Med.* **352**, 2285-2293 (2005).
24. R. M. Plenge, E. M. Scolnick, D. Altshuler, Validating therapeutic targets through human genetics. *Nat. Rev. Drug Discov.* **12**, 581-594 (2013).
 25. J. P. Overington, B. Al-Lazikani, A. L. Hopkins, How many drug targets are there? *Nat. Rev. Drug Discov.* **5**, 993-996 (2006).
 26. C. A. Lipinski, F. Lombardo, B. W. Dominy, P. J. Feeney, Experimental and computational approaches to estimate solubility and permeability in drug discovery and development settings. *Adv Drug Deliv Rev* **46**, 3-26 (2001).
 27. J. Lamb, E. D. Crawford, D. Peck, J. W. Modell, I. C. Blat, M. J. Wrobel, J. Lerner, J. P. Brunet, A. Subramanian, K. N. Ross, M. Reich, H. Hieronymus, G. Wei, S. A. Armstrong, S. J. Haggarty, P. A. Clemons, R. Wei, S. A. Carr, E. S. Lander, T. R. Golub, The Connectivity Map: using gene-expression signatures to connect small molecules, genes, and disease. *Science* **313**, 1929-1935 (2006).
 28. M. Iskar, M. Campillos, M. Kuhn, L. J. Jensen, V. van Noort, P. Bork, Drug-induced regulation of target expression. *PLoS Comput. Biol.* **6**, 1000925 (2010).
 29. R. Brynner, T. Stephens, *Dark Remedy: The Impact of Thalidomide and Its Revival as a Vital Medicine.* (Perseus Publishing, Cambridge, Cambridge, 2001).
 30. R. C. Renaud, H. Xuereb, Erectile-dysfunction therapies. *Nat. Rev. Drug Discov.* **1**, 663-664 (2002).
 31. M. Kotecki, P. S. Reddy, B. H. Cochran, Isolation and characterization of a near-haploid human cell line. *Exp. Cell Res.* **252**, 273-280 (1999).
 32. J. H. Reiling, C. B. Clish, J. E. Carette, M. Varadarajan, T. R. Brummelkamp, D. M. Sabatini, A haploid genetic screen identifies the major facilitator domain containing 2A (MFSD2A) transporter as a key mediator in the response to tunicamycin. *Proc. Natl. Acad. Sci. U. S. A.* **108**, 11756-11765 (2011).
 33. G. E. Winter, B. Radic, C. Mayor-Ruiz, V. A. Blomen, C. Trefzer, R. K. Kandasamy, K. V. Huber, M. Gridling, D. Chen, T. Klampfl, R. Kralovics, S. Kubicek, O. Fernandez-Capetillo, T. R. Brummelkamp, G. Superti-Furga, The solute carrier SLC35F2 enables YM155-mediated DNA damage toxicity. *Nat. Chem. Biol.* **10**, 768-773 (2014).
 34. C. I. Bliss, The toxicity of poisons applied jointly. *Ann. Appl. Biol.* **26**, 585-615 (1939).

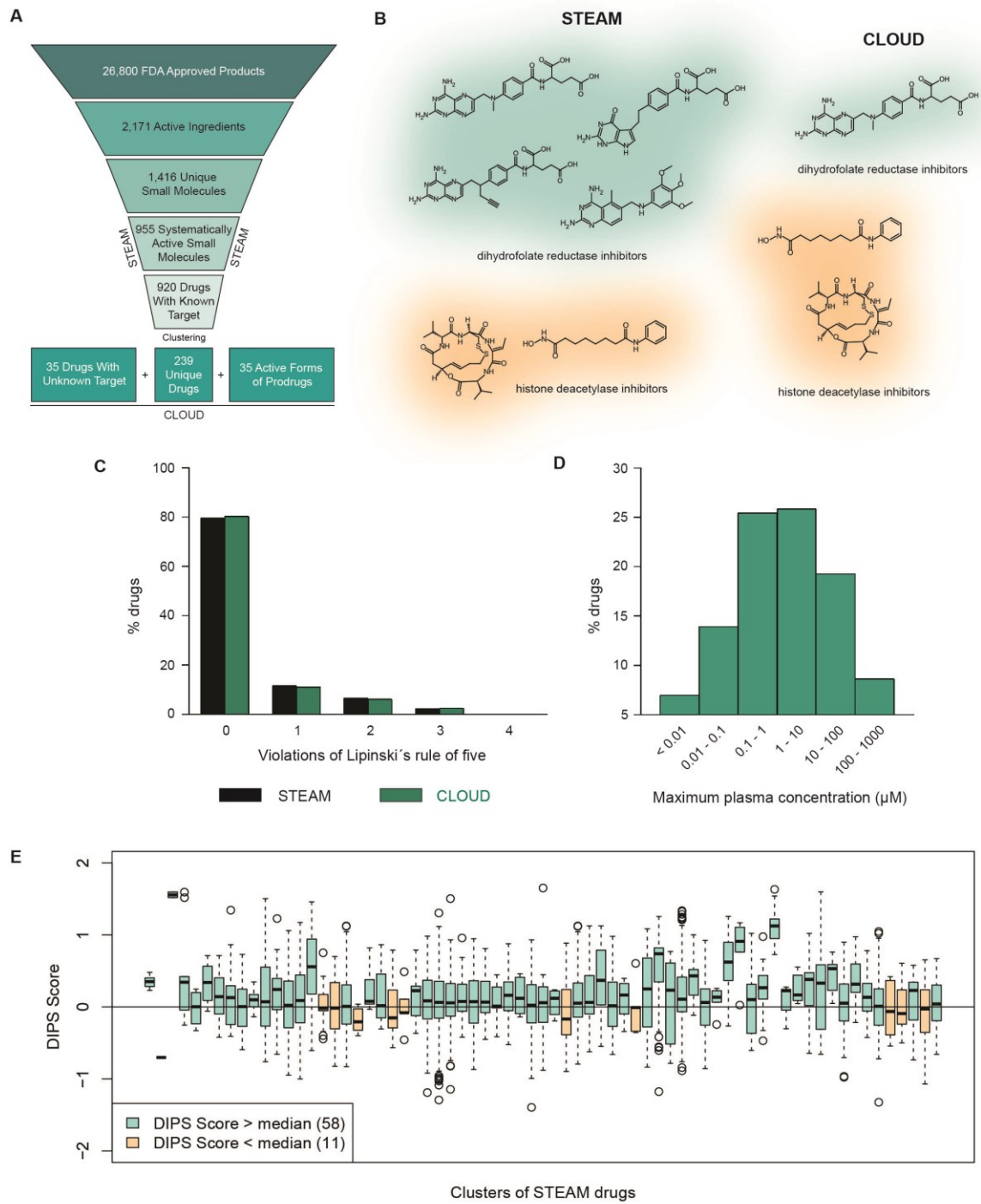
35. J. E. Carette, C. P. Guimaraes, M. Varadarajan, A. S. Park, I. Wuethrich, A. Godarova, M. Kotecki, B. H. Cochran, E. Spooner, H. L. Ploegh, T. R. Brummelkamp, Haploid genetic screens in human cells identify host factors used by pathogens. *Science* **326**, 1231-1235 (2009).
36. T. Burckstummer, C. Banning, P. Hainzl, R. Schobesberger, C. Kerzendorfer, F. M. Pauler, D. Chen, N. Them, F. Schischlik, M. Rebsamen, M. Smida, F. Fece de la Cruz, A. Lapao, M. Liszt, B. Eizinger, P. M. Guenzl, V. A. Blomen, T. Konopka, B. Gapp, K. Parapatics, B. Maier, J. Stockl, W. Fischl, S. Salic, M. R. Taba Casari, S. Knapp, K. L. Bennett, C. Bock, J. Colinge, R. Kralovics, G. Ammerer, G. Casari, T. R. Brummelkamp, G. Superti-Furga, S. M. Nijman, A reversible gene trap collection empowers haploid genetics in human cells. *Nat. Methods* **10**, 965-971 (2013).
37. S. M. Dehm, D. J. Tindall, Alternatively spliced androgen receptor variants. *Endocr. Relat. Cancer* **18**, 11-0141 (2011).
38. I. G. Mills, Maintaining and reprogramming genomic androgen receptor activity in prostate cancer. *Nature Reviews Cancer* **14**, 187-198 (2014).
39. M.-E. Taplin, Drug Insight: role of the androgen receptor in the development and progression of prostate cancer. *Nature Clinical Practice Oncology* **4**, 236-244 (2007).
40. C. D. Chen, D. S. Welsbie, C. Tran, S. H. Baek, R. Chen, R. Vessella, M. G. Rosenfeld, C. L. Sawyers, Molecular determinants of resistance to antiandrogen therapy. *Nat. Med.* **10**, 33-39 (2004).
41. F. Alimirah, J. Chen, Z. Basrawala, H. Xin, D. Choubey, DU-145 and PC-3 human prostate cancer cell lines express androgen receptor: implications for the androgen receptor functions and regulation. *FEBS Lett.* **580**, 2294-2300 (2006).
42. R. S. Bhattacharyya, A. V. Krishnan, S. Swami, D. Feldman, Fulvestrant (ICI 182,780) down-regulates androgen receptor expression and diminishes androgenic responses in LNCaP human prostate cancer cells. *Mol. Cancer Ther.* **5**, 1539-1549 (2006).
43. D. Martinez Molina, R. Jafari, M. Ignatushchenko, T. Seki, E. A. Larsson, C. Dan, L. Sreekumar, Y. Cao, P. Nordlund, Monitoring drug target engagement in cells and tissues using the cellular thermal shift assay. *Science* **341**, 84-87 (2013).

44. J. M. Grad, L. S. Lyons, D. M. Robins, K. L. Burnstein, The androgen receptor (AR) amino-terminus imposes androgen-specific regulation of AR gene expression via an exonic enhancer. *Endocrinology* **142**, 1107-1116 (2001).
45. M. P. Licciardello, M. K. Mullner, G. Durnberger, C. Kerzendorfer, B. Boidol, C. Trefzer, S. Sdelci, T. Berg, T. Penz, M. Schuster, C. Bock, R. Kralovics, G. Superti-Furga, J. Colinge, S. M. Nijman, S. Kubicek, NOTCH1 activation in breast cancer confers sensitivity to inhibition of SUMOylation. *Oncogene* **29**, 319 (2014).

Acknowledgments: We thank Murat Iskar (EMBL) and Peer Bork (EMBL) for providing us with DIPS scores; Georg Winter (CeMM) and Giulio Superti-Furga (CeMM) for thoughtful discussions and initializing synergy screenings at CeMM. We also thank Erika Schirghuber (CeMM) and Sara Sdelci (CeMM) for critical input on the manuscript.

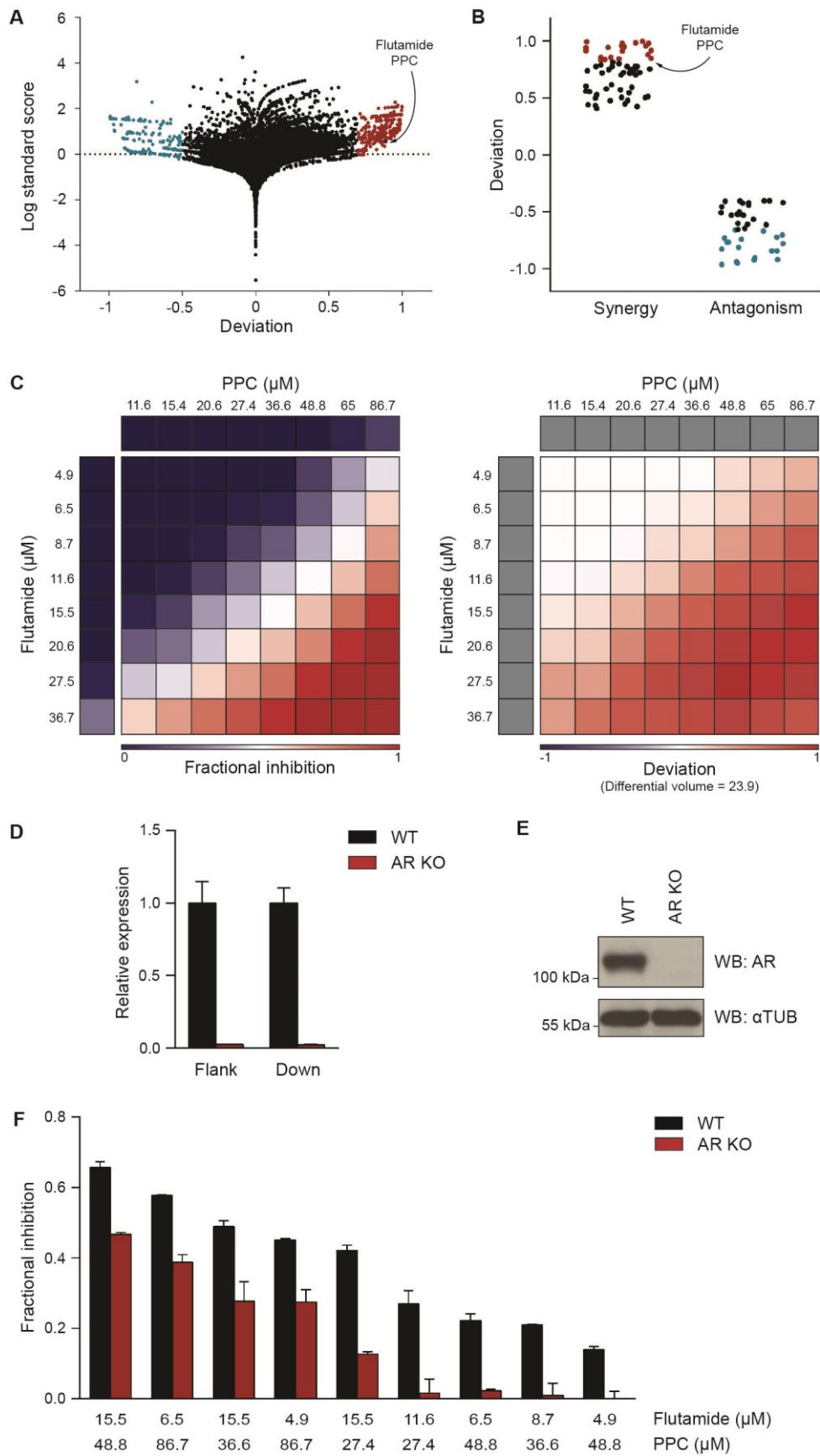
Funding: S.K. acknowledges support by a Marie Curie Career Integration Grant, the Austrian Federal Ministry of Science, Research and Economy and the National Foundation for Research, Technology, and Development. **Author contributions:** P.M., F.K. and S.K. designed and assembled the CLOUD. M.P.L., F.K. and C.H.L. designed and performed the screen of the CLOUD. M.P.L. and F.K. analyzed the data from the screen. M.P.L. designed and performed viability, RT-qPCR, western blotting and immunofluorescence experiments. G.D. and J.C. performed DIPS score analyses. V.I. synthesized, provided and quality controlled chemicals. M.P.L. and S.K. wrote the manuscript. **Competing interests:** The CLOUD will be distributed by Enamine, Ltd.

Figures:



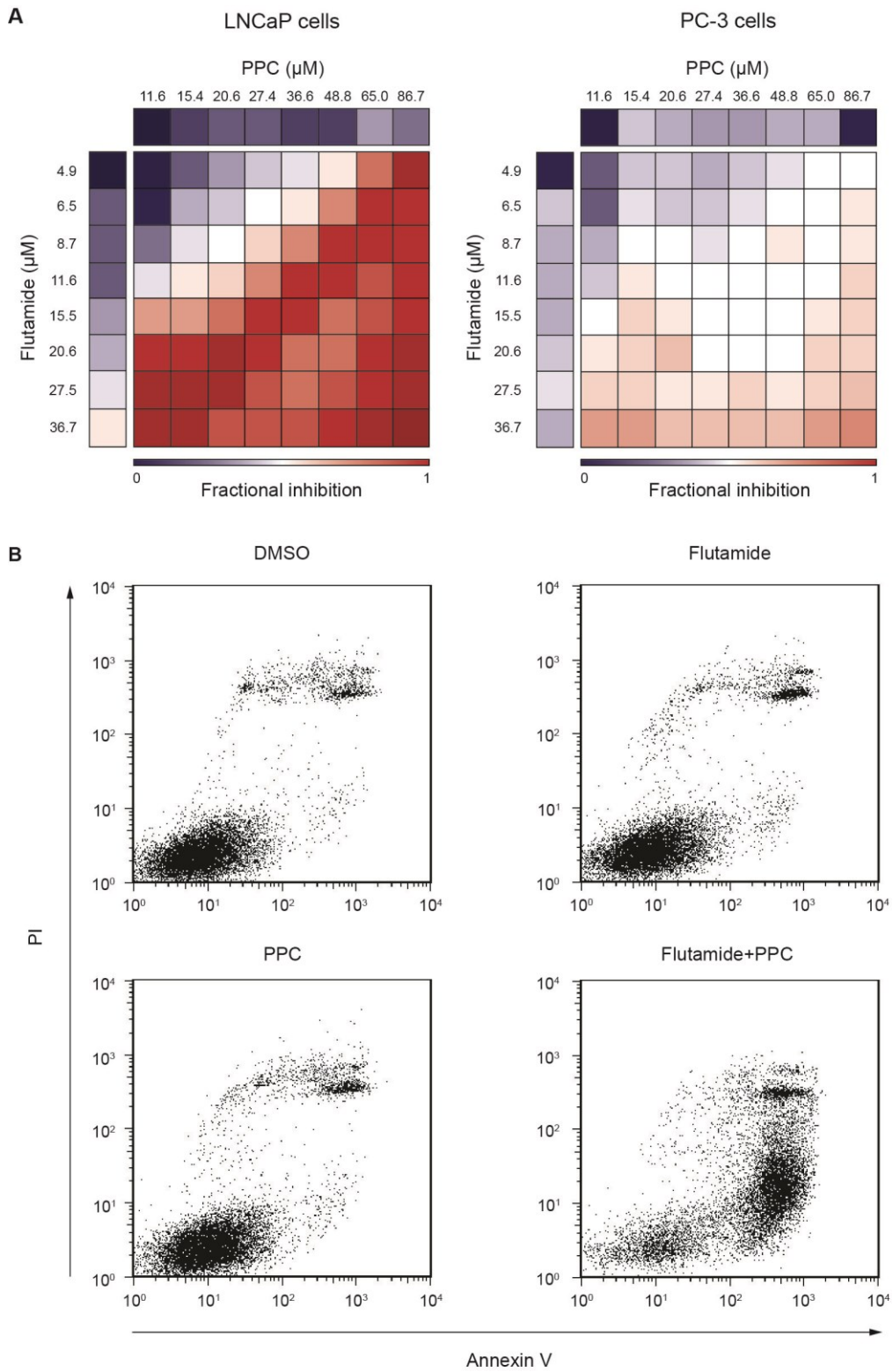
Licciardello et al, Figure 1

Fig. 1. The CeMM Library of Unique Drugs. **(A)** Schematic representation of the filtering and clustering procedure leading to the 309 CLOUD drugs. **(B)** Examples of STEAM drug clusters and selected representative CLOUD drugs. The cluster of dihydrofolate reductase inhibitors centers on methotrexate which was then selected for the CLOUD (top); the two structurally very different histone deacetylase inhibitors are both kept in the CLOUD (bottom). A complete list of clusters and selected CLOUD drugs can be found in table S1. **(C)** Violations of Lipinski's rule of five by STEAM and CLOUD drugs. **(D)** Maximum plasma concentration ranges of all CLOUD drugs. **(E)** Pairwise DIPS scores within 69 STEAM clusters. 58 clusters show median pairwise DIPS score above the overall median DIPS score (turquoise) while only 11 clusters have median DIPS scores below the overall median (orange).



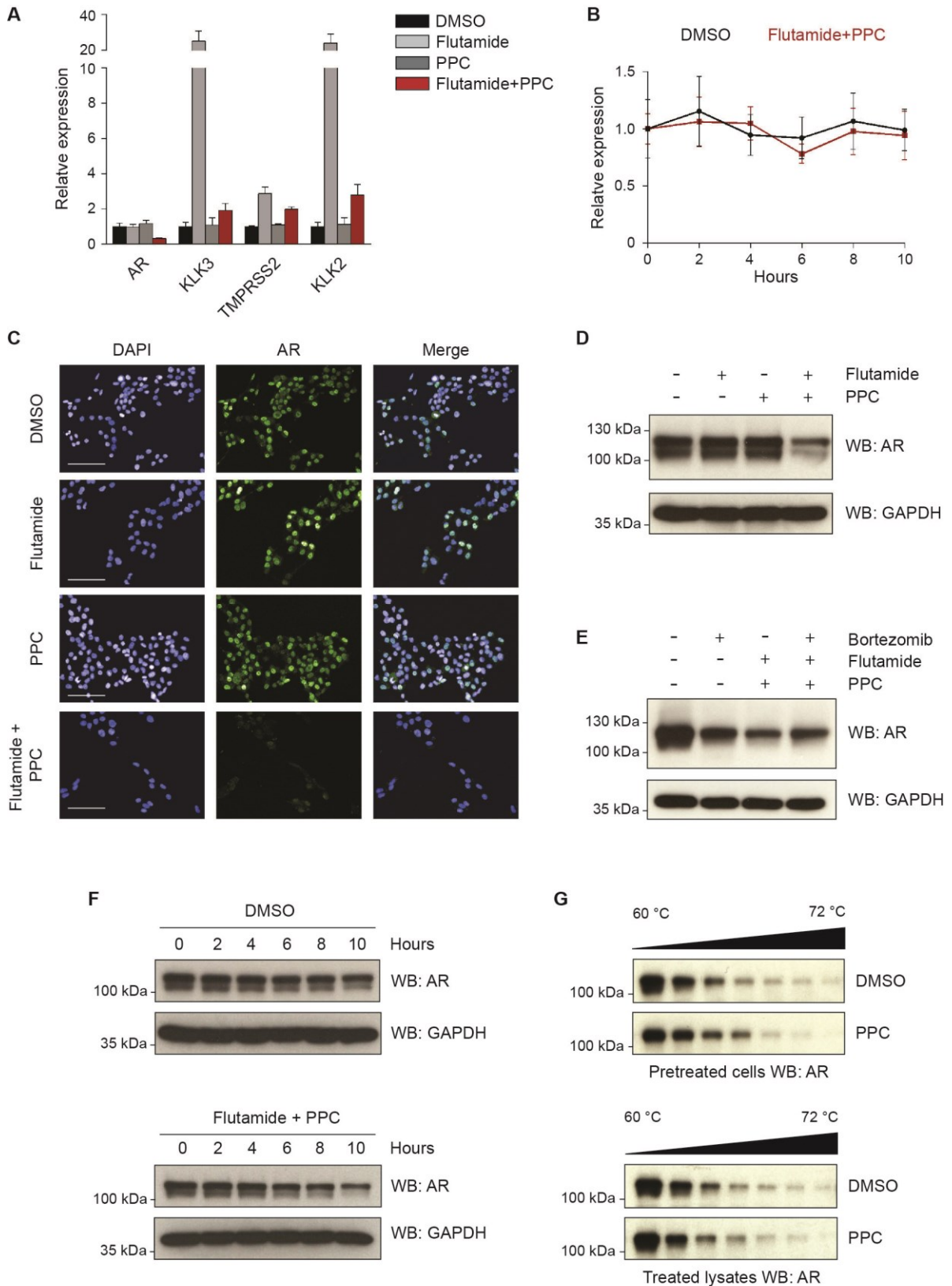
Licciardello et al, Figure 2

Fig. 2. A combinatorial HTS of the CLOUD uncovers the synergy between flutamide and PPC. **(A)** Butterfly plot summarizing the results from the screen. Dots represent combinations of two CLOUD drugs. The deviation from Bliss independence and the Log of the standard score of the deviation are illustrated. Synergies with a deviation > 0.7 (red) and antagonisms with a deviation < -0.5 (blue) are indicated. The combination of flutamide and PPC is highlighted. **(B)** Synergies and antagonisms validated in the counter-screen are reported. The top 20 synergies (red) and antagonisms (blue) are indicated. The combination of flutamide and PPC is highlighted. **(C)** Dose-response matrix of KBM7 cells treated with flutamide and PPC at the indicated concentrations for 3 days. The average fractional inhibition of viability of two biological replicates (left) and deviations from Bliss (right) are reported. The differential volume is the sum of all deviations. **(D)** RT-qPCR confirming knockout of the AR in the AR KO KBM7 clone. Primers flanking or downstream of the gene-trap were used. Data are normalized to actin expression and KBM7 WT values are set to 1. Error bars are s.d. of three biological replicates. **(E)** Western blotting confirming knockout of the AR in the AR KO KBM7 clone. Tubulin was used as a loading control. **(F)** Viability assay showing resistance of the AR KO KBM7 clone to the combination of flutamide and PPC compared to KBM7 WT after 3 days treatment at the indicated concentrations. Error bars are s.d. of two biological replicates.



Licciardello et al, Figure 3

Fig. 3. The combination of flutamide and PPC impairs the growth of LNCaP prostate cancer cells. **(A)** Dose-response matrix of LNCaP cells (left) and PC-3 cells (right) treated with flutamide and PPC at the indicated concentrations for 3 days. The average fractional inhibition of viability of two biological replicates is reported. The corresponding deviations and differential volumes are illustrated in fig. S6. **(B)** Annexin V/propidium iodide staining of LNCaP cells treated with DMSO, 15 μ M flutamide, 35 μ M PPC or the combination for 3 days. Only the combination of the two drugs induces cellular apoptosis.



Licciardello et al, Figure 4

Fig. 4. Flutamide and PPC induce AR degradation. **(A)** RT-qPCR analysis of the expression levels of AR and canonical targets of the AR signaling in LNCaP cells cultured in steroid-deprived medium and treated with 15 μ M flutamide, 35 μ M PPC or the combination for 24 hours. Data are normalized to actin expression and DMSO treatment is set to 1. Error bars are s.d. of three biological replicates. **(B)** RT-qPCR measurements of AR transcript levels in LNCaP cells cultured in steroid-deprived medium and treated with either DMSO or the combination. After 24 hours, 4 μ M Actinomycin D was added to the medium and samples were harvested at the indicated time points. Data are normalized to actin expression and to the initial time point. Error bars are s.d. of three biological replicates. **(C)** Immunofluorescence analysis of LNCaP cells treated with 15 μ M flutamide, 35 μ M PPC or the combination for 24 hours showing reduced AR protein levels only upon treatment with the combination. Scale bar = 100 μ m. **(D)** Western blotting of LNCaP cells treated as in (C) showing reduction of AR protein levels in LNCaP cells treated with the combination of flutamide and PPC. GAPDH was used as a loading control. **(E)** Western blotting of LNCaP cells treated with 30 nM bortezomib, 15 μ M flutamide, 35 μ M PPC as indicated. GAPDH was used as a loading control. **(F)** Western blotting of LNCaP cells treated with either DMSO or the combination. After 24 hours, 2.5 μ g/ml cycloheximide was added to the medium and samples were harvested at the indicated time points. GAPDH was used as a loading control. **(G)** CETSA of LNCaP cells treated with either DMSO or 35 μ M PPC for 2 days (top) and LNCaP cell lysates treated with either DMSO or 100 μ M PPC for 30 min (bottom).

Supplementary Figures:

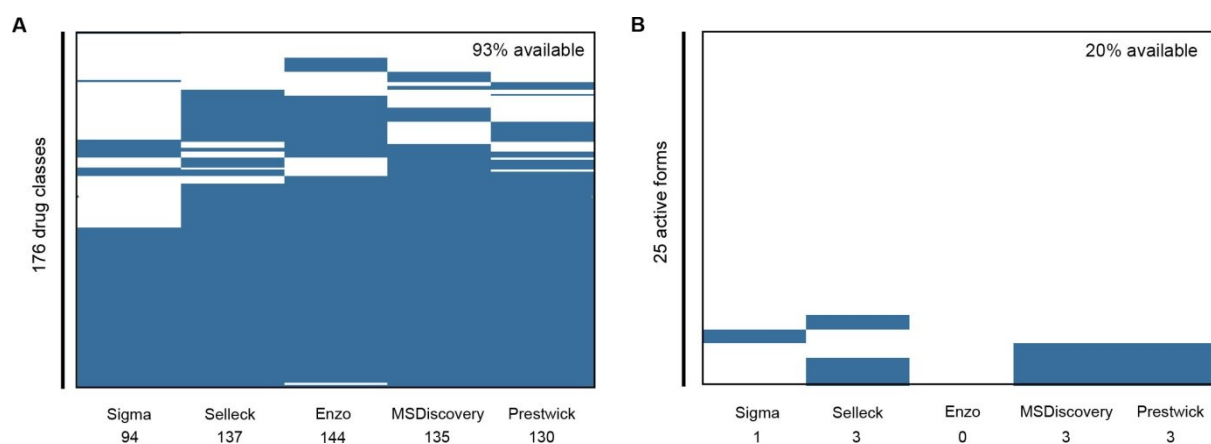


Fig. S1. The CLOUD compared to other commercial libraries. **(A)** Heatmap showing drug classes covered by commercially available libraries containing FDA-approved drugs. All commercial libraries together cover 93% of CLOUD drug classes. **(B)** Heatmap showing active forms of 25 CLOUD prodrugs listed in commercially available libraries. All commercial libraries together cover only 20% of CLOUD active forms.

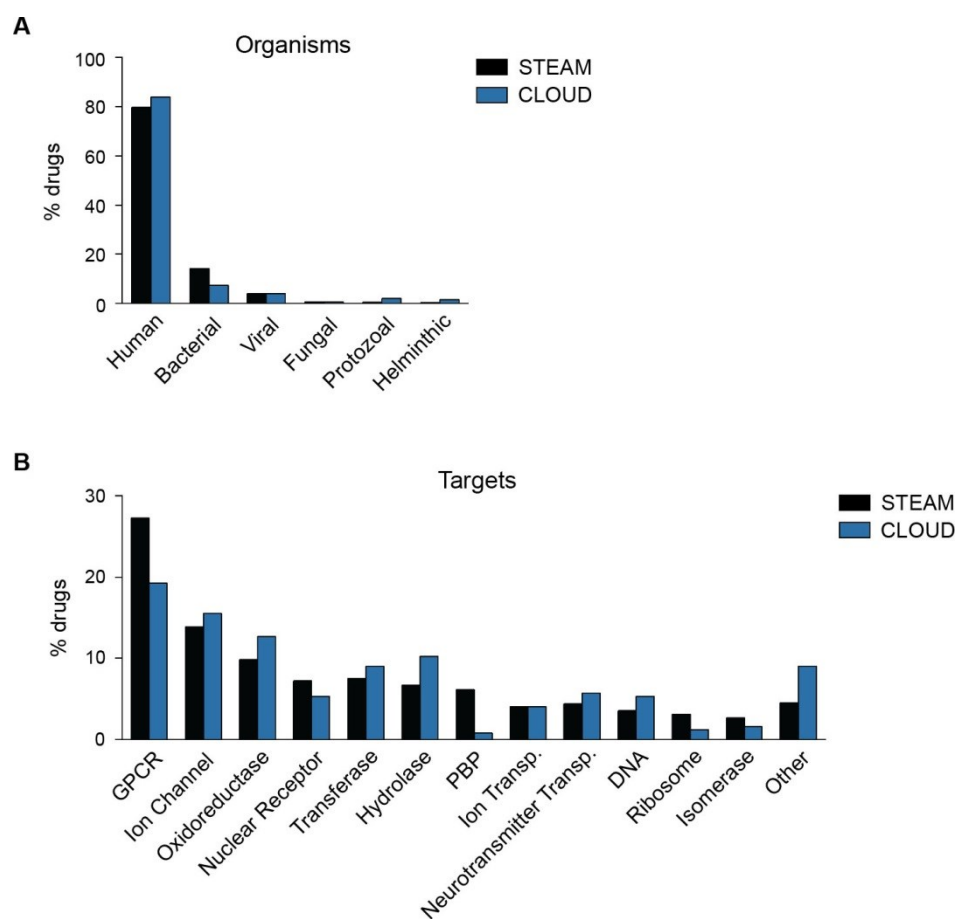


Fig. S2. STEAM and CLOUD distribution of organisms and targets. Percentage of STEAM and CLOUD drugs for a specific organism (**A**) or target class (**B**) are indicated.

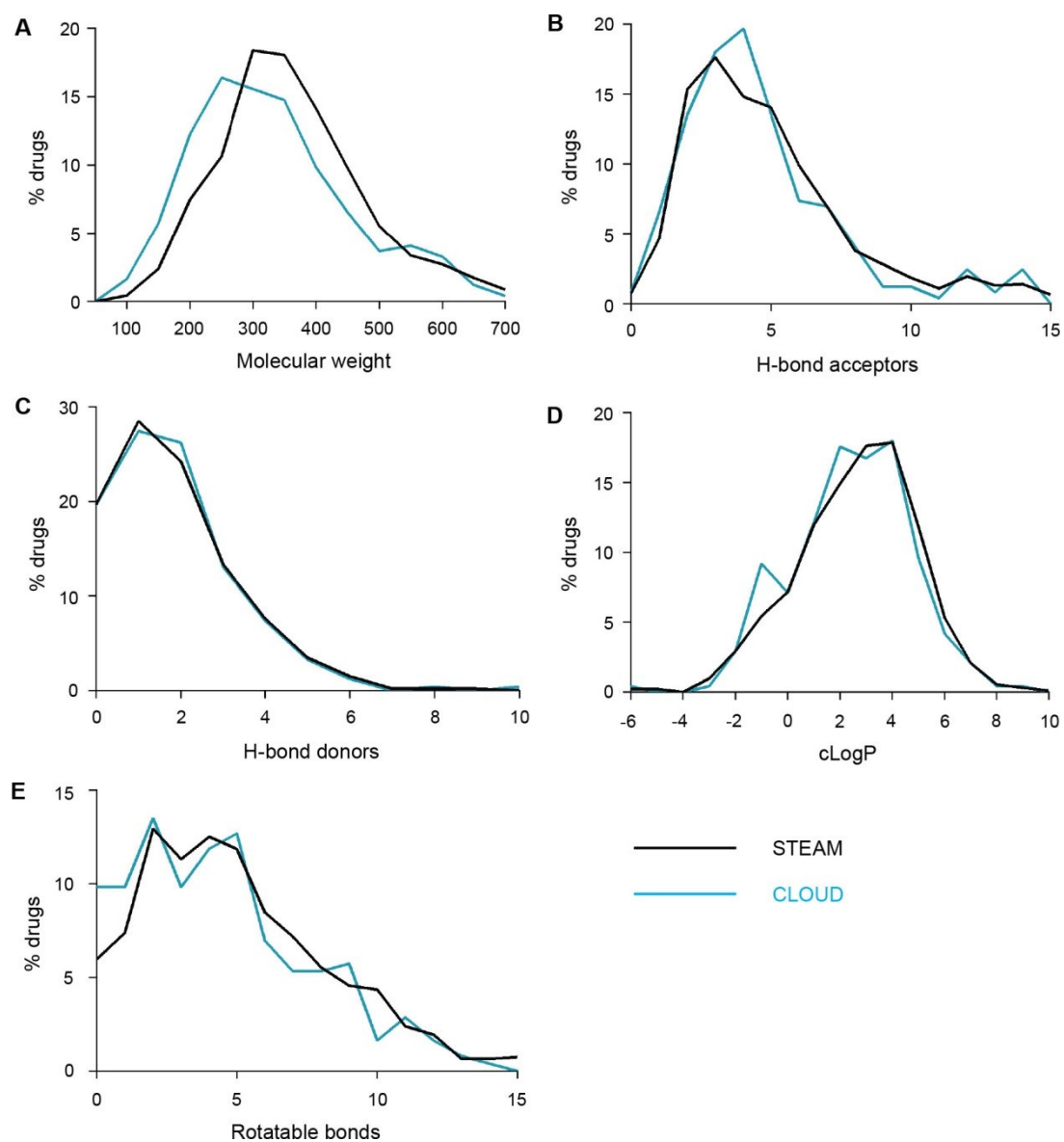


Fig. S3. Physicochemical properties of STEAM and CLOUD drugs. (A-E) Distribution of STEAM and CLOUD drugs physicochemical properties as indicated.

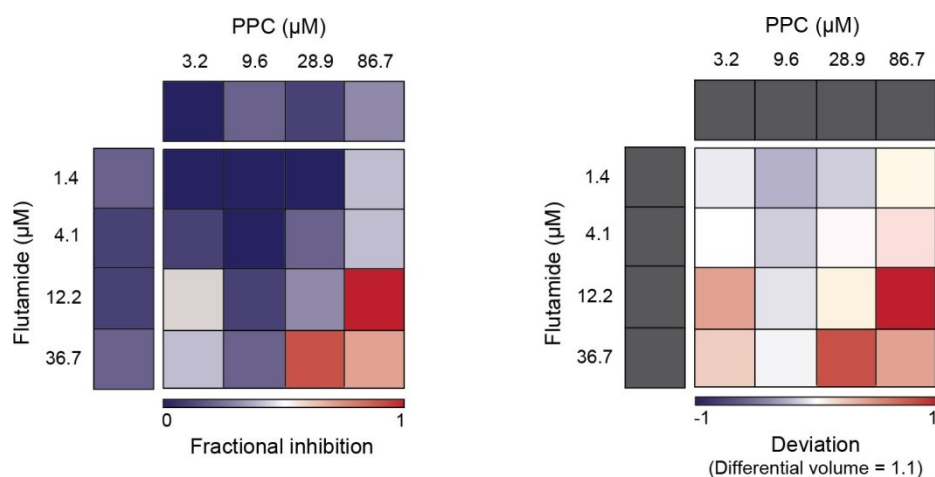


Fig. S4. Screen dose-response matrix for flutamide and PPC. Left, dose-response matrix showing fractional inhibition of KMB7 cells viability treated with flutamide and PPC at the indicated concentrations for 3 days. Average of two biological replicates is reported. Right, matrix showing deviations from Bliss. The differential volume is the sum of all deviation values within the matrix.

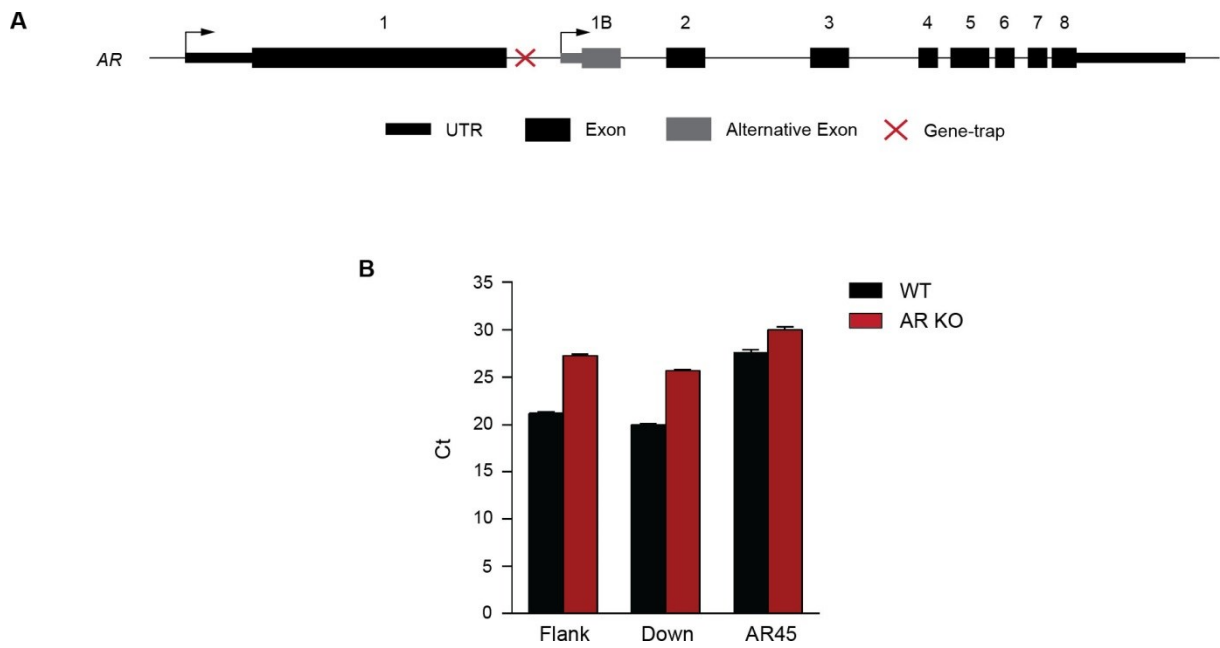


Fig. S5. AR KO KBM7 clone. **(A)** Schematic representation of the human AR gene. The gene-trap insertion site is indicated by a red cross. The transcriptional start site of the main isoform (exon 1) and AR45 isoform (alternative exon 1B) are also indicated. **(B)** Ct values showing residual transcription of the main AR and the AR45 isoform in AR KO KBM7 cells.

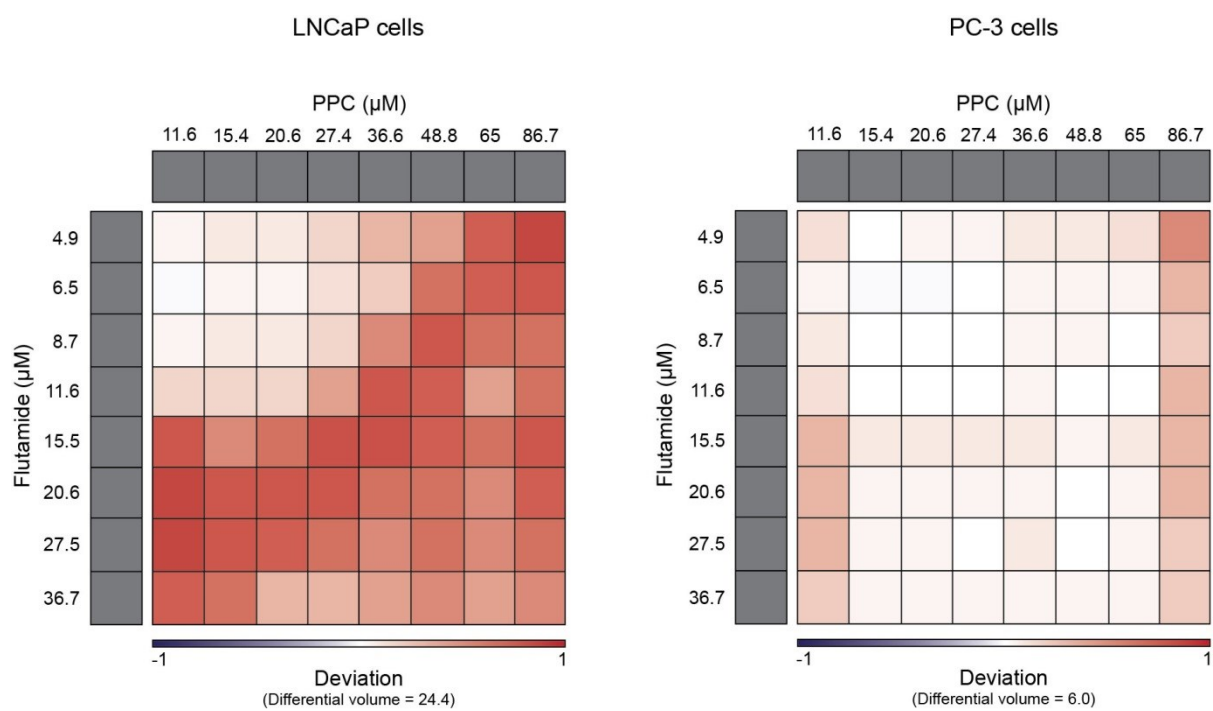


Fig. S6. Differential volumes of LNCaP and PC-3 cells. Dose-response matrices showing deviation values and differential volumes of LNCaP cells (left) and PC-3 cells (right) treated with flutamide and PPC at the indicated concentrations for 3 days. Values refer to the fractional inhibition dose-response matrices reported in **Fig. 3A**.

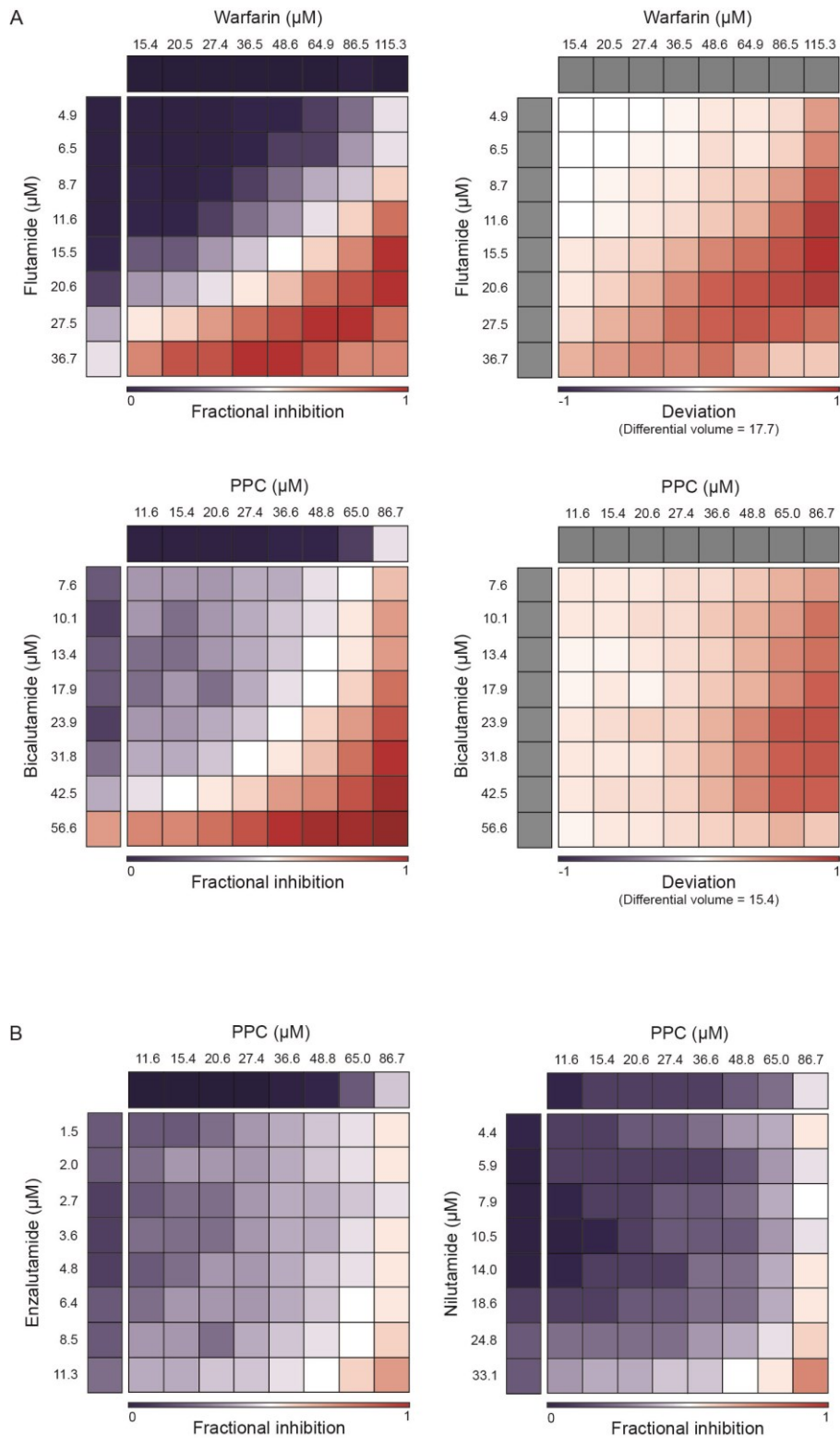


Fig. S7. Dose-response matrices of LNCaP cells treated with different VKORC1 inhibitors and antiandrogens. LNCaP cells were treated with flutamide and warfarin (**A**) or with PPC in combination with other antiandrogens (**A** and **B**) at the indicated concentrations for 3 days.

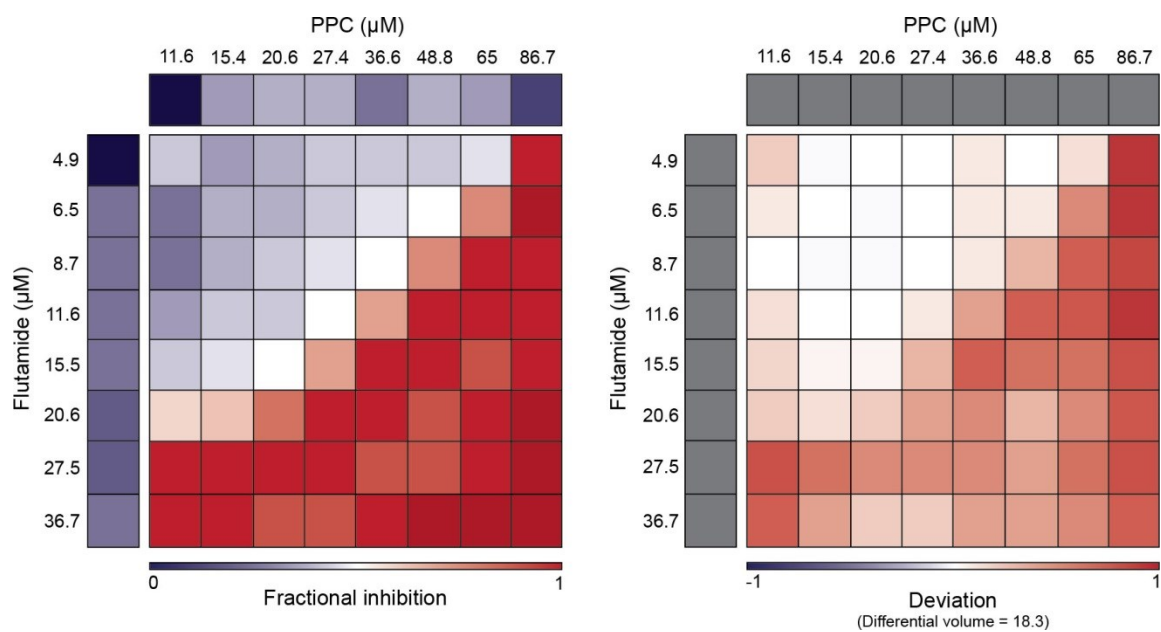


Fig. S8. Dose-response matrix of LNCaP cells in the absence of androgens. LNCaP cells were cultured for 3 days in steroid-deprived medium and then treated with flutamide and PPC at the indicated concentrations for 3 days.

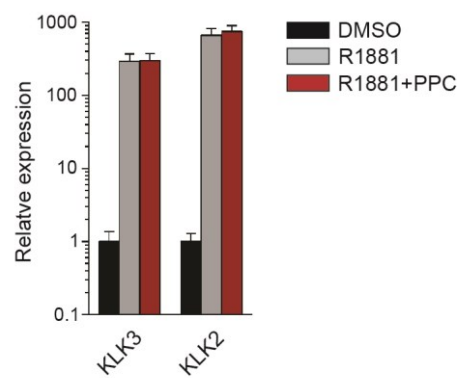


Fig. S9. AR signaling activation by R1881. RT-qPCR experiment showing unaltered expression of KLK3 and KLK2 in LNCaP cells treated with 10 nM R1881 \pm 35 μ M PPC for 24 hours.

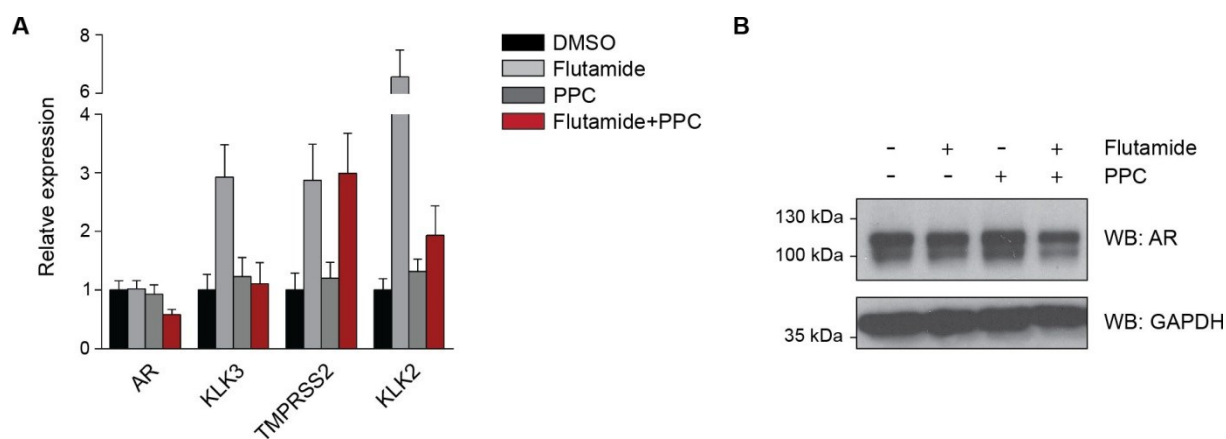


Fig. S10. AR and AR canonical targets downregulation. **(A)** RT-qPCR experiment showing restrained expression of KLK3 and KLK2 as well as downregulation of AR in LNCaP cells treated with 15 μ M flutamide and 35 μ M PPC for 8 hours. **(B)** Western blotting experiment showing downregulation of the AR in LNCaP cells treated with 15 μ M flutamide and 35 μ M PPC for 8 hours.

Supplementary Tables:

STEAM DRUG	MECHANISM OF ACTION	CLUSTER	CLOUD ID	PLASMA [μM]	SCREENING [μM]
Trilostane	3-beta-hydroxysteroid dehydrogenase inhibitor	1	CLOUD195	1.7	8.5
Nitisinone	4-hydroxyphenylpyruvate dioxygenase inhibitor	2	CLOUD190	23.7	118.6
Probucol	ATP-binding cassette transporter blocker	3	CLOUD224	7.6	37.7
Minoxidil	ATP-sensitive inward rectifier potassium channel opener	4	CLOUD040	1.2	6.0
Pinacidil	ATP-sensitive inward rectifier potassium channel opener	4	CLOUD258	1.7	8.3
Carboplatin	DNA alkylating-like	5	CLOUD250	67.0	67.0
Cisplatin	DNA alkylating-like	5			
Oxaliplatin	DNA alkylating-like	5			
Busulfan	DNA alkylator	6	CLOUD041	0.28	1.4
Chlorambucil	DNA alkylator	6	CLOUD046	1.6	8.1
Procarbazine	DNA alkylator	6	CLOUD099	2.7	13.3
Temozolomide	DNA alkylator	6	CLOUD164	70.6	352.9
Altretamine	DNA alkylator	6	CLOUD182	98.9	49.5
Carmustine	DNA alkylator	6	CLOUD225	0.040	0.18
Thiotepa	DNA alkylator	6	CLOUD277	9.7	8.5
Azathioprine	DNA alkylator	6			
Bendamustine	DNA alkylator	6			
Cyclophosphamide	DNA alkylator	6			
Dacarbazine	DNA alkylator	6			
Estramustine	DNA alkylator	6			
Ifosfamide	DNA alkylator	6			
Lomustine	DNA alkylator	6			
Mechlorethamine	DNA alkylator	6			
Melphalan	DNA alkylator	6			
Streptozocin	DNA alkylator	6			
Uracil Mustard	DNA alkylator	6			
Pipobroman	DNA alkylator	6			
Trioxsalen	DNA intercalator	7	CLOUD074	0.010	0.10
Plicamycin	DNA intercalator	7			
Thioguanine	DNA intercalator	7			
Doxorubicin	DNA intercalator; topoisomerase inhibitor	8	CLOUD053	0.040	0.20
Daunorubicin	DNA intercalator; topoisomerase inhibitor	8			
Epirubicin	DNA intercalator; topoisomerase inhibitor	8			
Idarubicin	DNA intercalator; topoisomerase inhibitor	8			
Valrubicin	DNA intercalator; topoisomerase inhibitor	8			
Azacitidine	DNA methyltransferase inhibitor	9	CLOUD115	3.1	15.4
Decitabine	DNA methyltransferase inhibitor	9			
Cytarabine	DNA polymerase inhibitor	10	CLOUD057	2.1	10.3

Fludarabine	DNA polymerase inhibitor	10			
Methyl dopa	DOPA decarboxylase inhibitor	11	CLOUD186	23.7	118.4
Carbidopa	DOPA decarboxylase inhibitor	11			
Valproate	GABA aminotransferase inhibitor	12	CLOUD249	693.4	3467.1
Vigabatrin	GABA aminotransferase inhibitor	12			
Ezetimibe	Niemann-Pick C1-Like 1 protein inhibitor	13	CLOUD066	0.17	0.90
Clopidogrel	P2Y receptor antagonist	14	CLOUD019	0.020	0.10
Prasugrel	P2Y receptor antagonist	14			
Ticlopidine	P2Y receptor antagonist	14			
Pyridostigmine Bromide	acetylcholinesterase inhibitor	15	CLOUD009	1.1	5.5
Tacrine	acetylcholinesterase inhibitor	15	CLOUD091	0.050	0.30
Galantamine	acetylcholinesterase inhibitor	15	CLOUD116	4.0	20.0
Amibenonium	acetylcholinesterase inhibitor	15			
Donepezil	acetylcholinesterase inhibitor	15			
Edrophonium	acetylcholinesterase inhibitor	15			
Hexafluorenium	acetylcholinesterase inhibitor	15			
Rivastigmine	acetylcholinesterase inhibitor	15			
Pentostatin	adenosine deaminase inhibitor	16	CLOUD138	11.2	55.9
Theophylline	adenosine receptor antagonist; phosphodiesterase inhibitor	17	CLOUD251	111.0	104.1
Aminophylline	adenosine receptor antagonist; phosphodiesterase inhibitor	17			
Oxtriphylline	adenosine receptor antagonist; phosphodiesterase inhibitor	17			
Dexmedetomidine	adrenergic receptor agonist	18	CLOUD004	0.010	0.042
Isoproterenol	adrenergic receptor agonist	18	CLOUD082	2.4	11.8
Epinephrine	adrenergic receptor agonist	18	CLOUD133	5.5	27.3
Guanfacine	adrenergic receptor agonist	18	CLOUD273	0.020	10.0
Arbutamine	adrenergic receptor agonist	18			
Clonidine	adrenergic receptor agonist	18			
Dobutamine	adrenergic receptor agonist	18			
Guanabenz	adrenergic receptor agonist	18			
Mephentermine	adrenergic receptor agonist	18			
Metaraminol	adrenergic receptor agonist	18			
Methoxamine	adrenergic receptor agonist	18			
Midodrine	adrenergic receptor agonist	18			
Norepinephrine	adrenergic receptor agonist	18			
Phenylephrine	adrenergic receptor agonist	18			
Phenylpropanolamine	adrenergic receptor agonist	18			
Protokylol	adrenergic receptor agonist	18			
Pseudoephedrine	adrenergic receptor agonist	18			
Ritodrine	adrenergic receptor agonist	18			
Salbutamol	adrenergic receptor agonist	18			
Terbutaline	adrenergic receptor agonist	18			
Tetrahydrozoline	adrenergic receptor agonist	18			
Tizanidine	adrenergic receptor agonist	18			
Dihydroergotamine	adrenergic receptor agonist; adrenergic receptor antagonist	19	CLOUD069	0.015	0.10
Ergotamine	adrenergic receptor agonist; adrenergic receptor antagonist	19			

RESULTS

Terazosin	adrenergic receptor antagonist	20	CLOUD110	0.21	1.0
Atenolol	adrenergic receptor antagonist	20	CLOUD124	3.8	18.8
Tolazoline	adrenergic receptor antagonist	20	CLOUD125	25.0	124.9
Acebutolol	adrenergic receptor antagonist	20			
Alfuzosin	adrenergic receptor antagonist	20			
Betaxolol	adrenergic receptor antagonist	20			
Bethanidine	adrenergic receptor antagonist	20			
Bisoprolol	adrenergic receptor antagonist	20			
Carvedilol	adrenergic receptor antagonist	20			
Doxazosin	adrenergic receptor antagonist	20			
Ergoloid	adrenergic receptor antagonist	20			
Esmolol	adrenergic receptor antagonist	20			
Labetalol	adrenergic receptor antagonist	20			
Metoprolol	adrenergic receptor antagonist	20			
Nadolol	adrenergic receptor antagonist	20			
Nebivolol	adrenergic receptor antagonist	20			
Oxprenolol	adrenergic receptor antagonist	20			
Penbutolol	adrenergic receptor antagonist	20			
Phenoxybenzamine	adrenergic receptor antagonist	20			
Phentolamine	adrenergic receptor antagonist	20			
Pindolol	adrenergic receptor antagonist	20			
Prazosin	adrenergic receptor antagonist	20			
Propranolol	adrenergic receptor antagonist	20			
Silodosin	adrenergic receptor antagonist	20			
Tamsulosin	adrenergic receptor antagonist	20			
Timolol	adrenergic receptor antagonist	20			
Propiomazine	adrenergic receptor antagonist	20			
Thiethylperazine	adrenergic receptor antagonist	20			
Mirtazapine	adrenergic receptor antagonist	20			
Fomepizole	alcohol dehydrogenase inhibitor	21	CLOUD242	299.6	1498.2
Disulfiram	aldehyde dehydrogenase inhibitor	22	CLOUD062	1.4	6.7
Acarbose	alpha glucosidase inhibitor	23	CLOUD075	0.44	2.2
Miglitol	alpha glucosidase inhibitor	23	CLOUD159	9.1	43.4
Amiloride	amiloride-sensitive sodium channel inhibitor	24	CLOUD017	0.22	1.1
Triamterene	amiloride-sensitive sodium channel inhibitor	24	CLOUD054	0.39	2.0
Testosterone	androgen receptor agonist	25	CLOUD051	0.030	0.20
Stanozolol	androgen receptor agonist	25	CLOUD158	12.5	57.8
Danazol	androgen receptor agonist	25			
Dromostanolone	androgen receptor agonist	25			
Ethylestrenol	androgen receptor agonist	25			
Fluoxymesterone	androgen receptor agonist	25			
Methyltestosterone	androgen receptor agonist	25			
Nandrolone	androgen receptor agonist	25			
Oxandrolone	androgen receptor agonist	25			
Oxymetholone	androgen receptor agonist	25			
Flutamide	androgen receptor antagonist	26	CLOUD142	5.4	27.2

Bicalutamide	androgen receptor antagonist	26			
Nilutamide	androgen receptor antagonist	26			
Enalaprilat	angiotensin converting enzyme inhibitor	27	CLOUD095	0.14	0.70
Benazepril	angiotensin converting enzyme inhibitor	27			
Captopril	angiotensin converting enzyme inhibitor	27			
Deserpidine	angiotensin converting enzyme inhibitor	27			
Enalapril	angiotensin converting enzyme inhibitor	27			
Fosinopril	angiotensin converting enzyme inhibitor	27			
Lisinopril	angiotensin converting enzyme inhibitor	27			
Moexipril	angiotensin converting enzyme inhibitor	27			
Perindopril	angiotensin converting enzyme inhibitor	27			
Quinapril	angiotensin converting enzyme inhibitor	27			
Ramipril	angiotensin converting enzyme inhibitor	27			
Rescinnamine	angiotensin converting enzyme inhibitor	27			
Spirapril	angiotensin converting enzyme inhibitor	27			
Trandolapril	angiotensin converting enzyme inhibitor	27			
Olmesartan Medoxomil	angiotensin receptor antagonist	28	CLOUD093	1.3	6.7
Candesartan	angiotensin receptor antagonist	28			
Eprosartan	angiotensin receptor antagonist	28			
Irbesartan	angiotensin receptor antagonist	28			
Losartan	angiotensin receptor antagonist	28			
Telmisartan	angiotensin receptor antagonist	28			
Valsartan	angiotensin receptor antagonist	28			
Anastrozole	aromatase inhibitor	29	CLOUD085	0.10	0.50
Testolactone	aromatase inhibitor	29	CLOUD281	10.0	10.0
Aminoglutethimide	aromatase inhibitor	29			
Exemestane	aromatase inhibitor	29			
Letrozole	aromatase inhibitor	29			
Metronidazole	bacterial DNA alkylator	30	CLOUD170	58.4	292.1
Furazolidone	bacterial DNA intercalator	31	CLOUD135	4.4	10.9
Clofazimine	bacterial DNA intercalator	31			
Mitomycin	bacterial DNA intercalator	31			
Isoniazid	bacterial InhA inhibitor	32	CLOUD171	72.9	364.6
Ethionamide	bacterial InhA inhibitor	32			
Rifabutin	bacterial RNA polymerase inhibitor	33	CLOUD086	0.18	0.90
Rifapentine	bacterial RNA polymerase inhibitor	33			
Rifaximin	bacterial RNA polymerase inhibitor	33			
D-Cycloserine	bacterial alanine racemase inhibitor; bacterial D-alanine--D-alanine ligase inhibitor	34	CLOUD177	98.0	122.4
Ethambutol	bacterial arabinosyltransferase inhibitor	35	CLOUD185	29.4	146.8
Sulbactam	bacterial beta-lactamase inhibitor	36	CLOUD214	343.0	1714.9
Clavulanate	bacterial beta-lactamase inhibitor	36			

RESULTS

Tazobactam	bacterial beta-lactamase inhibitor	36			
Trimethoprim	bacterial dihydrofolate reductase inhibitor	37	CLOUD144	8.6	43.1
Pyrimethamine	bacterial dihydrofolate reductase inhibitor	37			
Sulfameter	bacterial dihydropteroate synthase inhibitor	38	CLOUD161	321.1	1604.7
Sulfacytine	bacterial dihydropteroate synthase inhibitor	38			
Sulfadiazine	bacterial dihydropteroate synthase inhibitor	38			
Sulfadoxine	bacterial dihydropteroate synthase inhibitor	38			
Sulfamerazine	bacterial dihydropteroate synthase inhibitor	38			
Sulfamethazine	bacterial dihydropteroate synthase inhibitor	38			
Sulfamethizole	bacterial dihydropteroate synthase inhibitor	38			
Sulfamethoxazole	bacterial dihydropteroate synthase inhibitor	38			
Sulfaphenazole	bacterial dihydropteroate synthase inhibitor	38			
Sulfapyridine	bacterial dihydropteroate synthase inhibitor	38			
Sulfathiazole	bacterial dihydropteroate synthase inhibitor	38			
Sulfisoxazole	bacterial dihydropteroate synthase inhibitor	38			
Sulfoxone	bacterial dihydropteroate synthase inhibitor	38			
Fosfomycin	bacterial enolpyruvate transferase inhibitor	39	CLOUD252	231.8	3.1
Pyrazinamide	bacterial fatty acid synthase inhibitor	40	CLOUD245	609.2	609.3
Mycophenolic Acid	bacterial inosine-5-monophosphate dehydrogenase inhibitor	41	CLOUD165	15.6	78.0
Cefmenoxime	bacterial penicillin-binding protein inhibitor	42	CLOUD216	183.8	918.8
Amdinocillin	bacterial penicillin-binding protein inhibitor	42			
Amoxicillin	bacterial penicillin-binding protein inhibitor	42			
Ampicillin	bacterial penicillin-binding protein inhibitor	42			
Azlocillin	bacterial penicillin-binding protein inhibitor	42			
Aztreonam	bacterial penicillin-binding protein inhibitor	42			
Bacampicillin	bacterial penicillin-binding protein inhibitor	42			
Benzylpenicillin	bacterial penicillin-binding protein inhibitor	42			
Carbenicillin	bacterial penicillin-binding protein inhibitor	42			
Cefaclor	bacterial penicillin-binding protein inhibitor	42			
Cefadroxil	bacterial penicillin-binding protein inhibitor	42			
Cefalotin	bacterial penicillin-binding protein inhibitor	42			
Cefamandole	bacterial penicillin-binding protein inhibitor	42			
Cefazolin	bacterial penicillin-binding protein inhibitor	42			
Cefdinir	bacterial penicillin-binding protein inhibitor	42			
Cefditoren	bacterial penicillin-binding protein inhibitor	42			
Cefepime	bacterial penicillin-binding protein inhibitor	42			

Cefixime	bacterial penicillin-binding protein inhibitor	42			
Cefmetazole	bacterial penicillin-binding protein inhibitor	42			
Cefonicid	bacterial penicillin-binding protein inhibitor	42			
Cefoperazone	bacterial penicillin-binding protein inhibitor	42			
Ceforanide	bacterial penicillin-binding protein inhibitor	42			
Cefotaxime	bacterial penicillin-binding protein inhibitor	42			
Cefotetan	bacterial penicillin-binding protein inhibitor	42			
Cefotiam	bacterial penicillin-binding protein inhibitor	42			
Cefoxitin	bacterial penicillin-binding protein inhibitor	42			
Cefpiramide	bacterial penicillin-binding protein inhibitor	42			
Cefpodoxime	bacterial penicillin-binding protein inhibitor	42			
Cefprozil	bacterial penicillin-binding protein inhibitor	42			
Cefradine	bacterial penicillin-binding protein inhibitor	42			
Ceftazidime	bacterial penicillin-binding protein inhibitor	42			
Ceftibuten	bacterial penicillin-binding protein inhibitor	42			
Ceftizoxime	bacterial penicillin-binding protein inhibitor	42			
Ceftriaxone	bacterial penicillin-binding protein inhibitor	42			
Cefuroxime	bacterial penicillin-binding protein inhibitor	42			
Cephalexin	bacterial penicillin-binding protein inhibitor	42			
Cephaloglycin	bacterial penicillin-binding protein inhibitor	42			
Cephapirin	bacterial penicillin-binding protein inhibitor	42			
Cloxacillin	bacterial penicillin-binding protein inhibitor	42			
Cyclacillin	bacterial penicillin-binding protein inhibitor	42			
Dicloxacillin	bacterial penicillin-binding protein inhibitor	42			
Doripenem	bacterial penicillin-binding protein inhibitor	42			
Ertapenem	bacterial penicillin-binding protein inhibitor	42			
Hetacillin	bacterial penicillin-binding protein inhibitor	42			
Imipenem	bacterial penicillin-binding protein inhibitor	42			
Loracarbef	bacterial penicillin-binding protein inhibitor	42			
Meropenem	bacterial penicillin-binding protein inhibitor	42			
Methicillin	bacterial penicillin-binding protein inhibitor	42			
Mezlocillin	bacterial penicillin-binding protein inhibitor	42			
Moxalactam	bacterial penicillin-binding protein inhibitor	42			
Nafcillin	bacterial penicillin-binding protein inhibitor	42			
Oxacillin	bacterial penicillin-binding protein inhibitor	42			
Penicillin G	bacterial penicillin-binding protein inhibitor	42			

RESULTS

Penicillin V	bacterial penicillin-binding protein inhibitor	42			
Piperacillin	bacterial penicillin-binding protein inhibitor	42			
Ticarcillin	bacterial penicillin-binding protein inhibitor	42			
Azithromycin	bacterial ribosome inhibitor	43	CLOUD081	1.3	6.7
Tetracycline	bacterial ribosome inhibitor	43	CLOUD160	9.0	45.0
Amikacin	bacterial ribosome inhibitor	43			
Capreomycin	bacterial ribosome inhibitor	43			
Clarithromycin	bacterial ribosome inhibitor	43			
Clindamycin	bacterial ribosome inhibitor	43			
Dalfopristin	bacterial ribosome inhibitor	43			
Demeclocycline	bacterial ribosome inhibitor	43			
Dirithromycin	bacterial ribosome inhibitor	43			
Doxycycline	bacterial ribosome inhibitor	43			
Erythromycin	bacterial ribosome inhibitor	43			
Kanamycin	bacterial ribosome inhibitor	43			
Lincomycin	bacterial ribosome inhibitor	43			
Linezolid	bacterial ribosome inhibitor	43			
Lymecycline	bacterial ribosome inhibitor	43			
Methacycline	bacterial ribosome inhibitor	43			
Minocycline	bacterial ribosome inhibitor	43			
Netilmicin	bacterial ribosome inhibitor	43			
Nitrofurantoin	bacterial ribosome inhibitor	43			
Oxytetracycline	bacterial ribosome inhibitor	43			
Quinupristin	bacterial ribosome inhibitor	43			
Rifampin	bacterial ribosome inhibitor	43			
Spectinomycin	bacterial ribosome inhibitor	43			
Streptomycin	bacterial ribosome inhibitor	43			
Telithromycin	bacterial ribosome inhibitor	43			
Tigecycline	bacterial ribosome inhibitor	43			
Troleandomycin	bacterial ribosome inhibitor	43			
Viomycin	bacterial ribosome inhibitor	43			
Enoxacin	bacterial topoisomerase inhibitor	44	CLOUD156	12.5	62.4
Novobiocin	bacterial topoisomerase inhibitor	44	CLOUD231	90.6	510.1
Alatrofloxacin	bacterial topoisomerase inhibitor	44			
Cinoxacin	bacterial topoisomerase inhibitor	44			
Ciprofloxacin	bacterial topoisomerase inhibitor	44			
Gemifloxacin	bacterial topoisomerase inhibitor	44			
Grepafloxacin	bacterial topoisomerase inhibitor	44			
Levofloxacin	bacterial topoisomerase inhibitor	44			
Lomefloxacin	bacterial topoisomerase inhibitor	44			
Moxifloxacin	bacterial topoisomerase inhibitor	44			
Nalidixic Acid	bacterial topoisomerase inhibitor	44			
Norfloxacin	bacterial topoisomerase inhibitor	44			
Ofloxacin	bacterial topoisomerase inhibitor	44			
Sparfloxacin	bacterial topoisomerase inhibitor	44			
Trovafloxacin	bacterial topoisomerase inhibitor	44			

Acetohydroxamic Acid	bacterial urease inhibitor	45	CLOUD227	523.5	523.5
Bumetanide	bumetanide sensitive sodium-potassium-chloride cotransporter inhibitor	46	CLOUD056	0.20	1.0
Ethacrynic Acid	bumetanide sensitive sodium-potassium-chloride cotransporter inhibitor	46			
Furosemide	bumetanide sensitive sodium-potassium-chloride cotransporter inhibitor	46			
Torasemide	bumetanide sensitive sodium-potassium-chloride cotransporter inhibitor	46			
Tacrolimus	calcineurin inhibitor	47	CLOUD119	0.020	0.090
Cinacalcet	calcium sensing receptor agonist	48	CLOUD222	0.080	0.40
Nabilone	cannabinoid receptor agonist	49	CLOUD286	0.0054	0.027
Marinol	cannabinoid receptor agonist	49			
Carglumic Acid	carbamoyl-phosphate synthase activator	50	CLOUD162	13.7	68.4
Acetazolamide	carbonic anhydrase inhibitor	51	CLOUD192	90.0	90.0
Dichlorphenamide	carbonic anhydrase inhibitor	51	CLOUD241	214.8	214.8
Ethoxzolamide	carbonic anhydrase inhibitor	51			
Methazolamide	carbonic anhydrase inhibitor	51			
Acetohexamide	carbonic anhydrase inhibitor; sulfonyleurea receptor agonist	52	CLOUD240	215.8	1079.0
Entacapone	catechol O-methyltransferase inhibitor	53	CLOUD076	3.3	16.4
Tolcapone	catechol O-methyltransferase inhibitor	53			
Miglustat	ceramide glucosyltransferase inhibitor	54	CLOUD223	92.6	92.6
Maraviroc	chemokine receptor antagonist	55	CLOUD026	2.3	11.4
Plerixafor	chemokine receptor antagonist	55	CLOUD293	5.1	Not Tested
Doxapram	chemoreceptor agonist	56	CLOUD157	13.2	66.1
Oxyphenbutazone	cyclooxygenase inhibitor	57	CLOUD193	308.3	308.3
Fenoprofen	cyclooxygenase inhibitor	57	CLOUD230	247.7	1238.3
Acetaminophen	cyclooxygenase inhibitor	57			
Acetylsalicylic Acid	cyclooxygenase inhibitor	57			
Carpofen	cyclooxygenase inhibitor	57			
Celecoxib	cyclooxygenase inhibitor	57			
Diclofenac	cyclooxygenase inhibitor	57			
Diffunisal	cyclooxygenase inhibitor	57			
Etodolac	cyclooxygenase inhibitor	57			
Flurbiprofen	cyclooxygenase inhibitor	57			
Ibuprofen	cyclooxygenase inhibitor	57			
Indomethacin	cyclooxygenase inhibitor	57			
Ketoprofen	cyclooxygenase inhibitor	57			
Ketorolac	cyclooxygenase inhibitor	57			
Mefenamic Acid	cyclooxygenase inhibitor	57			
Meloxicam	cyclooxygenase inhibitor	57			
Nabumetone	cyclooxygenase inhibitor	57			
Naproxen	cyclooxygenase inhibitor	57			
Oxaprozin	cyclooxygenase inhibitor	57			
Phenylbutazone	cyclooxygenase inhibitor	57			
Piroxicam	cyclooxygenase inhibitor	57			

RESULTS

Rofecoxib	cyclooxygenase inhibitor	57			
Sulindac	cyclooxygenase inhibitor	57			
Tolmetin	cyclooxygenase inhibitor	57			
Valdecoxib	cyclooxygenase inhibitor	57			
Meclofenamic Acid	cyclooxygenase inhibitor; phospholipase inhibitor	58	CLOUD166	16.2	81.1
Atovaquone	cytochrome bc1 inhibitor	59	CLOUD218	37.9	47.4
Methotrexate	dihydrofolate reductase inhibitor	60	CLOUD089	0.090	0.40
Pralatrexate	dihydrofolate reductase inhibitor	60			
Trimetrexate	dihydrofolate reductase inhibitor	60			
Pemetrexed	dihydrofolate reductase inhibitor	60			
Leflunomide	dihydroorotate dehydrogenase inhibitor	61	CLOUD243	66.6	333.1
Sitagliptin	dipeptidyl peptidase 4 inhibitor	62	CLOUD061	0.95	4.8
Saxagliptin	dipeptidyl peptidase 4 inhibitor	62	CLOUD065	0.080	0.40
Pramipexole	dopamine receptor agonist	63	CLOUD011	0.030	0.20
Dopamine	dopamine receptor agonist	63	CLOUD023	0.50	2.5
Apomorphine	dopamine receptor agonist	63			
Bromocriptine	dopamine receptor agonist	63			
Cabergoline	dopamine receptor agonist	63			
Levodopa	dopamine receptor agonist	63			
Pergolide	dopamine receptor agonist	63			
Ropinirole	dopamine receptor agonist	63			
Rotigotine	dopamine receptor agonist	63			
Methylergonovine	dopamine receptor agonist; dopamine receptor antagonist	64	CLOUD126	0.010	0.044
Aripiprazole	dopamine receptor agonist; dopamine receptor antagonist; serotonin receptor agonist; serotonin receptor antagonist	65	CLOUD084	0.67	3.3
Trifluoperazine	dopamine receptor antagonist	66	CLOUD025	0.020	0.10
Acetophenazine	dopamine receptor antagonist	66			
Carphenazine	dopamine receptor antagonist	66			
Chlorprothixene	dopamine receptor antagonist	66			
Droperidol	dopamine receptor antagonist	66			
Fenoldopam	dopamine receptor antagonist	66			
Fluphenazine	dopamine receptor antagonist	66			
Haloperidol	dopamine receptor antagonist	66			
Loxapine	dopamine receptor antagonist	66			
Metoclopramide	dopamine receptor antagonist	66			
Molindone	dopamine receptor antagonist	66			
Perphenazine	dopamine receptor antagonist	66			
Pimozide	dopamine receptor antagonist	66			
Prochlorperazine	dopamine receptor antagonist	66			
Thioridazine	dopamine receptor antagonist	66			
Thiothixene	dopamine receptor antagonist	66			
Clozapine	dopamine receptor antagonist	66			
Iloperidone	dopamine receptor antagonist	66			
Mesoridazine	dopamine receptor antagonist	66			
Paliperidone	dopamine receptor antagonist	66			

Quetiapine	dopamine receptor antagonist	66			
Olanzapine	dopamine receptor antagonist	66			
Triflupromazine	dopamine receptor antagonist; histamine receptor antagonist; serotonin receptor antagonist; muscarinic acetylcholine receptor antagonist; alpha adrenergic receptor antagonist	67	CLOUD256	0.28	1.4
Chlorpromazine	dopamine receptor antagonist; histamine receptor antagonist; serotonin receptor antagonist; muscarinic acetylcholine receptor antagonist; alpha adrenergic receptor antagonist	67			
Promazine	dopamine receptor antagonist; histamine receptor antagonist; serotonin receptor antagonist; muscarinic acetylcholine receptor antagonist; alpha adrenergic receptor antagonist	67			
Armodafinil	dopamine transporter inhibitor	68	CLOUD201	27.1	27.1
Methylphenidate	dopamine transporter inhibitor	68			
Bupropion	dopamine transporter inhibitor	68			
Amphetamine	dopamine transporter substrate; norepinephrine transporter substrate	69	Controlled		
Benzphetamine	dopamine transporter substrate; norepinephrine transporter substrate	69	Controlled		
Dextroamphetamine	dopamine transporter substrate; norepinephrine transporter substrate	69	Controlled		
Lisdexamfetamine	dopamine transporter substrate; norepinephrine transporter substrate	69	Controlled		
Methamphetamine	dopamine transporter substrate; norepinephrine transporter substrate	69	Controlled		
Phenmetrazine	dopamine transporter substrate; norepinephrine transporter substrate	69	Controlled		
Bosentan	endothelin receptor antagonist	70	CLOUD206	6.7	10.0
Ambrisentan	endothelin receptor antagonist	70			
Ethinyl Estradiol	estrogen receptor agonist	71	CLOUD088	0.00046	0.0023
Chlorotrianisene	estrogen receptor agonist	71			
Diethylstilbestrol	estrogen receptor agonist	71			
Estradiol	estrogen receptor agonist	71			
Estrone	estrogen receptor agonist	71			
Mestranol	estrogen receptor agonist	71			
Polyestradiol	estrogen receptor agonist	71			
Quinestrol	estrogen receptor agonist	71			
Clomifene	estrogen receptor agonist	71			
Raloxifene	estrogen receptor agonist	71			
Toremifene	estrogen receptor agonist	71			
Tamoxifen	estrogen receptor antagonist	72	CLOUD064	1.4	6.7
Fulvestrant	estrogen receptor antagonist	72			
Itraconazole	fungal lanosterol 14-alpha demethylase inhibitor	73	CLOUD113	2.8	14.2
Fluconazole	fungal lanosterol 14-alpha demethylase inhibitor	73			
Ketoconazole	fungal lanosterol 14-alpha demethylase inhibitor	73			

RESULTS

Miconazole	fungal lanosterol 14-alpha demethylase inhibitor	73			
Posaconazole	fungal lanosterol 14-alpha demethylase inhibitor	73			
Voriconazole	fungal lanosterol 14-alpha demethylase inhibitor	73			
Albendazole	fungal tubulin polymerization inhibitor	74	CLOUD143	5.7	28.3
Prednisolone	glucocorticoid receptor agonist	75	CLOUD106	2.8	13.9
Betamethasone	glucocorticoid receptor agonist	75			
Cortisone	glucocorticoid receptor agonist	75			
Dexamethasone	glucocorticoid receptor agonist	75			
Fludrocortisone	glucocorticoid receptor agonist	75			
Fluprednisolone	glucocorticoid receptor agonist	75			
Hydrocortisone	glucocorticoid receptor agonist	75			
Meprednisone	glucocorticoid receptor agonist	75			
Methylprednisolone	glucocorticoid receptor agonist	75			
Paramethasone	glucocorticoid receptor agonist	75			
Prednisone	glucocorticoid receptor agonist	75			
Eptifibatide	glycoprotein IIb-IIIa receptor inhibitor	76	CLOUD090	1.1	5.3
Tirofiban	glycoprotein IIb-IIIa receptor inhibitor	76			
Isosorbide Dinitrate	guanylate cyclase activator	77	CLOUD007	0.030	0.10
Isosorbide Mononitrate	guanylate cyclase activator	77			
Nitroglycerin	guanylate cyclase activator	77			
Oxamniquine	helminthic DNA alkylator	78	CLOUD289	7.1	Not Tested
Ivermectin	helminthic glutamate-gated chloride channel activator	79	CLOUD280	0.029	0.14
Levamisole	helminthic nicotinic acetylcholine receptor agonist	80	CLOUD097	2.4	11.7
Mebendazole	helminthic tubulin polymerization inhibitor	81	CLOUD087	0.34	1.7
Amodiaquine	histamine N-methyltransferase inhibitor	82	CLOUD015	0.14	0.70
Azatadine	histamine receptor antagonist	83	CLOUD010	0.090	0.40
Nizatidine	histamine receptor antagonist	83	CLOUD118	1.5	7.5
Dexchlorpheniramine	histamine receptor antagonist	83	CLOUD204	0.030	0.13
Acrivastine	histamine receptor antagonist	83			
Bromodiphenhydramine	histamine receptor antagonist	83			
Brompheniramine	histamine receptor antagonist	83			
Bucizine	histamine receptor antagonist	83			
Carbinoxamine	histamine receptor antagonist	83			
Cetirizine	histamine receptor antagonist	83			
Chlophedianol	histamine receptor antagonist	83			
Chlorpheniramine	histamine receptor antagonist	83			
Cimetidine	histamine receptor antagonist	83			
Clemastine	histamine receptor antagonist	83			
Cyclizine	histamine receptor antagonist	83			
Cyproheptadine	histamine receptor antagonist	83			
Desloratadine	histamine receptor antagonist	83			
Dexbrompheniramine	histamine receptor antagonist	83			
Dimenhydrinate	histamine receptor antagonist	83			
Diphenhydramine	histamine receptor antagonist	83			

Diphenylpyraline	histamine receptor antagonist	83			
Doxepin	histamine receptor antagonist	83			
Doxylamine	histamine receptor antagonist	83			
Famotidine	histamine receptor antagonist	83			
Fexofenadine	histamine receptor antagonist	83			
Hydroxyzine	histamine receptor antagonist	83			
Levocetirizine	histamine receptor antagonist	83			
Loratadine	histamine receptor antagonist	83			
Meclizine	histamine receptor antagonist	83			
Mepyramine	histamine receptor antagonist	83			
Methdilazine	histamine receptor antagonist	83			
Olopatadine	histamine receptor antagonist	83			
Promethazine	histamine receptor antagonist	83			
Ranitidine	histamine receptor antagonist	83			
Trimeprazine	histamine receptor antagonist	83			
Tripelennamine	histamine receptor antagonist	83			
Triprolidine	histamine receptor antagonist	83			
Vorinostat	histone deacetylase inhibitor	84	CLOUD112	1.2	9.8
Romidepsin	histone deacetylase inhibitor	84	CLOUD292	0.70	Not Tested
Cerivastatin	hydroxymethylglutaryl coenzyme A reductase inhibitor	85	CLOUD104	0.090	0.46
Atorvastatin	hydroxymethylglutaryl coenzyme A reductase inhibitor	85			
Fluvastatin	hydroxymethylglutaryl coenzyme A reductase inhibitor	85			
Lovastatin	hydroxymethylglutaryl coenzyme A reductase inhibitor	85			
Pitavastatin	hydroxymethylglutaryl coenzyme A reductase inhibitor	85			
Pravastatin	hydroxymethylglutaryl coenzyme A reductase inhibitor	85			
Rosuvastatin	hydroxymethylglutaryl coenzyme A reductase inhibitor	85			
Simvastatin	hydroxymethylglutaryl coenzyme A reductase inhibitor	85			
Zaleplon	ionotropic GABA receptor agonist	86	CLOUD005	0.33	1.6
Carisoprodol	ionotropic GABA receptor agonist	86	CLOUD188	115.2	576.3
Etomidate	ionotropic GABA receptor agonist	86	CLOUD200	2.1	10.3
Primidone	ionotropic GABA receptor agonist	86	CLOUD226	55.0	275.3
Alprazolam	ionotropic GABA receptor agonist	86			
Butabarbital	ionotropic GABA receptor agonist	86			
Butalbital	ionotropic GABA receptor agonist	86			
Chlordiazepoxide	ionotropic GABA receptor agonist	86			
Chlormezanone	ionotropic GABA receptor agonist	86			
Clonazepam	ionotropic GABA receptor agonist	86			
Clorazepate	ionotropic GABA receptor agonist	86			
Diazepam	ionotropic GABA receptor agonist	86			
Estazolam	ionotropic GABA receptor agonist	86			
Eszopiclone	ionotropic GABA receptor agonist	86			
Flurazepam	ionotropic GABA receptor agonist	86			
Fospropofol	ionotropic GABA receptor agonist	86			
Glutethimide	ionotropic GABA receptor agonist	86			
Halazepam	ionotropic GABA receptor agonist	86			

RESULTS

Lorazepam	ionotropic GABA receptor agonist	86			
Meprobamate	ionotropic GABA receptor agonist	86			
Metharbital	ionotropic GABA receptor agonist	86			
Methohexital	ionotropic GABA receptor agonist	86			
Methyprylon	ionotropic GABA receptor agonist	86			
Midazolam	ionotropic GABA receptor agonist	86			
Oxazepam	ionotropic GABA receptor agonist	86			
Pentobarbital	ionotropic GABA receptor agonist	86			
Prazepam	ionotropic GABA receptor agonist	86			
Quazepam	ionotropic GABA receptor agonist	86			
Secobarbital	ionotropic GABA receptor agonist	86			
Talbutal	ionotropic GABA receptor agonist	86			
Temazepam	ionotropic GABA receptor agonist	86			
Thiamylal	ionotropic GABA receptor agonist	86			
Thiopental	ionotropic GABA receptor agonist	86			
Triazolam	ionotropic GABA receptor agonist	86			
Zolpidem	ionotropic GABA receptor agonist	86			
Gamma Hydroxybutyric Acid	ionotropic GABA receptor agonist; metabotropic GABA receptor agonist	87	Controlled		
Flumazenil	ionotropic GABA receptor antagonist	88	CLOUD045	0.33	1.6
Memantine	ionotropic glutamate receptor antagonist	89	CLOUD032	0.26	1.3
Acamprosate	ionotropic glutamate receptor antagonist	89	CLOUD272	3.6	10.0
Desflurane	ionotropic glutamate receptor antagonist	89			
Enflurane	ionotropic glutamate receptor antagonist	89			
Halothane	ionotropic glutamate receptor antagonist	89			
Isoflurane	ionotropic glutamate receptor antagonist	89			
Ketamine	ionotropic glutamate receptor antagonist	89			
Methoxyflurane	ionotropic glutamate receptor antagonist	89			
Sevoflurane	ionotropic glutamate receptor antagonist	89			
Triclofos	ionotropic glutamate receptor antagonist	89			
Dextromethorphan	ionotropic glutamate receptor antagonist; sigma-1 receptor agonist	90	CLOUD287	0.15	0.74
Zafirlukast	leukotriene receptor antagonist	91	CLOUD092	0.050	0.26
Montelukast	leukotriene receptor antagonist	91			
Zileuton	leukotriene synthase inhibitor	92	CLOUD187	21.1	105.4
Ramelteon	melatonin receptor agonist	93	CLOUD107	0.030	0.13
Baclofen	metabotropic GABA receptor agonist	94	CLOUD246	2.8	14.0
Piperazine Hexahydrate	metabotropic GABA receptor agonist	94	CLOUD254	1.2	5.8
Propofol	metabotropic GABA receptor agonist	94			
Desoxycorticosterone Pivalate	mineralocorticoid receptor agonist	95	CLOUD001	0.14	0.70
Spironolactone	mineralocorticoid receptor antagonist	96	CLOUD072	0.60	3.0
Drospirenone	mineralocorticoid receptor antagonist	96			

Eplerenone	mineralocorticoid receptor antagonist	96			
Tranylcypromine	monoamine oxidase inhibitor	97	CLOUD020	1.5	7.5
Pargyline	monoamine oxidase inhibitor	97	CLOUD030	0.38	1.9
Isocarboxazid	monoamine oxidase inhibitor	97			
Phenelzine	monoamine oxidase inhibitor	97			
Rasagiline	monoamine oxidase inhibitor	97			
Selegiline	monoamine oxidase inhibitor	97			
Cevimeline	muscarinic acetylcholine receptor agonist	98	CLOUD055	0.30	1.5
Bethanechol	muscarinic acetylcholine receptor agonist	98			
Carbachol	muscarinic acetylcholine receptor agonist; nicotinic acetylcholine receptor agonist	99	CLOUD012	0.00073	0.037
Oxyphenonium Bromide	muscarinic acetylcholine receptor antagonist	100	CLOUD022	0.010	0.10
Trihexyphenidyl	muscarinic acetylcholine receptor antagonist	100	CLOUD042	0.66	3.3
Anisotropine	muscarinic acetylcholine receptor antagonist	100			
Atropine	muscarinic acetylcholine receptor antagonist	100			
Benztropine	muscarinic acetylcholine receptor antagonist	100			
Biperiden	muscarinic acetylcholine receptor antagonist	100			
Clidinium	muscarinic acetylcholine receptor antagonist	100			
Cycrimine	muscarinic acetylcholine receptor antagonist	100			
Darifenacin	muscarinic acetylcholine receptor antagonist	100			
Dicyclomine	muscarinic acetylcholine receptor antagonist	100			
Diphepanil	muscarinic acetylcholine receptor antagonist	100			
Ethopropazine	muscarinic acetylcholine receptor antagonist	100			
Fesoterodine	muscarinic acetylcholine receptor antagonist	100			
Glycopyrrolate	muscarinic acetylcholine receptor antagonist	100			
Hexocyclium	muscarinic acetylcholine receptor antagonist	100			
Isopropamide	muscarinic acetylcholine receptor antagonist	100			
Mepenzolate	muscarinic acetylcholine receptor antagonist	100			
Methantheline	muscarinic acetylcholine receptor antagonist	100			
Methylscopolamine	muscarinic acetylcholine receptor antagonist	100			
Metixene	muscarinic acetylcholine receptor antagonist	100			
Orphenadrine	muscarinic acetylcholine receptor antagonist	100			
Oxybutynin	muscarinic acetylcholine receptor antagonist	100			
Oxyphencyclimine	muscarinic acetylcholine receptor antagonist	100			
Procyclidine	muscarinic acetylcholine receptor antagonist	100			
Propantheline	muscarinic acetylcholine receptor antagonist	100			
Scopolamine	muscarinic acetylcholine receptor antagonist	100			
Solifenacin	muscarinic acetylcholine receptor antagonist	100			

RESULTS

Tiotropium	muscarinic acetylcholine receptor antagonist	100			
Tolterodine	muscarinic acetylcholine receptor antagonist	100			
Tridihexethyl	muscarinic acetylcholine receptor antagonist	100			
Tropium	muscarinic acetylcholine receptor antagonist	100			
Aprepitant	neurokinin receptor antagonist	101	CLOUD264	4.1	20.6
Varenicline	nicotinic acetylcholine receptor agonist	102	CLOUD267	0.047	0.24
Decamethonium	nicotinic acetylcholine receptor agonist	102			
Nicotine	nicotinic acetylcholine receptor agonist	102			
Vecuronium Bromide	nicotinic acetylcholine receptor antagonist	103	CLOUD039	0.66	3.3
Mecamylamine	nicotinic acetylcholine receptor antagonist	103	CLOUD098	0.71	3.6
Cisatracurium Besylate	nicotinic acetylcholine receptor antagonist	103	CLOUD137	3.6	18.1
Succinylcholine Chloride	nicotinic acetylcholine receptor antagonist	103	CLOUD261	2.5	12.6
Pentolinium Tartrate	nicotinic acetylcholine receptor antagonist	103	CLOUD285	6.2	6.2
Atracurium	nicotinic acetylcholine receptor antagonist	103			
Doxacurium	nicotinic acetylcholine receptor antagonist	103			
Gallamine	nicotinic acetylcholine receptor antagonist	103			
Metocurine	nicotinic acetylcholine receptor antagonist	103			
Mivacurium	nicotinic acetylcholine receptor antagonist	103			
Pancuronium	nicotinic acetylcholine receptor antagonist	103			
Pipecuronium	nicotinic acetylcholine receptor antagonist	103			
Rapacuronium	nicotinic acetylcholine receptor antagonist	103			
Rocuronium	nicotinic acetylcholine receptor antagonist	103			
Trimethaphan	nicotinic acetylcholine receptor antagonist	103			
Tubocurarine	nicotinic acetylcholine receptor antagonist	103			
Metformin	non-specific serine-threonine protein kinase activator	104	CLOUD148	7.7	38.7
Everolimus	non-specific serine-threonine protein kinase inhibitor	105	CLOUD196	0.19	0.95
Sirolimus	non-specific serine-threonine protein kinase inhibitor	105			
Temsirolimus	non-specific serine-threonine protein kinase inhibitor	105			
Maprotiline	norepinephrine transporter inhibitor	106	CLOUD006	2.2	10.8
Imipramine	norepinephrine transporter inhibitor	106	CLOUD044	1.3	6.2
Amoxapine	norepinephrine transporter inhibitor	106	CLOUD109	1.9	9.6
Atomoxetine	norepinephrine transporter inhibitor	106			
Desipramine	norepinephrine transporter inhibitor	106			
Mazindol	norepinephrine transporter inhibitor	106			
Nortriptyline	norepinephrine transporter inhibitor	106			
Protriptyline	norepinephrine transporter inhibitor	106			

Trimipramine	norepinephrine transporter inhibitor	106			
Amitriptyline	norepinephrine transporter inhibitor	106			
Guanadrel	norepinephrine transporter substrate	107	CLOUD266	28.1	140.7
Diethylpropion	norepinephrine transporter substrate	107			
Guanethidine	norepinephrine transporter substrate	107			
Phentermine	norepinephrine transporter substrate	107			
Phendimetrazine	norepinephrine transporter substrate; dopamine transporter substrate	108	Controlled		
Loperamide	opioid receptor agonist	109	CLOUD058	0.010	0.032
Alfentanil	opioid receptor agonist	109			
Anileridine	opioid receptor agonist	109			
Butorphanol	opioid receptor agonist	109			
Codeine	opioid receptor agonist	109			
Difenoxin	opioid receptor agonist	109			
Dihydrocodeine	opioid receptor agonist	109			
Diphenoxylate	opioid receptor agonist	109			
Fentanyl	opioid receptor agonist	109			
Hydrocodone	opioid receptor agonist	109			
Hydromorphone	opioid receptor agonist	109			
Levomethadyl	opioid receptor agonist	109			
Levorphanol	opioid receptor agonist	109			
Meperidine	opioid receptor agonist	109			
Methadone	opioid receptor agonist	109			
Morphine	opioid receptor agonist	109			
Oxycodone	opioid receptor agonist	109			
Oxymorphone	opioid receptor agonist	109			
Propoxyphene	opioid receptor agonist	109			
Remifentanyl	opioid receptor agonist	109			
Sufentanyl	opioid receptor agonist	109			
Tramadol	opioid receptor agonist	109			
Tapentadol	opioid receptor agonist; norepinephrine transporter inhibitor	110	Controlled		
Buprenorphine	opioid receptor agonist; opioid receptor antagonist	111	Controlled		
Dezocine	opioid receptor agonist; opioid receptor antagonist	111	Controlled		
Nalbuphine	opioid receptor agonist; opioid receptor antagonist	111	Controlled		
Nalmefene	opioid receptor agonist; opioid receptor antagonist	111	Controlled		
Pentazocine	opioid receptor agonist; opioid receptor antagonist	111	Controlled		
Naltrexone	opioid receptor antagonist	112	CLOUD038	0.090	0.40
Alvimopan	opioid receptor antagonist	112			
Levallorphan	opioid receptor antagonist	112			
Methylnaltrexone	opioid receptor antagonist	112			
Naloxone	opioid receptor antagonist	112			
(+/-)-Sulfinpyrazone	organic anion transporter inhibitor	113	CLOUD229	42.0	210.1
Probenecid	organic anion transporter inhibitor	113	CLOUD244	700.9	3504.3

RESULTS

Pamidronic Acid	osteoclastic proton pump inhibitor; protein-tyrosine phosphatase inhibitor	114	CLOUD276	4.3	21.3
Alendronate	osteoclastic proton pump inhibitor; protein-tyrosine phosphatase inhibitor	114			
Etidronic Acid	osteoclastic proton pump inhibitor; protein-tyrosine phosphatase inhibitor	114			
Ibandronate	osteoclastic proton pump inhibitor; protein-tyrosine phosphatase inhibitor	114			
Risedronate	osteoclastic proton pump inhibitor; protein-tyrosine phosphatase inhibitor	114			
Tiludronate	osteoclastic proton pump inhibitor; protein-tyrosine phosphatase inhibitor	114			
Zoledronate	osteoclastic proton pump inhibitor; protein-tyrosine phosphatase inhibitor	114			
Orlistat	pancreatic lipase inhibitor	115	CLOUD278	0.010	0.091
Rosiglitazone	peroxisome proliferator-activated receptor agonist	116	CLOUD016	0.84	4.2
Clofibrate	peroxisome proliferator-activated receptor agonist	116	CLOUD247	325.5	325.5
Fenofibrate	peroxisome proliferator-activated receptor agonist	116			
Gemfibrozil	peroxisome proliferator-activated receptor agonist	116			
Pioglitazone	peroxisome proliferator-activated receptor agonist	116			
Troglitazone	peroxisome proliferator-activated receptor agonist	116			
Sildenafil	phosphodiesterase inhibitor	117	CLOUD073	0.11	0.50
Milrinone	phosphodiesterase inhibitor	117	CLOUD079	1.2	5.9
Dipyridamole	phosphodiesterase inhibitor	117	CLOUD122	4.0	19.8
Anagrelide	phosphodiesterase inhibitor	117			
Cilostazol	phosphodiesterase inhibitor	117			
Dyphylline	phosphodiesterase inhibitor	117			
Inamrinone	phosphodiesterase inhibitor	117			
Pentoxifylline	phosphodiesterase inhibitor	117			
Tadalafil	phosphodiesterase inhibitor	117			
Vardenafil	phosphodiesterase inhibitor	117			
Caffeine	phosphodiesterase inhibitor; adenosine receptor antagonist	118	CLOUD295	51.5	Not Tested
Tranexamic Acid	plasminogen inhibitor	119	CLOUD253	318.0	8.0
Lansoprazole	potassium transporting ATPase inhibitor	120	CLOUD141	4.6	11.1
Dexlansoprazole	potassium transporting ATPase inhibitor	120			
Esomeprazole	potassium transporting ATPase inhibitor	120			
Omeprazole	potassium transporting ATPase inhibitor	120			
Pantoprazole	potassium transporting ATPase inhibitor	120			
Rabeprazole	potassium transporting ATPase inhibitor	120			
Levonorgestrel	progesterone receptor agonist	121	CLOUD043	0.050	0.20
Desogestrel	progesterone receptor agonist	121			
Dienogest	progesterone receptor agonist	121			
Dydrogesterone	progesterone receptor agonist	121			

Ethinodiol	progesterone receptor agonist	121			
Etonogestrel	progesterone receptor agonist	121			
Hydroxyprogesterone	progesterone receptor agonist	121			
Medroxyprogesterone	progesterone receptor agonist	121			
Megestrol	progesterone receptor agonist	121			
Norelgestromin	progesterone receptor agonist	121			
Norethindrone	progesterone receptor agonist	121			
Norethynodrel	progesterone receptor agonist	121			
Norgestimate	progesterone receptor agonist	121			
Progesterone	progesterone receptor agonist	121			
Ulipristal Acetate	progesterone receptor agonist; progesterone receptor antagonist	122	CLOUD027	0.78	3.9
Mifepristone	progesterone receptor antagonist; glucocorticoid receptor agonist	123	CLOUD296	4.6	Not Tested
Hydralazine	prolyl hydroxylase inhibitor	124	CLOUD105	3.1	15.6
Iloprost	prostaglandin receptor agonist	125	CLOUD147	0.00021	0.0010
Dinoprostone	prostaglandin receptor agonist	125	CLOUD270	0.00014	Not Tested
Alprostadil	prostaglandin receptor agonist	125			
Carboprost	prostaglandin receptor agonist	125			
Epoprostenol	prostaglandin receptor agonist	125			
Misoprostol	prostaglandin receptor agonist	125			
Treprostinil	prostaglandin receptor agonist	125			
Bortezomib	proteasome inhibitor	126	CLOUD024	0.31	1.6
Artemether	protozoal calcium transporting ATPase inhibitor	127	CLOUD111	0.77	3.9
Proguanil	protozoal dihydrofolate reductase inhibitor	128	CLOUD036	0.59	3.0
Eflornithine	protozoal ornithine decarboxylase inhibitor; ornithine decarboxylase inhibitor	129	CLOUD207	319.5	79.9
Nitazoxanide	protozoal pyruvate ferredoxin oxidoreductase substrate	130	CLOUD174	9.8	48.8
Paromomycin	protozoal ribosome inhibitor	131	CLOUD197	66.6	1.6
Sunitinib	receptor protein-tyrosine kinase inhibitor	132	CLOUD071	0.15	0.70
Imatinib	receptor protein-tyrosine kinase inhibitor	132	CLOUD114	2.8	14.0
Gefitinib	receptor protein-tyrosine kinase inhibitor	132	CLOUD205	6.9	10.0
Sorafenib	receptor protein-tyrosine kinase inhibitor	132	CLOUD219	16.4	105.5
Pazopanib	receptor protein-tyrosine kinase inhibitor	132	CLOUD234	132.6	4.4
Dasatinib	receptor protein-tyrosine kinase inhibitor	132			
Erlotinib	receptor protein-tyrosine kinase inhibitor	132			
Lapatinib	receptor protein-tyrosine kinase inhibitor	132			
Nilotinib	receptor protein-tyrosine kinase inhibitor	132			
Cilastatin	renal dipeptidase inhibitor	133	CLOUD208	153.4	153.4
Aliskiren	renin inhibitor	134	CLOUD002	0.76	2.5
Acitretin	retinoic acid receptor agonist	135	CLOUD080	1.5	7.7
Bexarotene	retinoic acid receptor agonist	135			
Etretinate	retinoic acid receptor agonist	135			

RESULTS

Isotretinoin	retinoic acid receptor agonist	135			
6-Mercaptopurine	ribonucleoside-diphosphate reductase inhibitor	136	CLOUD102	2.0	9.9
Hydroxyurea	ribonucleoside-diphosphate reductase inhibitor	136	CLOUD179	130.0	650.0
Clofarabine	ribonucleoside-diphosphate reductase inhibitor	136	CLOUD209	1.5	7.5
Cladribine	ribonucleoside-diphosphate reductase inhibitor	136			
Gemcitabine	ribonucleoside-diphosphate reductase inhibitor	136			
Nelarabine	ribonucleoside-diphosphate reductase inhibitor	136			
Dantrolene	ryanodine receptor antagonist	137	CLOUD132	4.8	23.9
Sumatriptan	serotonin receptor agonist	138	CLOUD060	0.20	1.0
Cisapride	serotonin receptor agonist	138	CLOUD067	0.17	0.90
Buspirone	serotonin receptor agonist	138	CLOUD262	0.010	0.050
Almotriptan	serotonin receptor agonist	138			
Eletriptan	serotonin receptor agonist	138			
Frovatriptan	serotonin receptor agonist	138			
Methysergide	serotonin receptor agonist	138			
Naratriptan	serotonin receptor agonist	138			
Rizatriptan	serotonin receptor agonist	138			
Tegaserod	serotonin receptor agonist	138			
Zolmitriptan	serotonin receptor agonist	138			
Palonosetron	serotonin receptor antagonist	139	CLOUD283	0.0082	10.0
Alosetron	serotonin receptor antagonist	139			
Dolasetron	serotonin receptor antagonist	139			
Granisetron	serotonin receptor antagonist	139			
Nefazodone	serotonin receptor antagonist	139			
Ondansetron	serotonin receptor antagonist	139			
Methotrimeprazine	serotonin receptor antagonist	139			
Ziprasidone	serotonin receptor antagonist	139			
Cyclobenzaprine	serotonin receptor antagonist	139			
Asenapine	serotonin receptor antagonist; dopamine receptor antagonist; alpha adrenergic receptor antagonist	140	CLOUD013	0.010	0.10
Risperidone	serotonin receptor antagonist; dopamine receptor antagonist; alpha adrenergic receptor antagonist	140	CLOUD068	0.015	0.10
Fluvoxamine	serotonin transporter inhibitor	141	CLOUD033	0.79	3.9
Sertraline	serotonin transporter inhibitor	141	CLOUD037	0.65	3.3
Trazodone	serotonin transporter inhibitor	141	CLOUD134	4.3	21.5
Citalopram	serotonin transporter inhibitor	141	CLOUD198	0.62	3.1
Escitalopram	serotonin transporter inhibitor	141			
Fluoxetine	serotonin transporter inhibitor	141			
Paroxetine	serotonin transporter inhibitor	141			
Clomipramine	serotonin transporter inhibitor	141			
Desvenlafaxine	serotonin transporter inhibitor	141			
Duloxetine	serotonin transporter inhibitor	141			
Milnacipran	serotonin transporter inhibitor	141			
Sibutramine	serotonin transporter inhibitor	141			

Venlafaxine	serotonin transporter inhibitor	141			
Chlorphentermine	serotonin transporter substrate	142	Controlled	1.29	Not Tested
Tiagabine	sodium- and chloride-dependent GABA transporter inhibitor	143	CLOUD108	0.53	2.7
Digitoxin	sodium-potassium transporting ATPase inhibitor	144	CLOUD077	0.030	0.20
Acetyldigitoxin	sodium-potassium transporting ATPase inhibitor	144			
Deslanoside	sodium-potassium transporting ATPase inhibitor	144			
Digoxin	sodium-potassium transporting ATPase inhibitor	144			
Dutasteride	steroid 5-alpha reductase inhibitor	145	CLOUD070	0.0024	0.011
Finasteride	steroid 5-alpha reductase inhibitor	145			
Nateglinide	sulfonylurea receptor agonist	146	CLOUD163	13.2	10.0
Chlorpropamide	sulfonylurea receptor agonist	146			
Glibenclamide	sulfonylurea receptor agonist	146			
Glimepiride	sulfonylurea receptor agonist	146			
Glipizide	sulfonylurea receptor agonist	146			
Repaglinide	sulfonylurea receptor agonist	146			
Tolazamide	sulfonylurea receptor agonist	146			
Tolbutamide	sulfonylurea receptor agonist	146			
Levetiracetam	synaptic vesicle glycoprotein 2A modulator	147	CLOUD274	217.4	1086.9
Tetrabenazine	synaptic vesicular amine transporter inhibitor	148	CLOUD096	10.0	10.0
Reserpine	synaptic vesicular amine transporter inhibitor	148			
Methyclothiazide	thiazide sensitive sodium-chloride cotransporter inhibitor	149	CLOUD050	0.10	0.50
Diazoxide	thiazide sensitive sodium-chloride cotransporter inhibitor	149	CLOUD180	86.7	433.5
Bendroflumethiazide	thiazide sensitive sodium-chloride cotransporter inhibitor	149			
Benzthiazide	thiazide sensitive sodium-chloride cotransporter inhibitor	149			
Chlorothiazide	thiazide sensitive sodium-chloride cotransporter inhibitor	149			
Chlorthalidone	thiazide sensitive sodium-chloride cotransporter inhibitor	149			
Cyclothiazide	thiazide sensitive sodium-chloride cotransporter inhibitor	149			
Hydrochlorothiazide	thiazide sensitive sodium-chloride cotransporter inhibitor	149			
Hydroflumethiazide	thiazide sensitive sodium-chloride cotransporter inhibitor	149			
Indapamide	thiazide sensitive sodium-chloride cotransporter inhibitor	149			
Metolazone	thiazide sensitive sodium-chloride cotransporter inhibitor	149			
Polythiazide	thiazide sensitive sodium-chloride cotransporter inhibitor	149			
Quinethazone	thiazide sensitive sodium-chloride cotransporter inhibitor	149			
Trichlormethiazide	thiazide sensitive sodium-chloride cotransporter inhibitor	149			
Argatroban	thrombin inhibitor	150	CLOUD008	1.4	6.9
Eltrombopag	thrombopoietin receptor agonist	151	CLOUD279	16.5	82.5
5-Fluorouracil	thymidylate synthase inhibitor	152	CLOUD031	0.62	3.1
Capecitabine	thymidylate synthase inhibitor	152			
Floxuridine	thymidylate synthase inhibitor	152			
Flucytosine	thymidylate synthase inhibitor	152			

RESULTS

Liothyronine	thyroid hormone receptor agonist	153	CLOUD275	0.00003	0.00003
Dextrothyroxine	thyroid hormone receptor agonist	153			
Levothyroxine	thyroid hormone receptor agonist	153			
Propylthiouracil	thyroid peroxidase inhibitor	154	CLOUD175	18.0	90.0
Methimazole	thyroid peroxidase inhibitor	154			
Hydroxychloroquine	toll-like receptor antagonist	155	CLOUD018	0.30	1.5
Mitoxantrone	topoisomerase inhibitor	156	CLOUD063	0.67	3.4
Irinotecan	topoisomerase inhibitor	156	CLOUD117	3.4	16.8
Etoposide	topoisomerase inhibitor	156			
Teniposide	topoisomerase inhibitor	156			
Topotecan	topoisomerase inhibitor	156			
Docetaxel	tubulin depolymerization inhibitor	157	CLOUD139	4.5	22.7
Cabazitaxel	tubulin depolymerization inhibitor	157			
Ixabepilone	tubulin depolymerization inhibitor	157			
Paclitaxel	tubulin depolymerization inhibitor	157			
Vinblastine	tubulin polymerization inhibitor	158	CLOUD152	0.020	0.12
Colchicine	tubulin polymerization inhibitor	158			
Griseofulvin	tubulin polymerization inhibitor	158			
Vincristine	tubulin polymerization inhibitor	158			
Vinorelbine	tubulin polymerization inhibitor	158			
Metyrosine	tyrosine 3-monooxygenase inhibitor	159	CLOUD202	71.7	71.7
Tolvaptan	vasopressin receptor antagonist	160	CLOUD100	2.2	11.1
Conivaptan	vasopressin receptor antagonist	160			
Ganciclovir	viral DNA polymerase inhibitor	161	CLOUD233	19.6	97.9
Foscarnet	viral DNA polymerase inhibitor	161	CLOUD265	887.0	10.4
Aciclovir	viral DNA polymerase inhibitor	161			
Cidofovir	viral DNA polymerase inhibitor	161			
Didanosine	viral DNA polymerase inhibitor	161			
Entecavir	viral DNA polymerase inhibitor	161			
Famciclovir	viral DNA polymerase inhibitor	161			
Lamivudine	viral DNA polymerase inhibitor	161			
Telbivudine	viral DNA polymerase inhibitor	161			
Valaciclovir	viral DNA polymerase inhibitor	161			
Valganciclovir	viral DNA polymerase inhibitor	161			
Zidovudine	viral DNA polymerase inhibitor	161			
Ribavirin	viral RNA polymerase inhibitor	162	CLOUD178	15.1	16.0
Raltegravir	viral integrase inhibitor	163	CLOUD211	4.5	10.0
Amantadine	viral matrix protein 2 inhibitor	164	CLOUD260	4.0	19.8
Rimantadine	viral matrix protein 2 inhibitor	164			
Oseltamivir	viral neuraminidase inhibitor	165	CLOUD021	0.21	1.0
Amprenavir	viral protease inhibitor	166	CLOUD172	15.5	77.6
Atazanavir	viral protease inhibitor	166			
Darunavir	viral protease inhibitor	166			
Fosamprenavir	viral protease inhibitor	166			
Indinavir	viral protease inhibitor	166			
Lopinavir	viral protease inhibitor	166			
Nelfinavir	viral protease inhibitor	166			

Ritonavir	viral protease inhibitor	166			
Saquinavir	viral protease inhibitor	166			
Tipranavir	viral protease inhibitor	166			
Zalcitabine	viral reverse transcriptase inhibitor	167	CLOUD078	0.47	2.4
Abacavir	viral reverse transcriptase inhibitor	167	CLOUD146	13.5	55.7
Efavirenz	viral reverse transcriptase inhibitor	167	CLOUD221	28.8	28.8
Adefovir	viral reverse transcriptase inhibitor	167			
Delavirdine	viral reverse transcriptase inhibitor	167			
Emtricitabine	viral reverse transcriptase inhibitor	167			
Etravirine	viral reverse transcriptase inhibitor	167			
Nevirapine	viral reverse transcriptase inhibitor	167			
Stavudine	viral reverse transcriptase inhibitor	167			
Tenofovir	viral reverse transcriptase inhibitor	167			
Phenprocoumon	vitamin K epoxide reductase inhibitor	168	CLOUD167	12.8	64.2
Anisindione	vitamin K epoxide reductase inhibitor	168			
Dicumarol	vitamin K epoxide reductase inhibitor	168			
Phenindione	vitamin K epoxide reductase inhibitor	168			
Warfarin	vitamin K epoxide reductase inhibitor	168			
Nisoldipine	voltage-gated calcium channel blocker	169	CLOUD059	0.0026	0.013
Gabapentin	voltage-gated calcium channel blocker	169	CLOUD189	122.6	122.6
Trimethadione	voltage-gated calcium channel blocker	169	CLOUD288	5588.9	Not Tested
Amlodipine	voltage-gated calcium channel blocker	169			
Bepiridil	voltage-gated calcium channel blocker	169			
Clevidipine	voltage-gated calcium channel blocker	169			
Diltiazem	voltage-gated calcium channel blocker	169			
Ethosuximide	voltage-gated calcium channel blocker	169			
Felodipine	voltage-gated calcium channel blocker	169			
Flavoxate	voltage-gated calcium channel blocker	169			
Isradipine	voltage-gated calcium channel blocker	169			
Nicardipine	voltage-gated calcium channel blocker	169			
Nifedipine	voltage-gated calcium channel blocker	169			
Nimodipine	voltage-gated calcium channel blocker	169			
Paramethadione	voltage-gated calcium channel blocker	169			
Pregabalin	voltage-gated calcium channel blocker	169			
Verapamil	voltage-gated calcium channel blocker	169			
Lubiprostone	voltage-gated chloride channel activator	170	CLOUD123	0.00013	0.00064
Ibutilide	voltage-gated potassium channel blocker	171	CLOUD035	0.020	0.080

RESULTS

Bretylum Tosylate	voltage-gated potassium channel blocker	171	CLOUD140	9.9	84.1
Amiodarone	voltage-gated potassium channel blocker	171			
Dofetilide	voltage-gated potassium channel blocker	171			
Sotalol	voltage-gated potassium channel blocker	171			
Dronedarone	voltage-gated potassium channel blocker; voltage-gated sodium channel blocker; voltage-gated calcium channel blocker	172	CLOUD049	0.26	1.3
Lacosamide	voltage-gated sodium channel blocker	173	CLOUD145	49.9	217.8
Lamotrigine	voltage-gated sodium channel blocker	173	CLOUD155	54.7	273.3
Mephenytoin	voltage-gated sodium channel blocker	173	CLOUD181	68.7	343.8
Benzonate	voltage-gated sodium channel blocker	173			
Carbamazepine	voltage-gated sodium channel blocker	173			
Disopyramide	voltage-gated sodium channel blocker	173			
Ethotoin	voltage-gated sodium channel blocker	173			
Flecainide	voltage-gated sodium channel blocker	173			
Fosphenytoin	voltage-gated sodium channel blocker	173			
Indecainide	voltage-gated sodium channel blocker	173			
Mexiletine	voltage-gated sodium channel blocker	173			
Moricizine	voltage-gated sodium channel blocker	173			
Oxcarbazepine	voltage-gated sodium channel blocker	173			
Phenacemide	voltage-gated sodium channel blocker	173			
Phenytoin	voltage-gated sodium channel blocker	173			
Procainamide	voltage-gated sodium channel blocker	173			
Propafenone	voltage-gated sodium channel blocker	173			
Quinidine	voltage-gated sodium channel blocker	173			
Tocainide	voltage-gated sodium channel blocker	173			
Topiramate	voltage-gated sodium channel blocker; ionotropic glutamate receptor antagonist	174	CLOUD184	15.3	76.6
Zonisamide	voltage-gated sodium channel blocker; voltage-gated calcium channel blocker	175	CLOUD235	141.4	141.4
Allopurinol	xanthine dehydrogenase-oxidase inhibitor	176	CLOUD191	139.6	139.6
Febuxostat	xanthine dehydrogenase-oxidase inhibitor	176	CLOUD215	35.6	177.9
Chloroquine	Unknown		CLOUD003	0.94	4.7
Diphenidol	Unknown		CLOUD029	0.52	2.6
Pentamidine	Unknown		CLOUD047	1.5	7.4
Riluzole	Unknown		CLOUD052	0.85	4.3
Nicosamide	Unknown		CLOUD083	1.1	5.3
Diethylcarbamazine	Unknown		CLOUD094	1.3	6.3
Thalidomide	Unknown		CLOUD121	3.9	19.4

Mefloquine	Unknown		CLOUD129	2.6	13.2
Lumefantrine	Unknown		CLOUD130	17.0	82.3
Trimethobenzamide	Unknown		CLOUD131	5.2	25.7
Ranolazine	Unknown		CLOUD149	14.0	70.2
Lithium Citrate	Unknown		CLOUD150	1200.0	5783.4
Praziquantel	Unknown		CLOUD151	0.64	3.2
Metaxalone	Unknown		CLOUD153	7.7	40.7
Mesalazine	Unknown		CLOUD168	7.8	32.6
Mitotane	Unknown		CLOUD169	62.5	312.5
Thiabendazole	Unknown		CLOUD173	89.4	447.3
Chlorphenesin	Unknown		CLOUD183	83.9	444.2
4-Aminosalicylic Acid	Unknown		CLOUD194	130.6	130.6
Halofantrine	Unknown		CLOUD199	12.8	63.9
Chlorzoxazone	Unknown		CLOUD213	214.1	899.3
Rufinamide	Unknown		CLOUD217	202.1	50.5
Mebutamate	Unknown		CLOUD228	28.8	144.2
Quinine	Unknown		CLOUD232	21.6	107.9
Glatiramer Acetate	Unknown		CLOUD236	10.0	50.0
Tinidazole	Unknown		CLOUD238	192.9	192.9
Felbamate	Unknown		CLOUD239	205.7	205.7
Auranofin	Unknown		CLOUD255	1.5	7.3
Phensuximide	Unknown		CLOUD263	52.9	264.3
Pyrvinium Chloride Dihydrate	Unknown		CLOUD271	10.0	10.0
Benzquinamide	Unknown		CLOUD290	Unavailable	Not Tested
Piperacetazine	Unknown		CLOUD291	Unavailable	Not Tested
Ethchlorvynol	Unknown		Unavailable		
Ethinamate	Unknown		Unavailable		
Pemoline	Unknown		Unavailable		

Table S1. STEAM and CLOUD drugs

PRODRUG NAME	PRODRUG CLOUD ID	ACTIVE FORM NAME	ACTIVE FORM CLOUD ID	PLASMA [μ M]	SCREENING [μ M]
Cisapride	CLOUD067	Norcisapride	CLOUD014	0.080	0.30
Olmesartan Medoxomil	CLOUD093	Olmesartan	CLOUD028	2.0	10.1
Furazolidone	CLOUD135	3-Amino-2-Oxazolidinone	CLOUD034	9.8	49.0
Spirolactone	CLOUD072	Canrenone	CLOUD048	0.73	3.0
Tamoxifen	CLOUD064	Endoxifen	CLOUD101	1.4	6.8
Artemether	CLOUD111	Dihydroartemisinin	CLOUD103	2.6	10.4
Nitazoxanide	CLOUD174	Tizoxanide	CLOUD120	9.8	48.8
Minoxidil	CLOUD040	Minoxidil Sulfate	CLOUD127	0.86	4.3
Proguanil	CLOUD036	Cycloguanil	CLOUD128	0.59	3.4
Flutamide	CLOUD142	Hydroxyflutamide	CLOUD136	5.4	27.1
Ezetimibe	CLOUD066	Ezetimibe Glucuronide	CLOUD154	0.010	0.047
Ribavirin	CLOUD178	Ribavirin 5'-Triphosphate	CLOUD176	6.6	33.0
Leflunomide	CLOUD243	Teriflunomide	CLOUD203	66.6	66.9
Metronidazole	CLOUD170	Hydroxymetronidazole	CLOUD210	58.4	58.4
Clofibrate	CLOUD247	Clofibric Acid	CLOUD212	368.0	1840.1
Oseltamivir	CLOUD021	Oseltamivir Acid	CLOUD220	2.3	10.0
Irinotecan	CLOUD117	7-Ethyl-10-Hydroxy-Camptothecin	CLOUD237	5.0	25.1
Pyrazinamide	CLOUD245	Pyrazinoic Acid	CLOUD248	604.4	604.2
Buspirone	CLOUD262	6-Hydroxybuspirone	CLOUD257	0.010	0.050
Disulfiram	CLOUD062	Sodium Diethyldithiocarbamate Trihydrate	CLOUD259	2.7	13.2
Amodiaquine	CLOUD015	Desethylamodiaquine	CLOUD268	0.15	Not Tested
Zalcitabine	CLOUD078	Dideoxycytidine 5'-Triphosphate	CLOUD269	0.22	2.4
Clofarabine	CLOUD209	Clofarabine Triphosphate	CLOUD282	3.0	10.0
Isosorbide Dinitrate	CLOUD007	Nitrosoglutathione	CLOUD284	0.021	1.5
Cytarabine	CLOUD057	Cytosine Arabinoside Triphosphate	CLOUD294	10	Not Tested
Abacavir	CLOUD146	(-)-Carbovir Triphosphate	Unavailable		
Azacididine	CLOUD115	Azacididine Triphosphate	Unavailable		
Thiotepa	CLOUD277	Aziridine	Unavailable		
Clopidogrel	CLOUD019	Clopidogrel Acid	Unavailable		
Dextromethorphan	CLOUD287	Dextrorphan	Unavailable		
Acetohexamide	CLOUD240	Hydroxyhexamide	Unavailable		
Trazodone	CLOUD134	m-Chlorophenylpiperazine	Unavailable		
Altretamine	CLOUD182	N-(Hydroxymethyl)Melamine	Unavailable		
Oxamniquine	CLOUD289	Oxamniquine Sulfate Ester	Unavailable		
Romidepsin	CLOUD292	Romidepsin Reduced	Unavailable		

Table S2. Prodrugs and active forms

CLOUD IDs	DRUG NAMES	DEVIATION
CLOUD039, CLOUD136	Vecuronium Bromide, Hydroxyflutamide	1.00
CLOUD014, CLOUD176	Norcisapride, Ribavirin 5'-Triphosphate	1.00
CLOUD054, CLOUD195	Triamterene, Trilostane	0.99
CLOUD214, CLOUD224	Sulbactam, Probucof	0.98
CLOUD130, CLOUD162	Lumefantrine, Carglumic Acid	0.98
CLOUD214, CLOUD154	Sulbactam, Ezetimibe Glucuronide	0.96
CLOUD084, CLOUD123	Aripiprazole, Lubiprostone	0.96
CLOUD237, CLOUD217	7-Ethyl-10-Hydroxy-Camptothecin, Rufinamide	0.95
CLOUD051, CLOUD130	Testosterone, Lumefantrine	0.95
CLOUD035, CLOUD244	Ibutilide, Probenecid	0.94
CLOUD287, CLOUD035	Dextromethorphan, Ibutilide	0.92
CLOUD278, CLOUD023	Orlistat, Dopamine	0.92
CLOUD287, CLOUD153	Dextromethorphan, Metaxalone	0.91
CLOUD285, CLOUD227	Pentolinium Tartrate, Acetohydroxamic Acid	0.88
CLOUD287, CLOUD037	Dextromethorphan, Sertraline	0.86
CLOUD280, CLOUD082	Ivermectin, Isoproterenol	0.86
CLOUD167, CLOUD142	Phenprocoumon, Flutamide	0.85
CLOUD285, CLOUD229	Pentolinium Tartrate, (+/-)-Sulfinpyrazone	0.85
CLOUD286, CLOUD082	Nabilone, Isoproterenol	0.84
CLOUD272, CLOUD164	Acamprosate, Temozolomide	0.83
CLOUD175, CLOUD259	Propylthiouracil, Sodium Diethyldithiocarbamate Trihydrate	-0.66
CLOUD071, CLOUD165	Sunitinib, Mycophenolic Acid	-0.67
CLOUD054, CLOUD174	Triamterene, Nitazoxanide	-0.70
CLOUD114, CLOUD235	Imatinib, Zonisamide	-0.72
CLOUD006, CLOUD114	Maprotiline, Imatinib	-0.73
CLOUD165, CLOUD183	Mycophenolic Acid, Chlorphenesin	-0.74
CLOUD247, CLOUD062	Clofibrate, Disulfiram	-0.77
CLOUD041, CLOUD139	Busulfan, Docetaxel	-0.77
CLOUD114, CLOUD229	Imatinib, (+/-)-Sulfinpyrazone	-0.77
CLOUD114, CLOUD241	Imatinib, Dichlorphenamide	-0.78
CLOUD053, CLOUD252	Doxorubicin, Fosfomycin	-0.81
CLOUD013, CLOUD114	Asenapine, Imatinib	-0.83
CLOUD012, CLOUD114	Carbachol, Imatinib	-0.84
CLOUD114, CLOUD231	Imatinib, Novobiocin	-0.84
CLOUD133, CLOUD238	Epinephrine, Tinidazole	-0.90
CLOUD112, CLOUD066	Vorinostat, Ezetimibe	-0.92
CLOUD246, CLOUD165	Baclofen, Mycophenolic Acid	-0.92
CLOUD133, CLOUD235	Epinephrine, Zonisamide	-0.94
CLOUD211, CLOUD165	Raltegravir, Mycophenolic Acid	-0.95
CLOUD216, CLOUD259	Cefmenoxime, Sodium Diethyldithiocarbamate Trihydrate	-0.96

Table S3. Top 20 synergies and antagonisms

PRIMER	5'-SEQUENCE-3'
AR_flank_FW	GAAAGCGACTTCACCGCAC
AR_flank_RV	AAAACATGGTCCCTGGCAGT
AR_down_FW	TGTACACGTGGTCAAGTGGG
AR_down_RV	TGTGCATGCGGTACTCATTG
AR45_FW	ACTCTGGCTTCACAGTTTGGGA
AR45_RV	CGCACAGGTACTTCTGTTTCC
KLK3_FW	GGTGACCAAGTTCATGCTGTG
KLK3_RV	GTGTCCTTGATCCACTCCG
TMPRSS2_FW	CTGCCAAGGTGCTTCTCATT
TMPRSS2_RV	CTGTCACCCTGGCAAGAATC
KLK2_FW	CTGTCAGAGCCTGCCAAGAT
KLK2_RV	GCAAGAACTCCTCTGGTTCCG
ACT_FW	CTGTCTGGCGGCACCACCAT
ACT_RV	GCAACTAAGTCATAGTCCGC

Table S4. RT-qPCR primers used

DISCUSSION

According to recent projections the number of individuals with a history of cancer will rise up to nearly 18,000,000 only in the United States by 2022 while currently one in two men or two in three women will develop cancer during their lifetime (Siegel et al, 2012). Significant progress has been made in the understanding of cancer mechanisms and the development of treatments. However, current therapeutic regimens are not able to completely eradicate the disease in most of the cases. Moreover, genetic heterogeneity and the development of resistance have hampered the success of a limited arsenal of cancer drugs. Therefore, there is an urgent need for the development of more efficient and patient-tailored cancer therapeutics.

Cancer genome profiling and new insights into the rewired cancer circuitry have revealed an evolving and complex disease that cannot be addressed with the relatively straightforward approaches successfully employed for the treatment of other diseases (i.e. the “magic bullet” approach) (Ehrlich, 1913). Malignant neoplasms are intricate molecular machines that have developed a range of powerful mechanisms to sustain their uncontrolled proliferation. Importantly, the redundant functional network of cellular processes confers the plasticity they need in order to survive under different conditions and respond to various external perturbations. These sophisticated machines have, however, their Achilles’ heels and can be disrupted by means of specific pharmacological regimens. It has been said that it is relatively easy to kill malignant cells; after all they are cells and even though control over proliferation seems to have gone awry in these systems, there is plenty of molecules that would extinguish them with ease. The problem is that most of these molecules are very likely to damage also healthy tissues and would never translate into safe drugs. Cancer therapy must specifically target malignant cells (Kaelin, 2005). Drugs approved over the last 15 years have started embodying this concept addressing those addictions (oncogene- or non-oncogene-dependent) that are intrinsic to tumor cells. However, due to our limited knowledge about cancer heterogeneity and resistance mechanisms prior to the establishment of cost-effective next-generation sequencing technologies, most of these treatments did not meet the high expectations of both researchers and patients. There are many different driving mutations that can contribute to the tumorigenic process and

induce malignant transformation of cells belonging to the same tissue. We cannot address such a complex landscape with a handful of drugs: we need to expand the number of “druggable” targets and develop novel and more personalized treatments to deal with this plethora of genetic aberrations. Moreover, the evolving and redundant cancer network can easily circumvent the effect produced by single molecules and would be better addressed by multicomponent therapeutics. Here, we have applied longitudinal approaches to define novel targets and treatments with the intent to expand the therapeutic arsenal at our disposal against cancer. Our research has contributed to the draft of a precision cancer medicine global project (Collins & Varmus, 2015).

Targeting NOTCH1 breast cancer through inhibition of SUMOylation

Current breast cancer therapies have been developed based on simplistic classifications of different tumor specimens relying on the expression of few biomarkers or general gene expression profiles. Recent comprehensive stratifications of breast cancer samples have revealed a much broader collection of driver mutations involving, among others, chromatin-related genes. These updated molecular portraits complicate the genetic landscape of the disease but offer at the same time an invaluable resource for the development of more personalized treatments. Notably, many breast cancer-causing genes are tumor suppressors or oncogenes that are intrinsically difficult to target with small molecules. Chromatin-related proteins control different cellular processes, are “capacitors” for synthetic lethal interactions and include “druggable” enzymes. In an attempt to expand the number of cancer targets that could be pharmacologically modulated, we performed a loss-of-function screen on an *in vitro* breast cancer model. Due to their low genetic complexity, isogenic cell lines allow for more straightforward mechanistic interpretations of phenotypes and provide an ideal system for high-throughput gene-gene interaction studies. In this regard, we used a collection of isogenic cell lines capturing the genetic heterogeneity of breast cancer and derived from the precursor MCF10A, a cell line that resembles more the healthy tissue of the breast (Soule et al, 1990). This isogenic model has been previously described and successfully employed for the identification of an important resistance mechanism in the context of breast tumors (Muellner et al, 2011). In particular, we made use of MCF10A cells

overexpressing oncogenes that have been previously linked to neoplasms of the mammary gland. These genes included *AKT1*, *CCND1*, *FGFR1*, *HER2*, *IKBKE*, *MYC*, *MIR10B*, *NOTCH1*, *RHOC*, *TBL1XR1*, and *ZNF127* (Muellner et al, 2011). On this panel, we screened an epigenome-focused shRNA library opting for a multiplexed pooled approach that we established. By means of next-generation sequencing, we monitored the impact of chromatin-related protein knockdowns on the fitness of the cells retrieving hairpin abundance. With this approach, we analyzed in total more than 3000 gene-gene interactions. At first, we evaluated the performance of the screen and concluded that robust results can be obtained with two biological replicates per cell line ($R^2 > 0.7$ in correlation plots) and that the technology had been successfully implemented. Using already described hit scoring criteria (Luo et al, 2008; Moffat et al, 2006), we then obtained a list of chromatin-related genes significantly depleted (i.e. impairing cellular fitness) in our isogenic cell lines. Among the top hits we prioritized those genes that could be directly targeted with available inhibitors and proceeded with single hairpin validation experiments. Some hits could not be validated in such experiments, as hairpins could not impair the cellular growth when tested separately or did not show significant differences between oncogene-expressing isogenic cell lines and the wild type MCF10A control. The source of such screening false positive remains unclear but could be ascribed to poor knockdown efficiency or intrinsic limitations of the technology (e.g. a given knockdown phenotype might be affected by factors secreted by neighboring cells in the pool where a different knockdown has occurred). However, using different experimental approaches we were able to validate the specific interaction between activation of the NOTCH1 signaling pathway (Kopan & Ilagan, 2009) and knockdown of *UBE2I*, the gene coding for the UBC9 E2 conjugating enzyme of the SUMOylation cascade (Geiss-Friedlander & Melchior, 2007). Activation of the NOTCH1 signaling pathway through mutations, translocations or overexpression of the receptor as well as through decreased expression of the negative regulator NUMB has been described in a fraction of breast cancer samples (Al-Hussaini et al, 2010; CGAN, 2012; Mazzone et al, 2010). MCF10A cells overexpressing the intracellular domain of the potent NOTCH1 oncogene (NOTCH1 cells) proliferate faster, and compete away the wild type line in co-cultures. However, we showed that upon knockdown of *UBE2I*, NOTCH1 cells lose their growth advantage. Recurrence of the phenotype using different shRNA sequences targeting the *UBE2I* gene validated the finding of the screen and ruled out off-target effects frequently

observed with RNAi technologies. Importantly, upon overexpression of an shRNA-resistant UBC9 construct, we managed to rescue the growth impairment of NOTCH1 cells underlining the specificity of the interaction. These experiments associate the SUMOylation cascade to the NOTCH1 signaling pathway for the first time and imply a therapeutic potential for the enzymes in the SUMOylation cascades. Indeed, among our screening hits we were particularly interested in the interaction between NOTCH1 signaling and SUMOylation because small molecule inhibitors of this post-translational modification have already been described (Fukuda et al, 2009). Ginkgolic acid (GA) inhibits the SAE1/UBA2 E1 activating complex of the SUMOylation cascade and, similarly to knockdown of *UBE2I*, impaired the growth of NOTCH1 cells revealing a therapeutic window between the oncogene-expressing isogenic model and wild type MCF10A cells. We have used the SUMOylation inhibitor also in a γ -secretase-dependent NOTCH1 breast cancer model (Jarriault et al, 1995). Here, we could show a partial rescue of the phenotype upon treatment with a GSI, strengthening the link between NOTCH1 signaling activation and sensitivity to inhibition of the SUMOylation cascade. By means of gene expression profiling and cell cycle analysis we observed impairments in the S and G2/M phase of the cell cycle. Indeed, different proteins involved in the progression through these two distinct phases have been reported to be SUMOylated (Hay, 2005; Pfander et al, 2005). Given that we also observed prominent induction of apoptosis in NOTCH1 cells treated with GA, we concluded that inhibition of the SUMOylation cascade undermines the S and G2/M phase of the cell cycle eventually leading to cell death. Of note, a recent study observed sensitivity to inhibition of the SUMOylation cascade in MYC overexpressing breast cancer cells (Kessler et al, 2011). In this report, downregulation of a subset of MYC-regulated genes (SMS – SUMOylation-dependent MYC switchers) upon knockdown of SAE1 induced G2/M arrest and cell death. *MYC* is a canonical target regulated by NOTCH1 signaling. However, we did not observe complete G2/M arrest or downregulation of SMS genes in NOTCH1 cells treated with GA. Moreover, the MYC cells of our isogenic panel showed only weak depletion of *UBE2I* hairpins. As reported in the study, sensitivity to SUMOylation inhibition correlates to MYC dependence providing a potential explanation for such differences. SUMOylation affects the cellular localization, activity and interaction partners of many nuclear (but also cytosolic) proteins (Gill, 2004; Seeler & Dejean, 2003). Notably, it plays many important roles in the maintenance of cellular homeostasis. Nevertheless,

NOTCH1 cells showed an exquisite sensitivity to GA compared to their wild type counterpart. Western blotting and immunofluorescence experiments revealed a dramatic decrease in global SUMOylation specifically in the NOTCH1 cells treated with the SUMOylation inhibitor, while wild type MCF10A were virtually unaffected. These changes in global protein SUMOylation prompted us to check the amount of unconjugated SUMO protein in our panel of isogenic cell lines. Strikingly, NOTCH1 cells were the only cell line of the panel showing depleted levels of unconjugated SUMO1 and SUMO2/3 isoforms. The γ -secretase-dependent NOTCH1 breast cancer model further emphasized the link with NOTCH1 signaling activation as levels of unconjugated SUMO1 increased upon treatment with a GSI. From these experiments we hypothesized that activation of NOTCH1 signaling depletes unconjugated SUMO thereby conferring sensitivity to inhibition of the SUMOylation cascade. Notably, knockdown of SUMO1 or SUMO2/3 in wild type MCF10A cells increased sensitivity to inhibition of SUMOylation while SUMO3 overexpression rescued NOTCH1 cells from GA treatment corroborating our hypothesis. Isogenic models are genetically convenient systems that allow for an easier mechanistic dissection of molecular interactions. However, they do not perfectly mimic the genetic complexity or real tumors. For this reason, we evaluated the importance of our finding in a more clinically relevant context. We collected a series of patient-derived breast cancer cell lines recently reported to harbor genomic translocations involving *NOTCH1* and *NOTCH2* genes and activating the corresponding signaling (Robinson et al, 2011). These cell lines showed pronounced differences in the levels of unconjugated SUMO1 and SUMO2/3. Importantly, sensitivity to GA treatment correlated with levels of unconjugated SUMO validating our discovery in a genetic context closer to patients. Of note, activation of NOTCH1 signaling has been reported to be one of the major drivers of T-cell acute lymphoblastic leukemia (T-ALL) (Aifantis et al, 2008). We evaluated the effect of GA on a panel of T-ALL cell lines and measured levels of unconjugated SUMO. However, none of the cell lines showed depletion of SUMO or sensitivity to GA (data not shown). These observations endorse SUMO depletion upon activation of the NOTCH1 signaling pathway as a breast cancer specific event, also in light of the extremely context-dependent functions of the NOTCH1 pathway (Al-Hussaini et al, 2010). An interesting question that remains open to further investigations is whether other genetic alterations in different cancers result in similar depletions of unconjugated SUMO.

As to how exactly NOTCH1 activation depletes unconjugated SUMO, we cannot provide a definite answer. We attempted to investigate changes in protein SUMOylation by mass spectrometry; unfortunately, due to technical limitations, we could not perform these experiments. We can speculate that activation of the NOTCH1 signaling pathway induces the expression of SUMOylated proteins that would deplete the endogenous pools conferring sensitivity to further perturbations of the SUMOylation cascade (i.e. SAE1/UBA2 inhibition by GA or knockdown of *UBE2I*). Alterations in SUMO turnover could provide another potential explanation but the exact mechanism remains to be addressed by further research.

Here, we have provided evidence that NOTCH1 activation in breast cancer depletes unconjugated SUMO and confers sensitivity to inhibitors of the SUMOylation cascade. GA is a natural compound contained in *Ginkgo biloba* leaf extracts, which are used as health supplements in the United States and Japan. The molecule has not been thoroughly profiled *in vivo* but physiological concentrations associated with the consumption of *Ginkgo biloba* extracts are unlikely to inhibit the SUMOylation cascade. Our research encourages the development of improved SUMOylation inhibitors and their evaluation in multicomponent therapy.

A combination of approved drugs addressing resistance to flutamide in T877A AR prostate cancer

Tumor heterogeneity and resistance to therapy have long hampered efficiency of cancer treatments. In line with the latest successful anti-HIV drugs, multicomponent therapeutics has been suggested as a valid strategy for the treatment of complex diseases such as cancer. In particular, combinations of approved drugs entail numerous advantages as they are chemically optimized molecules already profiled in the clinic. Repurposing of a combination of clinical compounds would only require evaluation of drug-drug interactions *in vivo* as the single entities have been already profiled in terms of adsorption, diffusion, metabolism, excretion and toxicity by themselves. Combinations of approved drugs are not easy to investigate systematically essentially because comprehensive libraries of clinical compounds are difficult to obtain but also because a pairwise combinatorial screen of 1,000 drugs (i.e. way less than currently approved

small molecules) generates already 499,500 data points, overcoming the throughput of most screening platforms. We have defined and assembled a library of approved small molecules representative of the chemical and biological space covered by approved drugs. We named this non-redundant collection the CeMM Library of Unique Drugs (CLOUD). To generate the CLOUD we filtered all FDA-approved products retaining only systemically active small molecules. By means of clustering procedures only structurally unique compounds covering all biological activities addressed by FDA-approved drugs were kept. The addition of 35 approved molecules with unknown target as well as the active form of 35 prodrugs yielded a final collection of 309 CLOUD drugs. This library conveniently represents all FDA-approved small molecules and allows for combinatorial HTS. In order to investigate potential synergistic interactions between approved drugs, we performed a combinatorial screen on KBM7 cells, a near haploid CML cell line. We chose this system mainly because of a range of experimental possibilities provided by the ease to generate gene knockouts with a haploid cell line. Importantly, to maintain physiological relevance we screened all CLOUD drugs in the range of their maximal plasma concentration. In all, we tested 40,470 pairwise combinations of CLOUD drugs and collected 254 hits. A counter-screen narrowed the number of top hits down to 20 synergies and 20 antagonisms that we validated in extended dose-response combinatorial matrices. Not all hits validated: specific compounds showed different effects in different screens, others resulted in multiple synergistic or antagonistic combinations. We reasoned these compounds might be either unstable or partly precipitated in the screening plate affecting their distribution over the screen. Other technical issues might have interfered with the readout such as unequal dispensing of viability detection reagents. However, the synergistic interaction between flutamide (Eulexin®) and phenprocoumon (PPC, Marcumar®) detected in our original screen robustly validated in all subsequent counter-screens. We therefore decided to follow up this combination and manually tested new batches of the two compounds in a dose-response matrix performed with KBM7 cells. The combination showed a remarkable effect on cell viability and a strong synergistic interaction over a range of concentrations as assessed by the Bliss independence model. Flutamide is a non-steroidal antiandrogen targeting the AR and clinically used for the treatment of prostate cancer (Liao et al, 1974). It competes with the endogenous ligand of the AR for the binding pocket of the receptor and behaves as an antagonist, inhibiting the activation of the pathway. PPC

binds to VKORC1 inhibiting γ -carboxylation of glutamic acid residues by the GGCX enzyme (Paikin et al, 2010). The importance of γ -carboxylation in the context of the blood coagulation cascade has led to the approval of PPC as an anticoagulant for the treatment of thromboembolic disorders. Increased resistance to the combination of these two drugs observed in AR knockout KBM7 cells supported the AR as an important player in the observed phenotype. The AR signaling pathway sustains neoplasms of the prostatic tissue and is the target of different drugs approved for the treatment of prostate cancer (Farooqi & Sarkar, 2015). Even though patients initially respond to pharmacological treatments, they inevitably develop resistance to drugs targeting AR signaling. Therefore, we evaluated the therapeutic potential of the synergistic interaction between flutamide and PPC in prostate cancer cell lines. Interestingly, the combination greatly impaired the viability of the androgen-dependent LNCaP cells but spared PC-3 cells, another prostate cancer cell line that expresses very low levels of AR (Alimirah et al, 2006). These results further endorsed the AR as a key target and indicated therapeutic relevance of the combination for prostate cancer stages expressing sustained levels of the receptor. Of note, we could show that flutamide and PPC induce apoptosis in LNCaP cells and that similar growth impairments are observed using other approved VKORC1 inhibitors (e.g. warfarin, Coumadin®) (Paikin et al, 2010) and antiandrogens (e.g. bicalutamide, Casodex®) (Feldman & Feldman, 2001) validating the concept behind the CLOUD. The sensitivity of LNCaP cells to the combination of flutamide and PPC has interesting therapeutic implications. LNCaP cells overexpress a mutated form of the AR carrying a T877A substitution in the ligand binding domain of the receptor (Veldscholte et al, 1992). This mutation has been observed in patients and has been linked to resistance to antiandrogens treatment (Gaddipati et al, 1994). In particular, it has been shown that flutamide behaves as an AR agonist upon binding of the T877A mutant and activates AR signaling. Notably, flutamide agonistic activity in LNCaP cells is lost upon co-administration of PPC as we have observed expression of canonical AR signaling targets such as *KLK3* (also known as PSA) and *KLK2* reduced almost down to vehicle treatment. Interestingly, treatment of LNCaP cells with the combination also led to downregulation of the AR at the mRNA and protein levels. As PPC did not alter AR signaling induced by the potent agonist R1881, we inferred that flutamide would also still bind to the receptor in the presence of PPC. We analyzed AR downregulation in detail and observed that the two drugs in combination affect

transcription of the AR itself without significantly interfering with mRNA stability. However, they also induce proteasomal degradation of the receptor as bortezomib could partly restore the levels of AR upon treatment with flutamide and PPC. We also monitored changes in protein turnover and observed faster degradation of AR upon treatment with the combination. We reasoned that the AR might incur into destabilizing conformational changes upon treatment with both flutamide and PPC. In particular, we hypothesized that the AR could be γ -carboxylated and that PPC might interfere with this post-translational modification. To corroborate this hypothesis we performed a cellular thermal shift assay (CETSA) for the AR in LNCaP cells treated only with PPC for two days. Indeed, treatment with PPC increased AR thermal stability supporting a role for γ -carboxylation in the conformation of the receptor. Importantly, a 30 minutes treatment of LNCaP cell lysates with PPC could not induce the same increase in thermal stability arguing against direct binding of PPC to the AR. This experiment suggests that the AR is γ -carboxylated and that by preventing this post-translational modification PPC increases the thermal stability of the receptor. However, upon binding of flutamide the uncarboxylated AR would incur into further conformational changes jeopardizing its stability and leading to protein degradation. The loss of the receptor dictates eventually the death of AR-dependent LNCaP cells. To ultimately prove γ -carboxylation of the AR receptor we have designed mass spectrometry and 2D-gel electrophoresis experiments that are currently underway. Another important question that remains to be elucidated is the exact location of this modification on the AR as γ -carboxylation occurs on glutamic acid and the AR contains 55 of these residues. Up to date, only the structure of the ligand-binding domain of the AR has been solved. A full three-dimensional picture of the protein could further explain the importance of γ -carboxylation in the stability of the receptor and its interaction with flutamide.

In summary, we have uncovered a synergistic interaction between two approved drugs targeting the AR. Both compounds have already been clinically profiled and their combination could be easily translated into a new multicomponent regimen for the treatment of prostate cancer patients harboring AR mutations such as T877A. Interestingly, recent clinical studies have evaluated the preventive effect of pre-diagnosis use of anticoagulants on prostate cancer survival. However, contrasting results have been reported (O'Rorke et al, 2015; Sorensen, 2007; Tagalakis & Tamim, 2010; Tagalakis et al, 2013). Overall, our approach defines an efficient strategy for

repurposing of approved drugs and has expanded the number of possible therapeutic cancer treatments.

Conclusion & future prospects

We made use of molecularly stratified and combinatorial approaches to unravel novel targets and develop alternative cancer treatments. Our findings entail exciting translational potential for a new breast cancer target and therapy as well as a novel multicomponent regimen for the treatment of prostate tumors. Our approaches aimed at more patient-specific considerations and, in this regard, provided evidence for more personalized treatments (i.e. for NOTCH1 breast cancer or T877A AR prostate cancer patients). Additional efforts will have to address the remaining challenges posed by cancer heterogeneity and we regard recently established genome editing approaches such as the CRISPR-Cas9 (Cong et al, 2013; Mali et al, 2013) system or more sophisticated experimental set ups (e.g. three-compound combinatorial screens) as promising tools for the consolidation of precision cancer medicine.

REFERENCES

- Abbas-Terki T, Blanco-Bose W, Deglon N, Pralong W, Aebischer P (2002) Lentiviral-mediated RNA interference. *Hum Gene Ther* **13**: 2197-2201
- Adams JM, Cory S (2007) The Bcl-2 apoptotic switch in cancer development and therapy. *Oncogene* **26**: 1324-1337
- Aifantis I, Raetz E, Buonamici S (2008) Molecular pathogenesis of T-cell leukaemia and lymphoma. *Nature Reviews Immunology* **8**: 380-390
- Al-Hussaini H, Subramanyam D, Reedijk M, Sridhar SS (2010) Notch Signaling Pathway as a Therapeutic Target in Breast Cancer. *Mol Cancer Ther* **10**: 9-15
- Al-Lazikani B, Banerji U, Workman P (2012) Combinatorial drug therapy for cancer in the post-genomic era. *Nat Biotechnol* **30**: 679-692
- Albain KS, Barlow WE, Ravdin PM, Farrar WB, Burton GV, Ketchel SJ, Cobau CD, Levine EG, Ingle JN, Pritchard KI, Lichter AS, Schneider DJ, Abeloff MD, Henderson IC, Muss HB, Green SJ, Lew D, Livingston RB, Martino S, Osborne CK (2009) Adjuvant chemotherapy and timing of tamoxifen in postmenopausal patients with endocrine-responsive, node-positive breast cancer: a phase 3, open-label, randomised controlled trial. *Lancet* **374**: 2055-2063
- Alimirah F, Chen J, Basrawala Z, Xin H, Choubey D (2006) DU-145 and PC-3 human prostate cancer cell lines express androgen receptor: implications for the androgen receptor functions and regulation. *FEBS Lett* **580**: 2294-2300
- Allo M, Buggiano V, Fededa JP, Petrillo E, Schor I, de la Mata M, Agirre E, Plass M, Eyraas E, Elela SA, Klinck R, Chabot B, Kornblihtt AR (2009) Control of alternative splicing through siRNA-mediated transcriptional gene silencing. *Nat Struct Mol Biol* **16**: 717-724
- Armitage P, Doll R (1954) The age distribution of cancer and a multi-stage theory of carcinogenesis. *Br J Cancer* **8**: 1-12
- Ashburn TT, Thor KB (2004) Drug repositioning: identifying and developing new uses for existing drugs. *Nat Rev Drug Discov* **3**: 673-683
- Beck JT, Hortobagyi GN, Campone M, Lebrun F, Deleu I, Rugo HS, Pistilli B, Masuda N, Hart L, Melichar B, Dakhil S, Geberth M, Nunzi M, Heng DY, Brechenmacher T, El-Hashimy M, Douma S, Ringeisen F, Piccart M (2014) Everolimus plus exemestane as first-line therapy in HR(+), HER2(-) advanced breast cancer in BOLERO-2. *Breast Cancer Res Treat* **143**: 459-467
- Benvenuti S, Sartore-Bianchi A, Di Nicolantonio F, Zanon C, Moroni M, Veronese S, Siena S, Bardelli A (2007) Oncogenic activation of the RAS/RAF signaling pathway impairs the response of metastatic colorectal cancers to anti-epidermal growth factor receptor antibody therapies. *Cancer Res* **67**: 2643-2648

- Berenbaum MC (1989) What is synergy? *Pharmacol Rev* **41**: 93-141
- Bernards R, Brummelkamp TR, Beijersbergen RL (2006) shRNA libraries and their use in cancer genetics. *Nat Methods* **3**: 701-706
- Berns K, Horlings HM, Hennessy BT, Madiredjo M, Hijmans EM, Beelen K, Linn SC, Gonzalez-Angulo AM, Stemke-Hale K, Hauptmann M, Beijersbergen RL, Mills GB, van de Vijver MJ, Bernards R (2007) A Functional Genetic Approach Identifies the PI3K Pathway as a Major Determinant of Trastuzumab Resistance in Breast Cancer. *Cancer Cell* **12**: 395-402
- Bertos NR, Park M (2011) Breast cancer - one term, many entities? *J Clin Invest* **121**: 3789-3796
- Bliss CI (1939) The toxicity of poisons applied jointly. *Ann Appl Biol* **26**: 585-615
- Bock C, Lengauer T (2012) Managing drug resistance in cancer: lessons from HIV therapy. *Nat Rev Cancer* **12**: 494-501
- Borisy AA, Elliott PJ, Hurst NW, Lee MS, Lehar J, Price ER, Serbedzija G, Zimmermann GR, Foley MA, Stockwell BR, Keith CT (2003) Systematic discovery of multicomponent therapeutics. *Proc Natl Acad Sci U S A* **100**: 7977-7982
- Bridges CB (1922) The Origin of Variations in Sexual and Sex-Limited Characters. *The American Naturalist* **56**: 51-63
- Brockman RW (1963) Mechanisms of Resistance to Anticancer Agents. *Adv Cancer Res* **7**: 129-234
- Brummelkamp TR, Bernards R, Agami R (2002a) Stable suppression of tumorigenicity by virus-mediated RNA interference. *Cancer Cell* **2**: 243-247
- Brummelkamp TR, Bernards R, Agami R (2002b) A system for stable expression of short interfering RNAs in mammalian cells. *Science* **296**: 550-553
- Brummelkamp TR, Fabius AW, Mullenders J, Madiredjo M, Velds A, Kerkhoven RM, Bernards R, Beijersbergen RL (2006) An shRNA barcode screen provides insight into cancer cell vulnerability to MDM2 inhibitors. *Nat Chem Biol* **2**: 202-206
- Bryant HE, Schultz N, Thomas HD, Parker KM, Flower D, Lopez E, Kyle S, Meuth M, Curtin NJ, Helleday T (2005) Specific killing of BRCA2-deficient tumours with inhibitors of poly(ADP-ribose) polymerase. *Nature* **434**: 913-917
- Byrne AB, Weirauch MT, Wong V, Koeva M, Dixon SJ, Stuart JM, Roy PJ (2007) A global analysis of genetic interactions in *Caenorhabditis elegans*. *J Biol* **6**: 26

- Campbell PJ, Pleasance ED, Stephens PJ, Dicks E, Rance R, Goodhead I, Follows GA, Green AR, Futreal PA, Stratton MR (2008) Subclonal phylogenetic structures in cancer revealed by ultra-deep sequencing. *Proc Natl Acad Sci U S A* **105**: 13081-13086
- Carpinelli P, Moll J (2008) Aurora kinases and their inhibitors: more than one target and one drug. *Adv Exp Med Biol* **610**: 54-73
- CGAN (2012) Comprehensive molecular portraits of human breast tumours. *Nature* **490**: 61-70
- Chabner BA, Roberts TG, Jr. (2005) Timeline: Chemotherapy and the war on cancer. *Nat Rev Cancer* **5**: 65-72
- Chin L, Tam A, Pomerantz J, Wong M, Holash J, Bardeesy N, Shen Q, O'Hagan R, Pantginis J, Zhou H, Horner JW, 2nd, Cordon-Cardo C, Yancopoulos GD, DePinho RA (1999) Essential role for oncogenic Ras in tumour maintenance. *Nature* **400**: 468-472
- Choi YL, Soda M, Yamashita Y, Ueno T, Takashima J, Nakajima T, Yatabe Y, Takeuchi K, Hamada T, Haruta H, Ishikawa Y, Kimura H, Mitsudomi T, Tanio Y, Mano H (2010) EML4-ALK mutations in lung cancer that confer resistance to ALK inhibitors. *N Engl J Med* **363**: 1734-1739
- Chou TC, Talalay P (1984) Quantitative analysis of dose-effect relationships: the combined effects of multiple drugs or enzyme inhibitors. *Adv Enzyme Regul* **22**: 27-55
- Collins FS, Varmus H (2015) A new initiative on precision medicine. *N Engl J Med* **372**: 793-795
- Cong L, Ran FA, Cox D, Lin S, Barretto R, Habib N, Hsu PD, Wu X, Jiang W, Marraffini LA, Zhang F (2013) Multiplex genome engineering using CRISPR/Cas systems. *Science* **339**: 819-823
- Costanzo M, Baryshnikova A, Bellay J, Kim Y, Spear ED, Sevier CS, Ding H, Koh JL, Toufighi K, Mostafavi S, Prinz J, St Onge RP, VanderSluis B, Makhnevych T, Vizeacoumar FJ, Alizadeh S, Bahr S, Brost RL, Chen Y, Cokol M, Deshpande R, Li Z, Lin ZY, Liang W, Marback M, Paw J, San Luis BJ, Shuteriqi E, Tong AH, van Dyk N, Wallace IM, Whitney JA, Weirauch MT, Zhong G, Zhu H, Houry WA, Brudno M, Ragibizadeh S, Papp B, Pal C, Roth FP, Giaever G, Nislow C, Troyanskaya OG, Bussey H, Bader GD, Gingras AC, Morris QD, Kim PM, Kaiser CA, Myers CL, Andrews BJ, Boone C (2010) The genetic landscape of a cell. *Science* **327**: 425-431
- Croom KF, Perry CM (2003) Imatinib mesylate: in the treatment of gastrointestinal stromal tumours. *Drugs* **63**: 513-522
- Cunningham D, Humblet Y, Siena S, Khayat D, Bleiberg H, Santoro A, Bets D, Mueser M, Harstrick A, Verslype C, Chau I, Van Cutsem E (2004) Cetuximab monotherapy and cetuximab plus irinotecan in irinotecan-refractory metastatic colorectal cancer. *N Engl J Med* **351**: 337-345

Curtis C, Shah SP, Chin SF, Turashvili G, Rueda OM, Dunning MJ, Speed D, Lynch AG, Samarajiwa S, Yuan Y, Graf S, Ha G, Haffari G, Bashashati A, Russell R, McKinney S, Langerod A, Green A, Provenzano E, Wishart G, Pinder S, Watson P, Markowitz F, Murphy L, Ellis I, Purushotham A, Borresen-Dale AL, Brenton JD, Tavare S, Caldas C, Aparicio S (2012) The genomic and transcriptomic architecture of 2,000 breast tumours reveals novel subgroups. *Nature* **486**: 346-352

Davies MA, Samuels Y (2010) Analysis of the genome to personalize therapy for melanoma. *Oncogene* **29**: 5545-5555

de Azambuja E, Holmes AP, Piccart-Gebhart M, Holmes E, Di Cosimo S, Swaby RF, Untch M, Jackisch C, Lang I, Smith I, Boyle F, Xu B, Barrios CH, Perez EA, Azim HA, Jr., Kim SB, Kuemmel S, Huang CS, Vuylsteke P, Hsieh RK, Gorbunova V, Eniu A, Dreosti L, Tavartkiladze N, Gelber RD, Eidtmann H, Baselga J (2014) Lapatinib with trastuzumab for HER2-positive early breast cancer (NeoALTTO): survival outcomes of a randomised, open-label, multicentre, phase 3 trial and their association with pathological complete response. *Lancet Oncol* **15**: 1137-1146

De Roock W, De Vriendt V, Normanno N, Ciardiello F, Tejpar S (2011) KRAS, BRAF, PIK3CA, and PTEN mutations: implications for targeted therapies in metastatic colorectal cancer. *Lancet Oncol* **12**: 594-603

Dean M, Annilo T (2005) Evolution of the ATP-binding cassette (ABC) transporter superfamily in vertebrates. *Annu Rev Genomics Hum Genet* **6**: 123-142

Debiec-Rychter M, Sciot R, Le Cesne A, Schlemmer M, Hohenberger P, van Oosterom AT, Blay JY, Leyvraz S, Stul M, Casali PG, Zalcberg J, Verweij J, Van Glabbeke M, Hagemeyer A, Judson I (2006) KIT mutations and dose selection for imatinib in patients with advanced gastrointestinal stromal tumours. *Eur J Cancer* **42**: 1093-1103

Delaney G, Jacob S, Featherstone C, Barton M (2005) The role of radiotherapy in cancer treatment: estimating optimal utilization from a review of evidence-based clinical guidelines. *Cancer* **104**: 1129-1137

Di Nicolantonio F, Martini M, Molinari F, Sartore-Bianchi A, Arena S, Saletti P, De Dosso S, Mazzucchelli L, Frattini M, Siena S, Bardelli A (2008) Wild-type BRAF is required for response to panitumumab or cetuximab in metastatic colorectal cancer. *J Clin Oncol* **26**: 5705-5712

Dobzhansky T (1946) Genetics of Natural Populations. Xiii. Recombination and Variability in Populations of *Drosophila Pseudoobscura*. *Genetics* **31**: 269-290

Dow LE, Prensirrut PK, Zuber J, Fellmann C, McJunkin K, Miething C, Park Y, Dickins RA, Hannon GJ, Lowe SW (2012) A pipeline for the generation of shRNA transgenic mice. *Nat Protoc* **7**: 374-393

Druker BJ, Tamura S, Buchdunger E, Ohno S, Segal GM, Fanning S, Zimmermann J, Lydon NB (1996) Effects of a selective inhibitor of the Abl tyrosine kinase on the growth of Bcr-Abl positive cells. *Nat Med* **2**: 561-566

- Echeverri CJ, Beachy PA, Baum B, Boutros M, Buchholz F, Chanda SK, Downward J, Ellenberg J, Fraser AG, Hacohen N, Hahn WC, Jackson AL, Kiger A, Linsley PS, Lum L, Ma Y, Mathey-Prevot B, Root DE, Sabatini DM, Taipale J, Perrimon N, Bernards R (2006) Minimizing the risk of reporting false positives in large-scale RNAi screens. *Nat Methods* **3**: 777-779
- Ehrlich P (1913) Chemotherapeutics: scientific principles, methods, and results. *Lancet* **2**: 445-451
- Elbashir SM, Harborth J, Lendeckel W, Yalcin A, Weber K, Tuschl T (2001) Duplexes of 21-nucleotide RNAs mediate RNA interference in cultured mammalian cells. *Nature* **411**: 494-498
- Farmer H, McCabe N, Lord CJ, Tutt AN, Johnson DA, Richardson TB, Santarosa M, Dillon KJ, Hickson I, Knights C, Martin NM, Jackson SP, Smith GC, Ashworth A (2005a) Targeting the DNA repair defect in BRCA mutant cells as a therapeutic strategy. *Nature* **434**: 917-921
- Farmer P, Bonnefoi H, Becette V, Tubiana-Hulin M, Fumoleau P, Larsimont D, Macgrogan G, Bergh J, Cameron D, Goldstein D, Duss S, Nicoulaz AL, Brisken C, Fiche M, Delorenzi M, Iggo R (2005b) Identification of molecular apocrine breast tumours by microarray analysis. *Oncogene* **24**: 4660-4671
- Farooqi AA, Sarkar FH (2015) Overview on the complexity of androgen receptor-targeted therapy for prostate cancer. *Cancer Cell Int* **15**: 014-0153
- Fearon ER (1997) Human cancer syndromes: clues to the origin and nature of cancer. *Science* **278**: 1043-1050
- Feldman BJ, Feldman D (2001) The development of androgen-independent prostate cancer. *Nat Rev Cancer* **1**: 34-45
- Felsher DW, Bishop JM (1999) Reversible tumorigenesis by MYC in hematopoietic lineages. *Mol Cell* **4**: 199-207
- Ferrara N, Hillan KJ, Gerber HP, Novotny W (2004) Discovery and development of bevacizumab, an anti-VEGF antibody for treating cancer. *Nat Rev Drug Discov* **3**: 391-400
- Fidler IJ (2011) The biology of cancer metastasis. *Semin Cancer Biol* **21**: 9
- Fire A, Xu S, Montgomery MK, Kostas SA, Driver SE, Mello CC (1998) Potent and specific genetic interference by double-stranded RNA in *Caenorhabditis elegans*. *Nature* **391**: 806-811
- Flaherty KT, Puzanov I, Kim KB, Ribas A, McArthur GA, Sosman JA, O'Dwyer PJ, Lee RJ, Grippo JF, Nolop K, Chapman PB (2010) Inhibition of Mutated, Activated BRAF in Metastatic Melanoma. *N Engl J Med* **363**: 809-819

Flynn RL, Cox KE, Jeitany M, Wakimoto H, Bryll AR, Ganem NJ, Bersani F, Pineda JR, Suva ML, Benes CH, Haber DA, Boussin FD, Zou L (2015) Alternative lengthening of telomeres renders cancer cells hypersensitive to ATR inhibitors. *Science* **347**: 273-277

Fong PC, Boss DS, Yap TA, Tutt A, Wu P, Mergui-Roelvink M, Mortimer P, Swaisland H, Lau A, O'Connor MJ, Ashworth A, Carmichael J, Kaye SB, Schellens JH, de Bono JS (2009) Inhibition of poly(ADP-ribose) polymerase in tumors from BRCA mutation carriers. *N Engl J Med* **361**: 123-134

Freedman A (2014) Follicular lymphoma: 2014 update on diagnosis and management. *Am J Hematol* **89**: 429-436

Fukuda I, Ito A, Hirai G, Nishimura S, Kawasaki H, Saitoh H, Kimura K-i, Sodeoka M, Yoshida M (2009) Ginkgolic Acid Inhibits Protein SUMOylation by Blocking Formation of the E1-SUMO Intermediate. *Chem Biol* **16**: 133-140

Futreal PA, Coin L, Marshall M, Down T, Hubbard T, Wooster R, Rahman N, Stratton MR (2004) A census of human cancer genes. *Nat Rev Cancer* **4**: 177-183

Gaddipati JP, McLeod DG, Heidenberg HB, Sesterhenn IA, Finger MJ, Moul JW, Srivastava S (1994) Frequent detection of codon 877 mutation in the androgen receptor gene in advanced prostate cancers. *Cancer Res* **54**: 2861-2864

Garraway LA, Janne PA (2012) Circumventing cancer drug resistance in the era of personalized medicine. *Cancer Discov* **2**: 214-226

Gazdar AF (2009) Activating and resistance mutations of EGFR in non-small-cell lung cancer: role in clinical response to EGFR tyrosine kinase inhibitors. *Oncogene* **28**: 198

Geiss-Friedlander R, Melchior F (2007) Concepts in sumoylation: a decade on. *Nature Reviews Molecular Cell Biology* **8**: 947-956

Gerlinger M, Rowan AJ, Horswell S, Larkin J, Endesfelder D, Gronroos E, Martinez P, Matthews N, Stewart A, Tarpey P, Varela I, Phillimore B, Begum S, McDonald NQ, Butler A, Jones D, Raine K, Latimer C, Santos CR, Nohadani M, Eklund AC, Spencer-Dene B, Clark G, Pickering L, Stamp G, Gore M, Szallasi Z, Downward J, Futreal PA, Swanton C (2012) Intratumor heterogeneity and branched evolution revealed by multiregion sequencing. *N Engl J Med* **366**: 883-892

Gill G (2004) SUMO and ubiquitin in the nucleus: different functions, similar mechanisms? *Genes Dev* **18**: 2046-2059

Girotti MR, Lopes F, Preece N, Niculescu-Duvaz D, Zambon A, Davies L, Whittaker S, Saturno G, Viros A, Pedersen M, Suijkerbuijk BM, Menard D, McLeary R, Johnson L, Fish L, Ejima S, Sanchez-Laorden B, Hohloch J, Carragher N, Macleod K, Ashton G, Marusiak AA, Fusi A, Brognard J, Frame M, Lorigan P, Marais R, Springer C (2015) Paradox-breaking RAF inhibitors that also target SRC are effective in drug-resistant BRAF mutant melanoma. *Cancer Cell* **27**: 85-96

- Goga A, Yang D, Tward AD, Morgan DO, Bishop JM (2007) Inhibition of CDK1 as a potential therapy for tumors over-expressing MYC. *Nat Med* **13**: 820-827
- Gonzalez de Castro D, Clarke PA, Al-Lazikani B, Workman P (2013) Personalized cancer medicine: molecular diagnostics, predictive biomarkers, and drug resistance. *Clin Pharmacol Ther* **93**: 252-259
- Gorre ME, Mohammed M, Ellwood K, Hsu N, Paquette R, Rao PN, Sawyers CL (2001) Clinical resistance to STI-571 cancer therapy caused by BCR-ABL gene mutation or amplification. *Science* **293**: 876-880
- Gottesman MM (2002) Mechanisms of cancer drug resistance. *Annu Rev Med* **53**: 615-627
- Greaves M, Maley CC (2012) Clonal evolution in cancer. *Nature* **481**: 306-313
- Gu S, Jin L, Zhang Y, Huang Y, Zhang F, Valdmanis PN, Kay MA (2012) The loop position of shRNAs and pre-miRNAs is critical for the accuracy of dicer processing in vivo. *Cell* **151**: 900-911
- Hanahan D, Folkman J (1996) Patterns and emerging mechanisms of the angiogenic switch during tumorigenesis. *Cell* **86**: 353-364
- Hanahan D, Weinberg RA (2000) The hallmarks of cancer. *Cell* **100**: 57-70
- Hanahan D, Weinberg RA (2011) Hallmarks of cancer: the next generation. *Cell* **144**: 646-674
- Hannon GJ (2002) RNA interference. *Nature* **418**: 244-251
- Hantschel O (2012) Allosteric BCR-ABL inhibitors in Philadelphia chromosome-positive acute lymphoblastic leukemia: novel opportunities for drug combinations to overcome resistance. *Haematologica* **97**: 157-159
- Hantschel O, Grebien F, Superti-Furga G (2011) Targeting allosteric regulatory modules in oncoproteins: "drugging the undruggable". *Oncotarget* **2**: 828-829
- Hartman JLt, Garvik B, Hartwell L (2001) Principles for the buffering of genetic variation. *Science* **291**: 1001-1004
- Hartwell LH, Szankasi P, Roberts CJ, Murray AW, Friend SH (1997) Integrating genetic approaches into the discovery of anticancer drugs. *Science* **278**: 1064-1068
- Hay RT (2005) Sumo: a History of Modification. *Mol Cell* **18**: 1-12
- Hediger MA, Romero MF, Peng JB, Rolfs A, Takanaga H, Bruford EA (2004) The ABCs of solute carriers: physiological, pathological and therapeutic implications of human membrane transport proteinsIntroduction. *Pflugers Arch* **447**: 465-468

Heinrich MC, Corless CL, Demetri GD, Blanke CD, von Mehren M, Joensuu H, McGreevey LS, Chen CJ, Van den Abbeele AD, Druker BJ, Kiese B, Eisenberg B, Roberts PJ, Singer S, Fletcher CD, Silberman S, Dimitrijevic S, Fletcher JA (2003) Kinase mutations and imatinib response in patients with metastatic gastrointestinal stromal tumor. *J Clin Oncol* **21**: 4342-4349

Hennessy BT, Gonzalez-Angulo AM, Stemke-Hale K, Gilcrease MZ, Krishnamurthy S, Lee JS, Fridlyand J, Sahin A, Agarwal R, Joy C, Liu W, Stivers D, Baggerly K, Carey M, Lluch A, Monteagudo C, He X, Weigman V, Fan C, Palazzo J, Hortobagyi GN, Nolden LK, Wang NJ, Valero V, Gray JW, Perou CM, Mills GB (2009) Characterization of a naturally occurring breast cancer subset enriched in epithelial-to-mesenchymal transition and stem cell characteristics. *Cancer Res* **69**: 4116-4124

Hornsby C, Page KM, Tomlinson IP (2007) What can we learn from the population incidence of cancer? Armitage and Doll revisited. *Lancet Oncol* **8**: 1030-1038

Huettnner CS, Zhang P, Van Etten RA, Tenen DG (2000) Reversibility of acute B-cell leukaemia induced by BCR-ABL1. *Nat Genet* **24**: 57-60

Hutvagner G (2005) Small RNA asymmetry in RNAi: function in RISC assembly and gene regulation. *FEBS Lett* **579**: 5850-5857

Jarriault S, Brou C, Logeat F, Schroeter EH, Kopan R, Israel A (1995) Signalling downstream of activated mammalian Notch. *Nature* **377**: 355-358

Jeffries CD, Fried HM, Perkins DO (2011) Nuclear and cytoplasmic localization of neural stem cell microRNAs. *RNA* **17**: 675-686

Johnson David G, Dent Sharon YR (2013) Chromatin: Receiver and Quarterback for Cellular Signals. *Cell* **152**: 685-689

Jordan VC, Brodie AM (2007) Development and evolution of therapies targeted to the estrogen receptor for the treatment and prevention of breast cancer. *Steroids* **72**: 7-25

Kaelin WG (2005) The Concept of Synthetic Lethality in the Context of Anticancer Therapy. *Nature Reviews Cancer* **5**: 689-698

Kaelin WG, Jr. (2009) Synthetic lethality: a framework for the development of wiser cancer therapeutics. *Genome Med* **1**: 99.91-99.96

Kantarjian H, Pasquini R, Levy V, Jootar S, Holowiecki J, Hamerschlak N, Hughes T, Bleickardt E, Dejardin D, Cortes J, Shah NP (2009) Dasatinib or high-dose imatinib for chronic-phase chronic myeloid leukemia resistant to imatinib at a dose of 400 to 600 milligrams daily: two-year follow-up of a randomized phase 2 study (START-R). *Cancer* **115**: 4136-4147

Kartner N, Riordan JR, Ling V (1983) Cell surface P-glycoprotein associated with multidrug resistance in mammalian cell lines. *Science* **221**: 1285-1288

- Keith CT, Borisy AA, Stockwell BR (2005) Multicomponent therapeutics for networked systems. *Nat Rev Drug Discov* **4**: 71-78
- Kessler JD, Kahle KT, Sun T, Meerbrey KL, Schlabach MR, Schmitt EM, Skinner SO, Xu Q, Li MZ, Hartman ZC, Rao M, Yu P, Dominguez-Vidana R, Liang AC, Solimini NL, Bernardi RJ, Yu B, Hsu T, Golding I, Luo J, Osborne CK, Creighton CJ, Hilsenbeck SG, Schiff R, Shaw CA, Elledge SJ, Westbrook TF (2011) A SUMOylation-Dependent Transcriptional Subprogram Is Required for Myc-Driven Tumorigenesis. *Science* **335**: 348-353
- Kim DH, Saetrom P, Snove O, Jr., Rossi JJ (2008) MicroRNA-directed transcriptional gene silencing in mammalian cells. *Proc Natl Acad Sci U S A* **105**: 16230-16235
- Kopan R, Ilagan MXG (2009) The Canonical Notch Signaling Pathway: Unfolding the Activation Mechanism. *Cell* **137**: 216-233
- Kwak EL, Bang YJ, Camidge DR, Shaw AT, Solomon B, Maki RG, Ou SH, Dezube BJ, Janne PA, Costa DB, Varella-Garcia M, Kim WH, Lynch TJ, Fidias P, Stubbs H, Engelman JA, Sequist LV, Tan W, Gandhi L, Mino-Kenudson M, Wei GC, Shreeve SM, Ratain MJ, Settleman J, Christensen JG, Haber DA, Wilner K, Salgia R, Shapiro GI, Clark JW, Iafrate AJ (2010) Anaplastic lymphoma kinase inhibition in non-small-cell lung cancer. *N Engl J Med* **363**: 1693-1703
- Lamontanara AJ, Gencer EB, Kuzyk O, Hantschel O (2013) Mechanisms of resistance to BCR-ABL and other kinase inhibitors. *Biochim Biophys Acta* **7**: 28
- Lee MJ, Ye AS, Gardino AK, Heijink AM, Sorger PK, MacBeath G, Yaffe MB (2012) Sequential application of anticancer drugs enhances cell death by rewiring apoptotic signaling networks. *Cell* **149**: 780-794
- Lehar J (2007) Chemical combination effects predict connectivity in biological systems. *Mol Syst Biol* **3**: 80
- Lehar J, Stockwell BR, Giaever G, Nislow C (2008) Combination chemical genetics. *Nat Chem Biol* **4**: 674-681
- Lehner B, Crombie C, Tischler J, Fortunato A, Fraser AG (2006) Systematic mapping of genetic interactions in *Caenorhabditis elegans* identifies common modifiers of diverse signaling pathways. *Nature Genet* **38**: 896-903
- Leucci E, Patella F, Waage J, Holmstrom K, Lindow M, Porse B, Kauppinen S, Lund AH (2013) microRNA-9 targets the long non-coding RNA MALAT1 for degradation in the nucleus. *Sci Rep* **3**: 1-6
- Li CI, Uribe DJ, Daling JR (2005) Clinical characteristics of different histologic types of breast cancer. *Br J Cancer* **93**: 1046-1052
- Liao S, Howell DK, Chang TM (1974) Action of a nonsteroidal antiandrogen, flutamide, on the receptor binding and nuclear retention of 5 alpha-dihydrotestosterone in rat ventral prostate. *Endocrinology* **94**: 1205-1209

- Lichtenstein P, Holm NV, Verkasalo PK, Iliadou A, Kaprio J, Koskenvuo M, Pukkala E, Skytthe A, Hemminki K (2000) Environmental and heritable factors in the causation of cancer--analyses of cohorts of twins from Sweden, Denmark, and Finland. *N Engl J Med* **343**: 78-85
- Little AS, Balmanno K, Sale MJ, Newman S, Dry JR, Hampson M, Edwards PA, Smith PD, Cook SJ (2011) Amplification of the driving oncogene, KRAS or BRAF, underpins acquired resistance to MEK1/2 inhibitors in colorectal cancer cells. *Sci Signal* **4**: 2001752
- Loewe S (1928) Die quantitation probleme der pharmakologie. *Ergeb Physiol* **27**: 47-187
- Loewe S (1953) The problem of synergism and antagonism of combined drugs. *Arzneimittelforschung* **3**: 285-290
- Luo B, Cheung HW, Subramanian A, Sharifnia T, Okamoto M, Yang X, Hinkle G, Boehm JS, Beroukhi R, Weir BA, Mermel C, Barbie DA, Awad T, Zhou X, Nguyen T, Piquani B, Li C, Golub TR, Meyerson M, Hacohen N, Hahn WC, Lander ES, Sabatini DM, Root DE (2008) Highly parallel identification of essential genes in cancer cells. *Proc Natl Acad Sci U S A* **105**: 20380-20385
- Luo J, Solimini NL, Elledge SJ (2009) Principles of Cancer Therapy: Oncogene and Non-oncogene Addiction. *Cell* **136**: 823-837
- Mahon FX, Hayette S, Lagarde V, Belloc F, Turcq B, Nicolini F, Belanger C, Manley PW, Leroy C, Etienne G, Roche S, Pasquet JM (2008) Evidence that resistance to nilotinib may be due to BCR-ABL, Pgp, or Src kinase overexpression. *Cancer Res* **68**: 9809-9816
- Mair B, Kubicek S, Nijman SM (2014) Exploiting epigenetic vulnerabilities for cancer therapeutics. *Trends Pharmacol Sci* **35**: 136-145
- Mali P, Yang L, Esvelt KM, Aach J, Guell M, DiCarlo JE, Norville JE, Church GM (2013) RNA-guided human genome engineering via Cas9. *Science* **339**: 823-826
- Marshall E (2014) Breast cancer. Dare to do less. *Science* **343**: 1454-1456
- Martini M, Vecchione L, Siena S, Tejpar S, Bardelli A (2011) Targeted therapies: how personal should we go? *Nat Rev Clin Oncol* **9**: 87-97
- Masel J, Siegal ML (2009) Robustness: mechanisms and consequences. *Trends Genet* **25**: 395-403
- Matthews LR, Vaglio P, Reboul J, Ge H, Davis BP, Garrels J, Vincent S, Vidal M (2001) Identification of potential interaction networks using sequence-based searches for conserved protein-protein interactions or "interologs". *Genome Res* **11**: 2120-2126
- Maxmen A (2012) The hard facts. *Nature* **485**: S50-51

- Mazzone M, Selfors LM, Albeck J, Overholtzer M, Sale S, Carroll DL, Pandya D, Lu Y, Mills GB, Aster JC, Artavanis-Tsakonas S, Brugge JS (2010) Dose-dependent induction of distinct phenotypic responses to Notch pathway activation in mammary epithelial cells. *Proceedings of the National Academy of Sciences* **107**: 5012-5017
- Moffat J, Grueneberg DA, Yang X, Kim SY, Kloepfer AM, Hinkle G, Piqani B, Eisenhaure TM, Luo B, Grenier JK, Carpenter AE, Foo SY, Stewart SA, Stockwell BR, Hacohen N, Hahn WC, Lander ES, Sabatini DM, Root DE (2006) A Lentiviral RNAi Library for Human and Mouse Genes Applied to an Arrayed Viral High-Content Screen. *Cell* **124**: 1283-1298
- Molenaar JJ, Ebus ME, Geerts D, Koster J, Lamers F, Valentijn LJ, Westerhout EM, Versteeg R, Caron HN (2009) Inactivation of CDK2 is synthetically lethal to MYCN over-expressing cancer cells. *Proc Natl Acad Sci U S A* **106**: 12968-12973
- Muellner MK, Uras IZ, Gapp BV, Kerzendorfer C, Smida M, Lechtermann H, Craig-Mueller N, Colinge J, Duernberger G, Nijman SMB (2011) A chemical-genetic screen reveals a mechanism of resistance to PI3K inhibitors in cancer. *Nat Chem Biol* **7**: 787-793
- Mullighan CG, Phillips LA, Su X, Ma J, Miller CB, Shurtleff SA, Downing JR (2008) Genomic analysis of the clonal origins of relapsed acute lymphoblastic leukemia. *Science* **322**: 1377-1380
- Nahta R, Hung MC, Esteva FJ (2004) The HER-2-targeting antibodies trastuzumab and pertuzumab synergistically inhibit the survival of breast cancer cells. *Cancer Res* **64**: 2343-2346
- Napoli C, Lemieux C, Jorgensen R (1990) Introduction of a Chimeric Chalcone Synthase Gene into Petunia Results in Reversible Co-Suppression of Homologous Genes in trans. *Plant Cell* **2**: 279-289
- Nastoupil LJ, Rose AC, Flowers CR (2012) Diffuse large B-cell lymphoma: current treatment approaches. *Oncology* **26**: 488-495
- Navin N, Kendall J, Troge J, Andrews P, Rodgers L, McIndoo J, Cook K, Stepansky A, Levy D, Esposito D, Muthuswamy L, Krasnitz A, McCombie WR, Hicks J, Wigler M (2011) Tumour evolution inferred by single-cell sequencing. *Nature* **472**: 90-94
- Ngo VN, Davis RE, Lamy L, Yu X, Zhao H, Lenz G, Lam LT, Dave S, Yang L, Powell J, Staudt LM (2006) A loss-of-function RNA interference screen for molecular targets in cancer. *Nature* **441**: 106-110
- Nijman SM, Friend SH (2013) Cancer. Potential of the synthetic lethality principle. *Science* **342**: 809-811
- Nijman SMB (2011) Synthetic lethality: General principles, utility and detection using genetic screens in human cells. *FEBS Lett* **585**: 1-6
- Nik-Zainal S, Van Loo P, Wedge DC, Alexandrov LB, Greenman CD, Lau KW, Raine K, Jones D, Marshall J, Ramakrishna M, Shlien A, Cooke SL, Hinton J, Menzies A, Stebbings

LA, Leroy C, Jia M, Rance R, Mudie LJ, Gamble SJ, Stephens PJ, McLaren S, Tarpey PS, Papaemmanuil E, Davies HR, Varela I, McBride DJ, Bignell GR, Leung K, Butler AP, Teague JW, Martin S, Jonsson G, Mariani O, Boyault S, Miron P, Fatima A, Langerod A, Aparicio SA, Tutt A, Sieuwerts AM, Borg A, Thomas G, Salomon AV, Richardson AL, Borresen-Dale AL, Futreal PA, Stratton MR, Campbell PJ (2012) The life history of 21 breast cancers. *Cell* **149**: 994-1007

Nowell PC (1976) The clonal evolution of tumor cell populations. *Science* **194**: 23-28

O'Rourke MA, Murray LJ, Hughes CM, Cantwell MM, Cardwell CR (2015) The effect of warfarin therapy on breast, colorectal, lung, and prostate cancer survival: a population-based cohort study using the Clinical Practice Research Datalink. *Cancer Causes Control* **26**: 355-366

Ocana A, Pandiella A (2008) Identifying breast cancer druggable oncogenic alterations: lessons learned and future targeted options. *Clin Cancer Res* **14**: 961-970

Paddison PJ, Caudy AA, Bernstein E, Hannon GJ, Conklin DS (2002) Short hairpin RNAs (shRNAs) induce sequence-specific silencing in mammalian cells. *Genes Dev* **16**: 948-958

Paddison PJ, Silva JM, Conklin DS, Schlabach M, Li M, Aruleba S, Baliya V, O'Shaughnessy A, Gnoj L, Scobie K, Chang K, Westbrook T, Cleary M, Sachidanandam R, McCombie WR, Elledge SJ, Hannon GJ (2004) A resource for large-scale RNA-interference-based screens in mammals. *Nature* **428**: 427-431

Paikin JS, Eikelboom JW, Cairns JA, Hirsh J (2010) New antithrombotic agents--insights from clinical trials. *Nat Rev Cardiol* **7**: 498-509

Park CW, Zeng Y, Zhang X, Subramanian S, Steer CJ (2010) Mature microRNAs identified in highly purified nuclei from HCT116 colon cancer cells. *RNA Biol* **7**: 606-614

Perou CM, Sorlie T, Eisen MB, van de Rijn M, Jeffrey SS, Rees CA, Pollack JR, Ross DT, Johnsen H, Akslen LA, Fluge O, Pergamenschikov A, Williams C, Zhu SX, Lonning PE, Borresen-Dale AL, Brown PO, Botstein D (2000) Molecular portraits of human breast tumours. *Nature* **406**: 747-752

Pfander B, Moldovan G-L, Sacher M, Hoege C, Jentsch S (2005) SUMO-modified PCNA recruits Srs2 to prevent recombination during S phase. *Nature*

Poulikakos PI, Persaud Y, Janakiraman M, Kong X, Ng C, Moriceau G, Shi H, Atefi M, Titz B, Gabay MT, Salton M, Dahlman KB, Tadi M, Wargo JA, Flaherty KT, Kelley MC, Misteli T, Chapman PB, Sosman JA, Graeber TG, Ribas A, Lo RS, Rosen N, Solit DB (2011) RAF inhibitor resistance is mediated by dimerization of aberrantly spliced BRAF(V600E). *Nature* **480**: 387-390

Prat A, Perou CM (2009) Mammary development meets cancer genomics. *Nat Med* **15**: 842-844

- Rampling R, James A, Papanastassiou V (2004) The present and future management of malignant brain tumours: surgery, radiotherapy, chemotherapy. *J Neurol Neurosurg Psychiatry* **75**: ii24-30
- Renan MJ (1993) How many mutations are required for tumorigenesis? Implications from human cancer data. *Mol Carcinog* **7**: 139-146
- Richardson PG, Mitsiades C, Hideshima T, Anderson KC (2006) Bortezomib: proteasome inhibition as an effective anticancer therapy. *Annu Rev Med* **57**: 33-47
- Roberts TC (2014) The MicroRNA Biology of the Mammalian Nucleus. *Mol Ther Nucleic Acids* **19**: 40
- Robinson DR, Kalyana-Sundaram S, Wu Y-M, Shankar S, Cao X, Ateeq B, Asangani IA, Iyer M, Maher CA, Grasso CS, Lonigro RJ, Quist M, Siddiqui J, Mehra R, Jing X, Giordano TJ, Sabel MS, Kleer CG, Palanisamy N, Natrajan R, Lambros MB, Reis-Filho JS, Kumar-Sinha C, Chinnaiyan AM (2011) Functionally recurrent rearrangements of the MAST kinase and Notch gene families in breast cancer. *Nat Med* **17**: 1646-1651
- Rutherford SL, Lindquist S (1998) Hsp90 as a capacitor for morphological evolution. *Nature* **396**: 336-342
- Sasaki T, Okuda K, Zheng W, Butrynski J, Capelletti M, Wang L, Gray NS, Wilner K, Christensen JG, Demetri G, Shapiro GI, Rodig SJ, Eck MJ, Janne PA (2010) The neuroblastoma-associated F1174L ALK mutation causes resistance to an ALK kinase inhibitor in ALK-translocated cancers. *Cancer Res* **70**: 10038-10043
- Scaltriti M, Nuciforo P, Bradbury I, Sperinde J, Agbor-Tarh D, Campbell C, Chenna A, Winslow J, Serra V, Parra JL, Prudkin L, Jimenez J, Aura C, Harbeck N, Pusztai L, Ellis C, Eidtmann H, Arribas J, Cortes J, de Azambuja E, Piccart M, Baselga J (2015) High HER2 expression correlates with response to the combination of lapatinib and trastuzumab. *Clin Cancer Res* **21**: 569-576
- Seeler J-S, Dejean A (2003) Nuclear and unclear functions of SUMO. *Nature Reviews Molecular Cell Biology* **4**: 690-699
- Siegel R, DeSantis C, Virgo K, Stein K, Mariotto A, Smith T, Cooper D, Gansler T, Lerro C, Fedewa S, Lin C, Leach C, Cannady RS, Cho H, Scoppa S, Hachey M, Kirch R, Jemal A, Ward E (2012) Cancer treatment and survivorship statistics, 2012. *CA Cancer J Clin* **62**: 220-241
- Siegel R, Naishadham D, Jemal A (2013) Cancer statistics, 2013. *CA Cancer J Clin* **63**: 11-30
- Silva JM, Li MZ, Chang K, Ge W, Golding MC, Rickles RJ, Siolas D, Hu G, Paddison PJ, Schlabach MR, Sheth N, Bradshaw J, Burchard J, Kulkarni A, Cavet G, Sachidanandam R, McCombie WR, Cleary MA, Elledge SJ, Hannon GJ (2005) Second-generation shRNA libraries covering the mouse and human genomes. *Nat Genet* **37**: 1281-1288

- Sims D, Mendes-Pereira AM, Frankum J, Burgess D, Cerone MA, Lombardelli C, Mitsopoulos C, Hakas J, Murugaesu N, Isacke CM, Fenwick K, Assiotis I, Kozarewa I, Zvelebil M, Ashworth A, Lord CJ (2011) High-throughput RNA interference screening using pooled shRNA libraries and next generation sequencing. *Genome Biol* **12**: 2011-2012
- Slamon DJ, Leyland-Jones B, Shak S, Fuchs H, Paton V, Bajamonde A, Fleming T, Eiermann W, Wolter J, Pegram M, Baselga J, Norton L (2001) Use of chemotherapy plus a monoclonal antibody against HER2 for metastatic breast cancer that overexpresses HER2. *N Engl J Med* **344**: 783-792
- Sorensen HT (2007) Warfarin and prevention of prostate cancer. *Lancet Oncol* **8**: 368-369
- Sorlie T, Perou CM, Tibshirani R, Aas T, Geisler S, Johnsen H, Hastie T, Eisen MB, van de Rijn M, Jeffrey SS, Thorsen T, Quist H, Matese JC, Brown PO, Botstein D, Lonning PE, Borresen-Dale AL (2001) Gene expression patterns of breast carcinomas distinguish tumor subclasses with clinical implications. *Proc Natl Acad Sci U S A* **98**: 10869-10874
- Soule HD, Maloney TM, Wolman SR, Peterson WD, Jr., Brenz R, McGrath CM, Russo J, Pauley RJ, Jones RF, Brooks SC (1990) Isolation and characterization of a spontaneously immortalized human breast epithelial cell line, MCF-10. *Cancer Res* **50**: 6075-6086
- Steiner E, Holzmann K, Elbling L, Micksche M, Berger W (2006) Cellular functions of vaults and their involvement in multidrug resistance. *Curr Drug Targets* **7**: 923-934
- Stephens PJ, Tarpey PS, Davies H, Van Loo P, Greenman C, Wedge DC, Nik-Zainal S, Martin S, Varela I, Bignell GR, Yates LR, Papaemmanuil E, Beare D, Butler A, Cheverton A, Gamble J, Hinton J, Jia M, Jayakumar A, Jones D, Latimer C, Lau KW, McLaren S, McBride DJ, Menzies A, Mudie L, Raine K, Rad R, Spencer Chapman M, Teague J, Easton D, Langerod A, Lee MTM, Shen C-Y, Tee BTK, Huimin BW, Broeks A, Vargas AC, Turashvili G, Martens J, Fatima A, Miron P, Chin S-F, Thomas G, Boyault S, Mariani O, Lakhani SR, van de Vijver M, van 't Veer L, Foekens J, Desmedt C, Sotiriou C, Tutt A, Caldas C, Reis-Filho JS, Aparicio SAJR, Salomon AV, Borresen-Dale A-L, Richardson AL, Campbell PJ, Futreal PA, Stratton MR (2012) The landscape of cancer genes and mutational processes in breast cancer. *Nature* **486**: 400-404
- Stratton MR (2011) Exploring the genomes of cancer cells: progress and promise. *Science* **331**: 1553-1558
- Stratton MR, Campbell PJ, Futreal PA (2009) The cancer genome. *Nature* **458**: 719-724
- Strebhardt K, Ullrich A (2006) Targeting polo-like kinase 1 for cancer therapy. *Nat Rev Cancer* **6**: 321-330
- Szakacs G, Paterson JK, Ludwig JA, Booth-Gentle C, Gottesman MM (2006) Targeting multidrug resistance in cancer. *Nat Rev Drug Discov* **5**: 219-234

- Tagalakakis V, Tamim H (2010) The effect of warfarin use on clinical stage and histological grade of prostate cancer. *Pharmacoepidemiol Drug Saf* **19**: 436-439
- Tagalakakis V, Tamim H, Blostein M, Hanley JA, Kahn SR (2013) Risk of prostate cancer death in long-term users of warfarin: a population-based case-control study. *Cancer Causes Control* **24**: 1079-1085
- Tischler J, Lehner B, Chen N, Fraser AG (2006) Combinatorial RNA interference in *Caenorhabditis elegans* reveals that redundancy between gene duplicates can be maintained for more than 80 million years of evolution. *Genome Biol* **7**: 2
- Tischler J, Lehner B, Fraser AG (2008) Evolutionary plasticity of genetic interaction networks. *Nature Genet* **40**: 390-391
- Tolcher AW, Khan K, Ong M, Banerji U, Papadimitrakopoulou V, Gandara DR, Patnaik A, Baird RD, Olmos D, Garrett CR, Skolnik JM, Rubin EH, Smith PD, Huang P, Learoyd M, Shannon KA, Morosky A, Tetteh E, Jou YM, Papadopoulos KP, Moreno V, Kaiser B, Yap TA, Yan L, de Bono JS (2015) Antitumor Activity in RAS-Driven Tumors by Blocking AKT and MEK. *Clin Cancer Res* **21**: 739-748
- Tomasetti C, Vogelstein B (2015) Cancer etiology. Variation in cancer risk among tissues can be explained by the number of stem cell divisions. *Science* **347**: 78-81
- Tong AH, Evangelista M, Parsons AB, Xu H, Bader GD, Page N, Robinson M, Raghibizadeh S, Hogue CW, Bussey H, Andrews B, Tyers M, Boone C (2001) Systematic genetic analysis with ordered arrays of yeast deletion mutants. *Science* **294**: 2364-2368
- Tong AH, Lesage G, Bader GD, Ding H, Xu H, Xin X, Young J, Berriz GF, Brost RL, Chang M, Chen Y, Cheng X, Chua G, Friesen H, Goldberg DS, Haynes J, Humphries C, He G, Hussein S, Ke L, Krogan N, Li Z, Levinson JN, Lu H, Menard P, Munyana C, Parsons AB, Ryan O, Tonikian R, Roberts T, Sdicu AM, Shapiro J, Sheikh B, Suter B, Wong SL, Zhang LV, Zhu H, Burd CG, Munro S, Sander C, Rine J, Greenblatt J, Peter M, Bretscher A, Bell G, Roth FP, Brown GW, Andrews B, Bussey H, Boone C (2004) Global mapping of the yeast genetic interaction network. *Science* **303**: 808-813
- Veldscholte J, Berrevoets CA, Ris-Stalpers C, Kuiper GG, Jenster G, Trapman J, Brinkmann AO, Mulder E (1992) The androgen receptor in LNCaP cells contains a mutation in the ligand binding domain which affects steroid binding characteristics and response to antiandrogens. *J Steroid Biochem Mol Biol* **41**: 665-669
- Wang Y, Waters J, Leung ML, Unruh A, Roh W, Shi X, Chen K, Scheet P, Vattathil S, Liang H, Multani A, Zhang H, Zhao R, Michor F, Meric-Bernstam F, Navin NE (2014) Clonal evolution in breast cancer revealed by single nucleus genome sequencing. *Nature* **512**: 155-160
- Weigelt B, Geyer FC, Reis-Filho JS (2010) Histological types of breast cancer: how special are they? *Mol Oncol* **4**: 192-208

Weinstein IB (2002) Addiction to Oncogenes--the Achilles Heal of Cancer. *Science* **297**: 63-64

Whitehurst AW, Bodemann BO, Cardenas J, Ferguson D, Girard L, Peyton M, Minna JD, Michnoff C, Hao W, Roth MG, Xie XJ, White MA (2007) Synthetic lethal screen identification of chemosensitizer loci in cancer cells. *Nature* **446**: 815-819

Whitesell L, Lindquist SL (2005) HSP90 and the chaperoning of cancer. *Nat Rev Cancer* **5**: 761-772

WHOECO (2012) EUCAN National Estimates - World Health Organization European Cancer Observatory.

WHOROE (2012) European Detailed Mortality Database - World Health Organization Regional Office for Europe

Winter GE, Radic B, Mayor-Ruiz C, Blomen VA, Trefzer C, Kandasamy RK, Huber KV, Gridling M, Chen D, Klampfl T, Kralovics R, Kubicek S, Fernandez-Capetillo O, Brummelkamp TR, Superti-Furga G (2014) The solute carrier SLC35F2 enables YM155-mediated DNA damage toxicity. *Nat Chem Biol* **10**: 768-773

Yuan TL, Cantley LC (2008) PI3K pathway alterations in cancer: variations on a theme. *Oncogene* **27**: 5497-5510

Yun CH, Mengwasser KE, Toms AV, Woo MS, Greulich H, Wong KK, Meyerson M, Eck MJ (2008) The T790M mutation in EGFR kinase causes drug resistance by increasing the affinity for ATP. *Proc Natl Acad Sci U S A* **105**: 2070-2075

Zamore PD, Tuschl T, Sharp PA, Bartel DP (2000) RNAi: double-stranded RNA directs the ATP-dependent cleavage of mRNA at 21 to 23 nucleotide intervals. *Cell* **101**: 25-33

Zuber J, McJunkin K, Fellmann C, Dow LE, Taylor MJ, Hannon GJ, Lowe SW (2011a) Toolkit for evaluating genes required for proliferation and survival using tetracycline-regulated RNAi. *Nat Biotechnol* **29**: 79-83

Zuber J, Shi J, Wang E, Rappaport AR, Herrmann H, Sison EA, Magoon D, Qi J, Blatt K, Wunderlich M, Taylor MJ, Johns C, Chicas A, Mulloy JC, Kogan SC, Brown P, Valent P, Bradner JE, Lowe SW, Vakoc CR (2011b) RNAi screen identifies Brd4 as a therapeutic target in acute myeloid leukaemia. *Nature* **478**: 524-528

CURRICULUM VITAE

Marco Paolo Licciardello

Ettenreichgasse 50/4/DG 52 1100 Vienna, Austria

Nationality: Italian

Date of birth: October, 7th 1984

Mobile: +43 680 553 57 40

Email: marco.licciardello@gmail.com

Education

- 2010 - Present **PhD in Molecular Medicine, Molecular Signal Transduction Program, Medical University of Vienna, Austria**
CeMM – Research Center for Molecular Medicine of the Austrian Academy of Sciences
Thesis: *“Molecularly stratified and combinatorial approaches for precision cancer therapy”*
Supervisor: Dr. Stefan Kubicek
- 2007 - 2009 **MSc in Biomolecular Chemistry (Hons), University of Catania, Italy**
Department of Chemistry
Thesis: *“DNA detection by digital microfluidics”*
Supervisor: Prof. Giuseppe Spoto
- 2003 - 2007 **BSc in Chemistry (Hons), University of Catania, Italy**
Department of Chemistry
Supervisor: Prof. Giuseppe Spoto

Further Research Experience

- February 2009 – June 2009 **Internship at CeMM – Research Center for Molecular Medicine of the Austrian Academy of Sciences**
Laboratory: Prof. Giulio Superti-Furga

Scholarships and Awards

- July 2012 Best Poster (2nd place) - European Chemical Biology Symposium 2012, Vienna, Austria
- 2003 -2009 Annual university scholarship based on merit

Conferences and Courses

AACR Annual Meeting 2015, Philadelphia, PA, USA (Poster)

ÖGMBT Annual Meeting 2014, Vienna, Austria (Selected Talk: “*NOTCH1 activation in breast cancer confers sensitivity to inhibition of SUMOylation*”)

Cell Symposia - Cancer Epigenomics 2013, Sitges, Spain (Poster)

Chromatin and Systems Biology Summer School 2013, Spetses, Greece (Poster)

European Chemical Biology Symposium 2012, Vienna, Austria (Best Poster – 2nd place)

Synthetic Lethality From Yeast to Man, EMBO Workshop 2012, Vienna, Austria (Poster)

Nature Chemical Biology Symposium 2011, Boston, MA, USA (Poster)

EMBO Meeting 2011, Vienna, Austria

Methods in Chemical Biology, EMBO Practical Course 2011, Heidelberg, Germany (Poster)

Publications

Licciardello, M. P., Markt, P., Klepsch, F., Lardeau C. -H., Dürnberger, G., Ivanov, V., Colinge, J. & Kubicek, S. “*A combinatorial screen of the CLOUD uncovers a synergy of approved drugs targeting the androgen receptor*”, (submitted)

Licciardello, M. P., Müllner, M. K., Dürnberger, G., Kerzendorfer, C., Boidol, B., Trefzer, C., Sdelci, S., Berg, T., Penz, T., Schuster, M., Bock, C., Kralovics, R., Superti-Furga, G., Colinge, J., Nijman, S. M. & Kubicek, S. “*NOTCH1 activation in breast cancer confers sensitivity to inhibition of SUMOylation*”, *Oncogene*, 2014, 1-11

Zanoli, L. M., **Licciardello, M. P.**, D’Agata, R., Lantano, C., Calabretta, A., Corradini, R., Marchelli, R. & Spoto, G. “*Peptide nucleic acid molecular beacons for the detection of PCR amplicons in droplet-based microfluidic devices*”, *Analytical and Bioanalytical Chemistry*, 2013, 405:615-624

Languages

Italian: native

English: full professional proficiency

German: professional working proficiency

Other Interests

Music

Travelling